Study of Non-Covalent Protein-Carbohydrate Interactions by Nanoelectrospray Ionization Mass Spectrometry and Surface Plasmon Resonance

by

Sanaz Nikjah

A thesis submitted to the Faculty of Graduate Studies and Research in partial fulfillment of the requirements for the degree of

Master of Science

Department of Chemistry
University of Alberta

Abstract

This thesis describes the application of electrospray ionization mass spectrometry (ESI-MS) techniques to identify and quantify antibody-antigen interactions in vitro. Also potential application of nanodiscs (ND) as membrane model in ESI-MS and surface plasmon resonance (SPR) spectroscopy has been investigated.

A direct nanoelectrospray mass spectrometry assay (nanoESI-MS) was developed for quantification of specific binding between a monoclonal antibody (mAb) and its cognate antigen. A qualitative investigation was performed on cross-reactivity of antibodies. NanoESI-MS was also employed to investigate the effects of fatty acid chain lengths on its degree of incorporation into ND. The results can be utilized for synthesis purposes where biologically important carbohydrates require a proper carbon chain for incorporation into ND.

ND technology was also employed to investigate protein-ligand interaction using SPR spectroscopy. The results open up further investigation on the effect of the position of ganglioside binding sites incorporated into ND and ability of their binding to the receptors in SPR.

Preface

This master's thesis includes two research projects that are original, independent and unpublished work of Sanaz Nikjah.

The derived binding formula in chapter 2 was done primarily by me with assistance of Dr. Elena Kitova and Ling Han. The monoclonal antibody CS-35 used was expressed and purified by Ruixiang Zheng.

Table of contents

List of Tables

List of Figures

CTB to 1%GM1-ND immobilized on the surface of CM5 sensor chip.

List of Abbreviations

Ab	Antibody
Ab	Abundance
AC	Alternative current
app	Apparent
BSA	Bovine serum albumin
C	Constant region
CBD	Chitin binding domain
CDR	Complementary-determining region
CID	Collision-induced dissociation
CRM	Charge residue model
CTB	Cholera toxin B subunit
Da	Dalton
DC	Direct current
DMPC	1,2-dimyristoyl-sn-glycero-3-phosphocholine
EDC	(N-(3-dimethylaminopropyl)-N'-ethylcarbodiimide hydrochloride
ELISA	Enzyme- linked immunosorbent assay
ESI	Electrospray ionization
ESI-MS	Electrospray ionization mass spectrometry

Fab	Fragment of antigen- binding
FC	Fragment crystallizable
FPLC	Fast protein ligand chromatography
G	Glycan
Gb3-Cer	Globotriaosylceramide (Gal(α1-4)Gal(β-4)Glc(β1)-ceramide
GD1b	bDGalp(1-3)bDGalNAc(1-4)[aNeu5Ac(2-8)aNeu5Ac(2-3)] bDGalp(1-4)bDGlcp(1-1)Cer
GD2	bDGalpNAc(1-4)[aNeu5Ac(2-8)aNeu5Ac(2-3)]bDGalp(1-4) bDGlcp(1-1)Cer
GM1	bDGalp(1-3)bDGalNAc[aNeu5Ac(2-3)]bDGalp(1-4)bDGlcp (1-1)Cer
GM3	aNeu5Ac(2-3)bDGalp(1-4)bDGlcp(1-1)Cer
H-Araf	Hexa-Arabinofuranoside
HEPES	4-(2-hydroxyethyl)-1-piperazineëthanesulfonic acid
IEM	Ion evaporation model
Ig	Immunoglobulin
IgG	Immunoglobulin γ
IS	Internal standard
ITC	Isothermal titration microcalorimetry
Ka	Binding constant
$K_{a,int}$	Intrinsic association constant
K_d	Dissociation constant
L	Ligand

LAM	Lipoarabinomannan
LB	Luria-Bertani
m/z	Mass-to-charge ratio
mAb	Monoclonal antibody
MALDI	Matrix-assisted laser desorption ionization
MS	Mass spectrometry
MSP	Membrane Scaffold protein
MW	Molecular weight
MWCO	Molecular weight cut-off
nanoESI	Nanoflow electrospray ionization
ND	Nanodisc
NHS	N-hydroxysuccinimide
NMR	Nuclear magnetic resonance
NTA	Nitrilitriacetic acid
P	Protein
P_{ref}	Reference protein
Q-IMS-TOF	Quadrupole ion-mobility separation time-of-flight
RF	Radio frequency
RF	Response factor
RU	Response unit
SDS-PAGE	Sodium dodecyl sulfate-polyacrylamide gel electrophoresis
SEC	Size exclusion chromatography
SPR	Surface plasmon resonance

Stx2	Shiga toxin 2
TB	Tuberculosis
TOF	Time of flight
V	Variable region

Chapter 1

Study of Non-covalent Protein-Ligand Interactions by Electrospray Ionization Mass Spectrometry

1.1 Introduction

Mass spectrometry (MS) is an analytical technique that is based on producing charged particles from molecules to obtain different information such as molecular weight from the sample. With the technological improvements of MS instrumentation in recent years, MS has emerged as a powerful method for research and industrial endeavors in the field of chemistry, biology, biophysics and biochemistry. A few examples of the numerous applications of MS are, for monitoring enzyme reactions[1], can be used in all stages of drug discovery and development[2], food safety[3], protein analysis[4], environmental research[5] and protein-ligand complex binding kinetics[6] and thermodynamics[7].

Among the applications of MS, in the field of glycomics, investigation of protein-carbohydrate interaction is of increasing importance. Many biological processes rely on protein-carbohydrate interactions for signal transduction, antibody antigen interaction, intra cellular communication and enzymatic catalysis[8]. As a result, having reliable techniques to identify and measure binding constants of protein-carbohydrate interactions is of utmost importance.

In addition to MS, other methods that have been used to investigate protein ligand interactions are fluorescence polarization[9], isothermal calorimetry (ITC)[10],

surface plasmon resonance (SPR) spectroscopy [11], enzyme- linked immunosorbent assay (ELISA)[12] and nuclear magnetic resonance (NMR) spectroscopy[13].

Fluorescence polarization is based on the rotation of molecules in solution. Smaller molecules rotate faster. Excitation of a fluorescent-labeled small molecule with a plane polarized light leads to depolarization of the emitted light caused by the fast movement of the molecules. If the fluorescent-labeled small molecule is bound to a molecule with a large molecular mass and is excited with a polarized light, the emitted light is less depolarized due to the restricted movement of the complex. A binding constant can be obtained by titrating a target protein against a fixed concentration of fluorescent-labeled small molecule. However, this method requires labeling and so is a disadvantage for measuring binding constant[9].

ITC is a real label free method and is known as the "gold standard" for studying thermodynamic parameters of biological complexes. In ITC, the heat changes (change in temperature) as sample is injected into the sample cell and forms complex with the ligand. Binding constant, entropy and enthalpy of the reaction, as well as free energy of binding, can be determined in just one single experiment[14]. However, the main drawback of this method is its low sensitivity and requirement of relatively large amount (~ mg) of pure protein and ligand for the experiment. To fulfill the problem, new ITC technologies has emerged such as the Nano ITC, which consume lower amount of sample and have better sensitivity.

SPR is one of the most frequently used methods for measuring kinetic and thermodynamic constants of protein-ligand interactions. First, this technique was developed to determine binding constant for macromolecular interactions[15]. With technological improvements of the SPR instrument, measuring of binding strength of small molecules such as drugs to macromolecules have become possible. Overall, SPR is sensitive and requires only a low amount of sample (~ ng) for each run. However, SPR is not a label-free technique as one of the binding partners (ligand) should be immobilized on the surface.

Some researchers have shown that kinetic and thermodynamic data obtained by SPR are not necessarily the same as ones have gained by solution based techniques such as ITC[16]. One reason is that immobilizing of one of the two partners (ligand) on the surface can restrict rotational freedom of the molecule and diffusional characteristics and as a result change the binding data and reaction thermodynamic.

ELISA is a powerful method for investigating protein-ligand interaction[17]. Different formats of ELISA are available for studying protein-ligand interactions, the common feature of them all is the immobilization of one sample on a solid surface either specifically or nonspecifically and incubation of the immobilized sample with a solution containing binding partner of the sample that is linked to an enzyme. After incubation a substance is added to react with the enzyme to produce a detectable signal. ELISA is easy to perform. It can be automated and is relatively sensitive; however non-specific binding due to a large surface area can

lead to an increased background. ELISA needs tedious washing steps and the results are highly dependent on the effectiveness of washing. Also the reaction between enzyme and the substrate is short-term and the plate must be read as soon as possible.

NMR spectroscopy is another useful technique for studying the interactions of proteins in solution and on an atomic level. However, the intrinsic insensitivity of the method is the greatest disadvantages of NMR spectroscopy and as a result a large amount of samples is required for analysis (typically mg range). In addition, NMR method is a time consuming process and restricted to small proteins with molecular weights (MWs) < 40 kDa[18].

Electrospray ionization mass spectrometry (ESI-MS) has recently emerged as a useful technique for identifying the stoichiometry and binding affinity of protein-ligand interactions. Even though the invention of MS goes back the beginning of 20th century[19], biological macromolecules could not be transferred into gas phase. After Fenn introduced ESI in late 1980's, the application of MS expanded to biological systems[20].

ESI-MS is a non-destructive technique that preserves noncovalent protein-ligand interaction in gas phase. In direct ESI-MS assay, the protein and protein-ligand complex ions are detected directly from the gas phase. The first binding measurement of carbohydrate-protein complex by direct ESI-MS was reported by Kitova *et al.* in 2001[21] and the reported K_a value were in good agreement with the ITC results[22]. Since then, a lot of research has been done to quantify carbohydrate

-protein interaction using the direct ESI-MS assay [23]. Before explaining direct ESI-MS assay, a brief description of ESI mechanism and mass instrumentation will be given below.

1.2 Electrospray ionization mass spectrometry (ESI-MS)

Electrospray (ES) is a method that uses electricity to produce fine liquid aerosol via electrostatic charging. The phenomenon first viewed by the physicist John Zeleny in 1914 [24]. By applying a high voltage to a liquid that pass through a nozzle, the liquid will get charged and at a critical point when the liquid cannot hold anymore electrical charge, it will break away into small highly charged droplets. From here, the term electrospray ionization (ESI) was derived from. Combination of ESI and MS makes a powerful and invaluable method for analysis of large biological molecules.

1.2.1 ESI mechanism

The mechanism of ESI can be divided into three stages according to Kebarle and coworkers[25] :

a) Production of charged droplets at the capillary tip of ESI (Droplet formation)
b) Shrinkage of the charged droplet as a result of solvent evaporation (Droplet shrinkage)

c) Production of gas phase ions from the small droplets (Gaseous ion formation)

Long before its combination with MS, ES was used to create aerosol particles and for electrostatic dispersion of liquids, the above first two steps are well understood and studied by researchers[26]. There have been predictions on the mechanism of the third step however the actual mechanism is still not fully understood. The two most popular and accepted mechanisms to explain the third step will be discussed below.

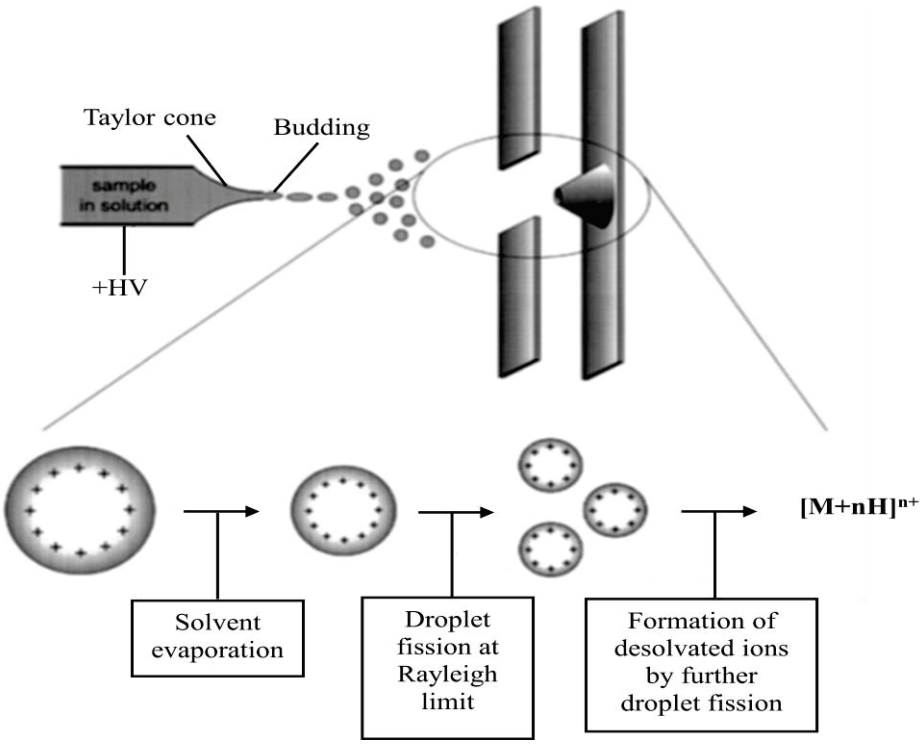

Figure 1.1 Droplet production in ESI in positive ion mode adapted from Ref 22.

a) Production of charged droplets at the capillary tip of ESI (Droplet formation):

Ions in ESI are produced at atmospheric pressure. Figure 1.1 shows ESI diagram in positive ion mode. A high positive voltage is applied to the small capillary that the sample solution is passing through. This induces charge separation in the solvent. The accumulated positive charges drift towards the liquid surface and are destabilized due to repulsion. Next, it deforms into a liquid cone called a Taylor cone[27]. From the apex of the cone, there is a fine jet of liquid that finally breaks up into small droplets[28]. The initial ESI droplets sizes have a narrow distribution in the micrometer range[27].

b) Shrinkage of the charged droplet as a result of solvent evaporation (Droplet shrinkage):

When the charged droplets are produced, they begin to shrink as their solvent starts to evaporate as neutral particles. This leads to an increase in the electric field at the surface of the droplet. The size of the droplet continues to decrease until it reaches the Rayleigh limit[27], the point at which Coulomb force of repulsion balances with the surface tension of the droplets. At this point Coulomb fission occurs and smaller offspring droplets release from the parent droplets. The process of evaporation/Coulomb fission repeats and yields the final charged nanodroplets[27].

c) Production of gas phase ions from the small droplets (Gaseous ion formation):

Two mechanisms for the formation of gas phase ions will be discussed here. Figure 1.2 shows schematic representation of the two models for formation of gas phase ions:

i) Charge Residue Model (CRM): This model proposed by Dole is based on formation of gas phase ions from the very small charged droplets. Using the Taylor cone mechanism and Rayleigh limit, it is possible to produce charged droplets that carry one analyte molecule. Desolvation of this droplet causes the charge at the surface of the droplet to be transferred to the analyte[29]. The model is well suited to explain electrospray ionization of analytes of high molecular mass such as native proteins, as shown by several studies, that the number of charges on large ions produced by ESI is about the same as the Rayleigh limiting charge of droplets with the same size as the big ions[30].

ii) Ion Evaporation Model (IEM): This model was proposed by Iribarne and Thomson[31] and assumes direct ion emission from small charged droplets. When the size of the droplets is decreased as a result of solvent evaporation and coulomb fission, the electric field at the surface of the droplet is quite strong to let direct emission of the ions. Typically after the radii of the droplets are less than 10 nm, the ion emission model dominates over Rayleigh fission. This model works well for small ions[31] with negligible hydrodynamic radius. The energy barrier to leave the droplet is significantly large for larger ions and this makes direct emission of larger ions significantly difficult[32].

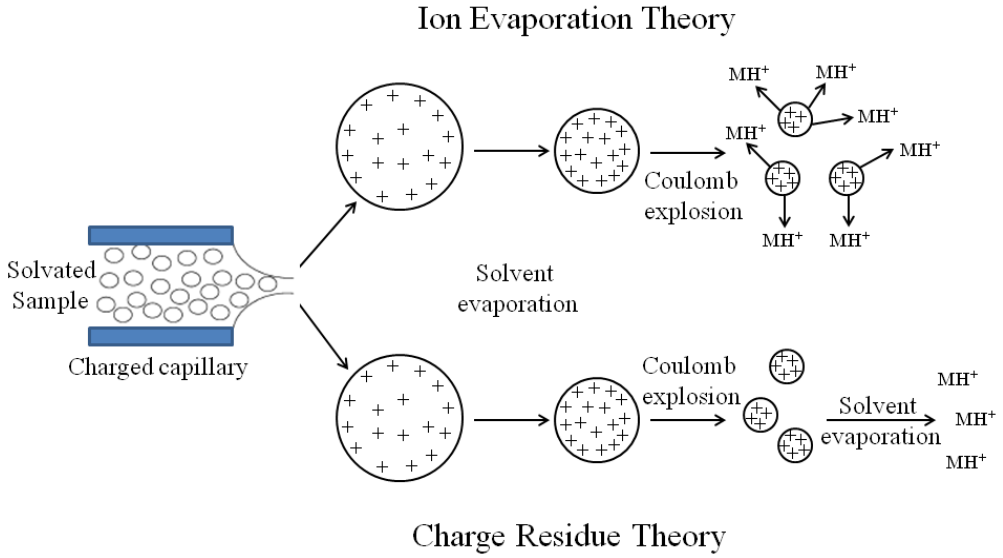

Figure 1.2 The formation of gas phase ions during electrospray ionization by different mechanism (Modified from Ref 29).

Different types of ESI have been used in biological research including: conventional ESI, nanoESI and ESSI (electrosonic spray ionization). A comparison of these three techniques has been done to show which method gives more reliable binding data for protein-ligand interaction[33]. Binding data was determined for a known model protein with the three techniques and results have shown that the values for all three methods are in good agreement with the binding data gained in solution phase methods. Although the closest binding data match was with ESSI technique, it is not as widely available as the other two techniques.

In my research project, nanoESI was used for all the experiments. The mechanism of nanoESI is the same as ESI, except for a few differences in

parameters and improved performance. Electric potentials between capillary and sampling orifice is lower for nanoESI compare to ESI (1-1.5 kV versus 3-5 kV for ESI), this allows transfer of non-covalent protein-ligand complexes to the gas phase more efficiently[34]. Droplet sizes in nanoESI are about 10 times smaller than droplets produced in conventional ESI (150 nm for nanoESI compared to 1.5 μm in diameter for conventional ESI), so under gentle condition of temperature and pressure desolvation is more efficient that leads to improved sensitivity[34].

In nanoESI narrow glass tips are used. To provide enough conductivity, the capillary can be coated with a conductive metal or a thin metal wire can be inserted inside the capillary. The capillary tubes are disposable which removes the possibility of contamination and memory effects. Since nanoESI works at lower flow rates (10-50 nL/min) compare to conventional ESI (1-10 μL/min)[35], less sample material is required per analysis. This is especially important when availability of sample is low (as is often the case in biological research).

In addition to the above advantages, nanoESI has greater tolerance against higher levels of salts and improved detectability for some classes of compounds compared to conventional ESI[36]. Due to solvent evaporation and droplet shrinkage the concentration of analyte and electrolyte increases in each droplet. The droplet size in nanoESI is ten times smaller than the one in conventional ESI. For nanoESI, the number of droplet shrinkage steps is less than conventional ESI as a result this leads to a lower concentration of salts in the sample solution. Certain compounds such as sugars and glycosides are known to be non-surface

active analytes. Surface active compounds preferentially go to the surface of droplets. Conventional ESI does not have enough sensitivity to detect non-surface active analytes, as they are found largely in the bulk of the droplet. However, nanoESI has a higher surface/volume ratio of droplets; so non-surface active compounds located in the bulk of droplets are more accessible[37]. The mechanisms are depicted in figure 1.3. Smaller droplets size in nanoESI has other advantages as well. A smaller droplets means that fewer analyte molecules exist per droplet, thus, nonspecific aggregations is minimized[38]. Moreover, conventional ESI is not a convenient method for using of solvents that have high surface tensions because spray stability is low, while with nanoESI these solvents can be successfully sprayed[39]. All these properties make nanoESI a useful method for investigating non covalent protein-ligand interactions.

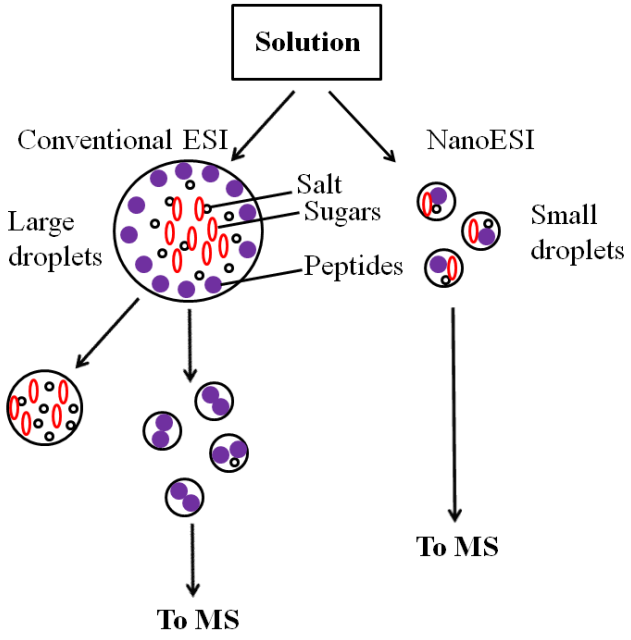

Figure 1.3 Comparison between conventional ESI and nanoESI[38].

1.2.2 Mass instrumentation

1.2.2.1 Hybrid quadrupole time of flight mass spectrometer

A Synapt G2S quadrupole ion-mobility separation time-of-flight (Q-IMS-TOF) mass spectrometer (Waters UK Ltd., Manchester, UK), equipped with a nanoflow ESI (nanoESI) source was used for the entire work.

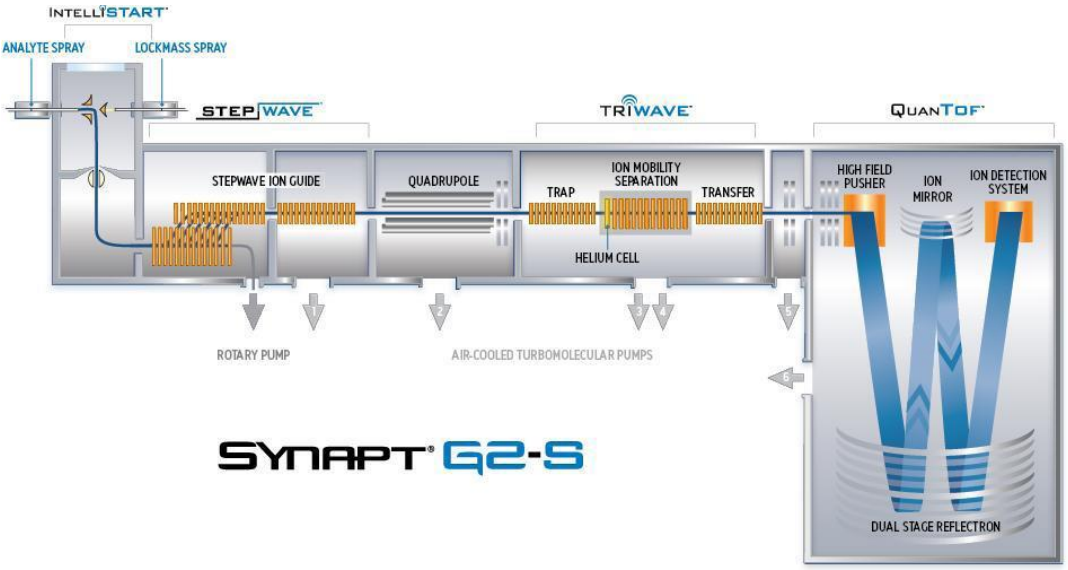

Figure 1.4 Schematic representation of the Waters Synapt G2S nanoESI Q-IMS-TOF mass spectrometer. The figure was adapted from Waters Corporation.

The analyzer can be considered as the heart of the mass spectrometer. As a quadrupole and time-of flight mass analyzer has been used in Waters Synapt G2S, a brief description of these two analyzers will be brought here.

1.2.2.1.1 Quadrupole

In a quadrupole, four parallel metal rods are kept at equal distance from each other. They act together as a mass separator. One set of opposite rods is connected electrically to a positive direct current (DC) potential and the other set connected to an equal but negative DC potential. A radio frequency (RF) alternating current (AC) voltage is superimposed with the DC potential and is applied on each set. By changing the RF and DC voltages simultaneously while the RF/DC ratio is kept constant, only the ions with the desired m/z (mass-to-charge) ratio have amplitudes of oscillation that are stable enough to travel, pass through the quadrupole and reach the detector. Other ions with an unstable trajectory will hit the rods and become neutralized. If the DC voltage is switched off and only the RF voltage is applied, the quadrupole will work as a transfer only device and act as a broad bandpass filter to focus the ions with a wide range of m/z into the mass spectrometer optics[40].

In the Synapt mass spectrometer the quadrupole consist of two parts, a main quadrupole and an RF only quadrupole prefilter which is mounted in front of it (Figure 1.5). The prefilter usually works at the same RF voltage as the main filter. The ions motion through the prefilter is complicated and has been demonstrated by numerical simulations of trajectories. Without the prefilter, ions may not be transmitted effectively to the quadrupole because of the effects of the fringing field. As such, the prefilter guides ions into the main quadrupole and increases the absolute sensitivity[41].

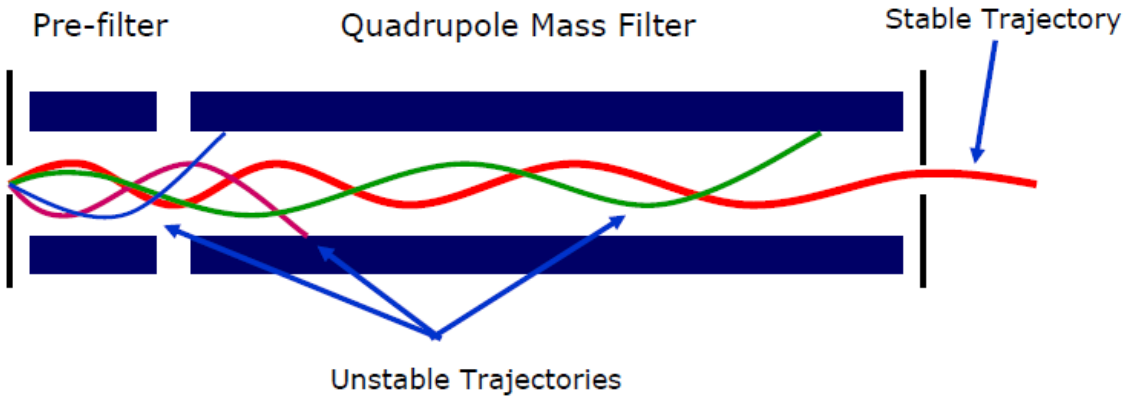

Figure 1.5 Schematic representation of the quadrupole in Waters Synapt G2S mass spectrometer[42].

1.2.2.1.2 Time of flight (TOF)

In a TOF mass analyzer, ions are accelerated by a high electric field pulse into a long straight flight tube which is kept at a low pressure. Ions with different m/z ratio attain different velocity. The time taken for an ion to pass the flight tube is inversely proportional to its velocity and thus proportional to its m/z ratio. By measuring the flight time of the ions their m/z values can be determined, according to equation (1):

$$(m/z)^{1/2} = t\left(\frac{\sqrt{2eV_s}}{L}\right) \qquad (1)$$

where m is the mass of the ion, z is the charge state of the ion, t is the flight time, e is the elementary charge, Vs is the acceleration potential and L is the length of the flight tube. Two different model of TOF include: linear TOF analyzer and reflectron TOF analyzer. In linear TOF, ions introduced into the flight tube have

different kinetic energies and as a result ions with equal m/z can reach the detector at different times. This will influence the resolving power. To overcome this drawback, reflectron TOF was developed to compensate for differences in the velocities of ions with equal m/z. The reflectron, an electrostatic ion mirror, is an ion optic device[43]. When ions reach sets of electric grids of increasing potential, they are turned around and sent back to a second flight towards the detector. Ions with the same m/z but with different kinetic energies penetrate different path lengths; ions with more kinetic energy arrive at the ion mirror first and penetrate the field deeper and spend more time in the reflectron than ions with less kinetic energy. So ions with the same m/z but different kinetic energies arrive at the detector at or about the same time. This along with increased travel path improves the resolution of the TOF analyzer[44].

After a brief description of ESI, nanoESI and mass instrumentation, the direct ESI-MS binding assay used in the present work will be given in the section below.

1.3 Direct ESI-MS binding assay

The direct ESI-MS binding assay is based on the detection and quantification of free and ligand-bound protein ions by ESI-MS. Beginning with solutions of known initial concentrations of protein ($[P]_0$) and ligand ($[L]_0$), the K_a values is determined from the ratio (R) of total abundance (*Ab*) of ligand-bound and unbound protein ions in the gas phase. The method is based on the

assumption that the gas-phase abundance ratio is the same as the concentration ratio in solution at equilibrium.

$$\mathrm{P} + \mathrm{L} \rightleftharpoons \mathrm{PL} \tag{2}$$

$$\frac{[\mathrm{PL}]_{eq}}{[\mathrm{P}]_{eq}} = \frac{Ab(\mathrm{PL})}{Ab(\mathrm{P})} = R \tag{3}$$

For a 1:1 protein-ligand complex, the K_a value is determined using equation (4):

$$\mathrm{K}_a = \frac{R}{[\mathrm{L}]_0 - \frac{R}{1+R}[\mathrm{P}]_0} \tag{4}$$

For determining K_a for a particular protein-ligand interaction, a titration experiment is required, wherein a fixed concentration of one analyte (normally P) is used against varying concentration of the other. The Ka value can be obtained using nonlinear regression analysis of the fraction of ligand-bound protein [R/(R+1)], using equation (5):

$$\frac{R}{R+1} = \frac{1 + \mathrm{K}_a[\mathrm{P}]_0 + \mathrm{K}_a[\mathrm{L}]_0 - \sqrt{4\mathrm{K}_a[\mathrm{L}]_0 + (1 + \mathrm{K}_a[\mathrm{P}]_0 - \mathrm{K}_a[\mathrm{L}]_0)^2}}{2\mathrm{K}_a[\mathrm{P}]_0} \tag{5}$$

1.4 Potential drawbacks in direct ESI-MS binding assay

There are some limitations that can affect the results of direct ESI-MS binding assay. Equilibrium abundance ratio of bound-to- free protein is an important parameter. Any physical and chemical steps that change this ratio during ESI and/or during the gas phase in relation to the original ratio in the bulk solution will result in an incorrect K_a calculation. Four common sources of error known to be related to the ESI-MS measurement are: 1) non-uniform response factors, 2) nonspecific ligand-protein binding, 3) in-source dissociation and 4) ESI-induced changes in solution pH and temperature. A brief description of these sources of error with some strategies to reduce their effect is brought here[45].

1.4.1 Non–uniform response factors

The abundance of gaseous P and PL ions measured by ESI-MS are correlated to the solution concentrations by response factors (RFs) which accounts for the detection efficiencies and ionization, equation (6):

$$\frac{[\mathrm{PL}]_{eq}}{[\mathrm{P}]_{eq}} = \frac{Ab(\mathrm{PL})/RF_{\mathrm{PL}}}{Ab(\mathrm{P})/RF_{\mathrm{p}}} = RF_{\mathrm{P/PL}}\frac{Ab(\mathrm{PL})}{Ab(\mathrm{P})} \qquad (6)$$

RF_{P} and RF_{PL} are the response factor of P and PL respectively and relative response factor, $RF_{\mathrm{P/PL}}$, is the ratio between the two *RF* values. Absolute *RF* depends on some parameters including the structure, size and surface properties of P and PL and also depends on solution composition and instrumental parameters of the measurement. However uniform *RF*s for P and PL are still expected when

the size and surface properties of the P and PL are about the same. This means that the L should be small compared to the P[46]. Overall, when the molecular weight of PL and P (MW_{PL} and MW_P) are similar in such a way that $MW_{PL}/MW_P \leq 110\%$, this approximation is considered to be valid[47]. There are examples when the *RF* of protein complex and free protein are quite different from each other[48]. In these cases some strategies have been introduced to minimize the effects of non-uniform *RF*s on obtaining K_a values by ESI-MS assay. In one method the $RF_{P/PL}$ term is introduced to the binding model as an adjustable parameter[48]. However this model contains multiple adjustable parameters that are required to be fitted to the titration data, so obtaining a reliable K_a value, requires higher quality experimental data[49]. In addition, another assumption should be considered when using this method is that $RF_{P/PL}$ is independent of concentration, at least for the ranges of the concentrations that is used in the experiment. Another approach, involves using an internal standard (IS). The IS should have similar molecular weight and surface activity to the analyte, but should not have specific binding to L[50].

1.4.2 Nonspecific binding

Nonspecific binding of L to P and PL (or PL_q in general) can occur during ESI because of concentration effects and hence, gives false positive results. One sign of occurrence of nonspecific binding is the presence of peaks from the target protein P bound to multiple ligands with a Poisson-like distribution. Another

indicator of occurrence of nonspecific binding is changes in the magnitude of K_a when the ligand concentration changes[45]. Decreasing the initial concentration of ligand is a general strategy to minimize the formation of nonspecific binding between protein and ligand. However high initial concentrations of ligand (> 0.05 mM) is typically necessary in dealing with very weak ligand interactions ($K_{a,int} < 10^4$ M^{-1}) in order to produce detectable level of complexes. In these cases the occurrence of nonspecific binding is inevitable[45].

There are a few methods that have been introduced to consider the occurrence of nonspecific binding to correct ESI mass spectra. One common approach is the reference protein method[51]. In this approach a reference protein (P_{ref}) is added to the solution but does not have specific binding to the protein and ligand of interest. The basic assumption of this method is that nonspecific binding is a random phenomenon that has equal effect on all protein species that exist in the ESI droplets. This is suggested based on mass spectra of nonspecifically bound molecules that resemble a Poisson process. By measuring the fractional abundance of nonspecific complexes of P_{ref} and L from mass spectra, the contribution of nonspecific binding to the mass spectra of protein and specific protein-ligand complexes can be measured. The true abundance (specific binding) of a given PL_q species can be obtained from the apparent (measured directly from the mass spectra) abundance of the PL_q species ($Ab_{app}(PL_q)$) and applying the correction according to the measured distribution of nonspecific $P_{ref}L_q$ species using the following equation:

$$Ab(\mathrm{PL_q}) = [Ab_{app}(\mathrm{PL_q}) - f_{1,\mathrm{Pref}}Ab(\mathrm{PL_{q-1}}) - \ldots f_{q,\mathrm{Pref}}Ab(\mathrm{P})]/f_{0,\mathrm{Pref}} \quad (7)$$

$f_{q,\mathrm{Pref}}$ is the fractional abundance of $\mathrm{P_{ref}}$ bound to q molecules of L. This widely tested method can be applied to correct nonspecific binding for some ligands such as amino acids, peptides, neutral and charged carbohydrates and divalent metal ions[52].

1.4.3 In-source dissociation

The Relative abundance of PL and P ions can be changed due to collision-induced dissociation (CID) of the gaseous complexes (PL) in the ion source. As a result the K_a value will decrease. False negative results occur in the case that all PL complex ions break down. If the R value changes as result of a change in ion source parameters, especially those parameters which influence the internal energy of ions such as voltage differences in high pressure regions, this indicates the occurrence of ion-source dissociation.

Conditions such as short accumulation times within external rf multiple storage devices (e.g. hexapole), low potentials across lens elements and low temperatures (sampling capillary, drying gas) are necessary to determine a reliable K_a value in the cases where PL complexes are prone to in-source dissociation. However, these conditions can lead to reduced signal intensities. So a balance must be kept to have sufficient protein ion signal and at the same time minimize in-source dissociation[45]. It is known that addition of small organic molecules such as imidazole to the ESI solution helps in minimizing the in-source

dissociation. There are some reasons for the stabilizing effect of imidazole: First, dissociation of nonspecific imidazole adducts from the gaseous PL ions can lead to improved evaporative cooling[53]. Secondly, imidazole has a relatively high gas phase basicity that causes the protein complex ions to obtain fewer charges[54]. Finally, using imidazole vapor in the ion source can protect complexes from in-source dissociation[55]. Even though these methods have been shown to be useful, the detection of very labile gas phase complexes by ESI remains challenging.

In the case that protein-ligand complexes are highly labile a competitive ESI-MS binding assay can be used[56]. In this assay, direct ESI along with a reference ligand (L_{ref}) is used. A suitable L_{ref} should have specific binding to P with a known binding affinity and forms a stable protein-ligand complex in the gas phase. The fraction of P that binds to $L_{ref,}$ is stable in the gas phase and can be obtained by direct ESI mass spectrum. This fraction is sensitive to the fraction of P that binds to L in solution and is unstable in the gas phase. Considering this assumption, the affinity of P for L can be determined.

1.4.4 ESI-induced changes in solution pH and temperature

It is known that the ESI technique itself may induce changes in the conformation of protein and the protein-ligand complexes, leading to errors in the measured K_a values. Changes in the pH and temperature of the solution during ESI-MS measurement impact the measured K_a value. The change in pH is more prominent in low solution flow rates (<100 nL/min)[57]. Two strategies have been

suggested to minimize changes in the solution pH. Using solutions with a high buffer capacity and spraying in short times (<10 min) can minimize pH changes. In most commercial ESI sources the droplets are heated (By N_2 or heated air) to speed up desolvation of ions to achieve better sensitivity. This can change the temperature by a few degrees. Overall, for reporting binding data, the solution temperature should be determined under standard operating conditions and be reported[45].

A brief description of SPR spectroscopy, another instrument used in the present work, is given in the next section. This follows by an introduction to antibodies and nanodisc (ND) as a synthetic membrane model, the molecules used in the present work.

1.5 Surface plasmon resonance (SPR)

SPR spectroscopy is an optical method for monitoring biomolecular interaction in solution. When a beam of light passes from a media with a high refractive index (e.g. glass) into the media with a low refractive index (e.g. water), the light will be refracted and or will be reflected at the boundary surface. In the case that the propagating light strikes the boundary in an angle greater than the critical angle, the light cannot pass through and is completely reflected. If the glass surface is coated with a thin layer of a noble metal (e.g. gold), the light is not completely reflected. Some of the light interacts with the electrons on the surface of the metal film and as a result the reflected light intensity decreases. There is an angle in which the loss of the reflected light intensity is greatest. This angle is called SPR angle. Surface plasmon is the oscillation of mobile electrons at the surface of the metal film[58]. When the energy of the photon of the incident light matches the quantum energy level of surface plasmon, the electrons at the metal surface resonate that is called SPR. These oscillating electrons generate an evanescent electromagnetic field in the opposite direction of the radiated light. This evanescent wave penetrates approximately 300 nm into the medium away from the metallic film surface[59].

Changes in refractive index of this medium due to analyte binding to the ligand on the surface of the metal plate cause the change in resonance frequency of the surface plasma wave and thus a shift in SPR angle. The change in the angle

is defined by resonance units or response units (RUs). A shift of 10^{-4} degrees equals to 1 RU[60].

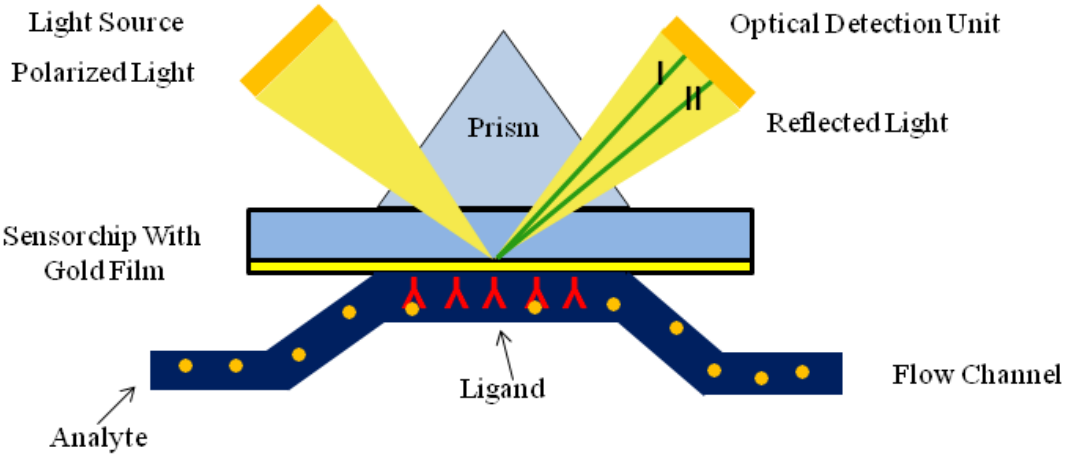

Figure 1.6 Principal of SPR detection, the figure adapted from Biacore sensor surface handbook.

In SPR instruments refractive index near the surface of a sensor chip (Biacore Instruments) is measured in the evanescent field area. To investigate the interaction between two molecules, one molecule (the ligand) is immobilized on the surface of the sensor chip and the binding partner (the analyte) flows over the sensor chip surface in aqueous solution (the sample buffer). Binding of the analyte to ligand induces changes in the refractive index at the surface of the sensor chip. These changes are measured in real time and the results are depicted as a sensorgram. A typical sensorgram is shown in figure 1.7. A sensorgram

contains kinetic information such as the association rate constant, dissociation rate constant and the equilibrium state.

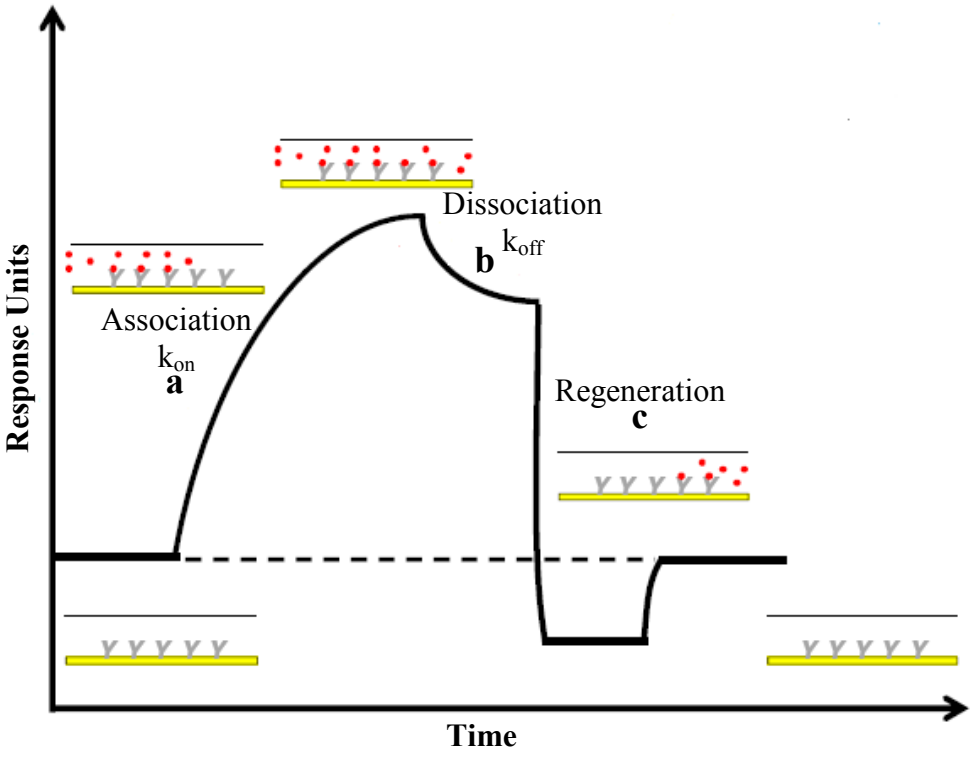

Figure 1.7 Schematic illustration of a typical sensorgram: a) injection of analyte molecules into the flow cell, b) removal of analyte molecules from the surface by continuous flow of running buffer, c) surface regeneration by washing off the analyte molecues, the figure adapted from reference[60].

1.6 Sensor chips

Generally sensor chips in SPR are glass slides in which one side of it is coated with a thin layer of an inert metal (e.g. gold). In SPR machines, sensor chip surfaces with different matrices are used according to the requirements of the

experiment[61]. CM5 sensor chip is a general-purpose and most versatile chip that is appropriate for immobilization of a wide variety of ligands. As CM5 sensor chip has been used in the presented work, a brief description of this sensor chip has been provided below.

1.6.1 CM5 sensor chip

The matrix of the CM5 sensor chip is carboxymethylated dextran that is covalently attached to a gold surface. The ligand is covalently coupled to the carboxyl moieties on the dextran. Ligands with functional groups such as NH2, SH, CHO and COOH can be used[62].

1.7 Experimental cycle

Each experimental cycle in a typical SPR experiment can be divided into several steps:

1.7.1 Immobilization: The first step is the immobilization of the ligand on the sensor chip surface without disrupting the ligand's activity. The immobilization can be done by covalent coupling which is permanent or by capturing which is transient.

1.7.2 Association: In the association step the analyte is passed over the sensor chip surface and binds to the ligand. Simultaneous association and dissociation happens.

1.7.3 Steady state: In the steady state the net rate of binding is zero since the analyte is added and removed from the surface at the same rate.

1.7.4 Dissociation: At the end of the injection of the analyte, the solution flowing over the surface of the sensor chip is changed to the flow buffer which does not contain analyte. Hence, the analyte-ligand complex will begin to dissociate. In an ideal condition, only dissociation should happen. However, some re-binding may occur.

1.7.5 Regeneration: The goal of regeneration is to remove all the noncovalently bound analyte while keeping the ligand active on the sensor chip surface. A common regeneration solution is a buffer with low pH such as 10 mM Glycine pH 1.5-2.5 [63].

1.8 Kinetic analysis with SPR

One application of SPR is the analysis of binding kinetics. A number of kinetic models are applied to the SPR data. By fitting the SPR data to an appropriate binding model, kinetic parameters can be obtained. It is always recommended to begin with the simplest fitting model, that is 1:1 Langmuir model[64]. In Langmuir model one ligand molecule interacts with one analyte molecule. The following equation is applied for this model:

$$A + B \underset{K_{off}}{\overset{K_{on}}{\rightleftharpoons}} AB \qquad (8)$$

where A is the analyte and B represent the ligand. K_{on} is the association rate constant and K_{off} is the dissociation rate constant. This model is based on the assumption that the analyte is monovalent and the solution is homogeneous and contributes to independent binding events.

Another model that is used in the present work is a bivalent model. In this case an analyte has two identical binding sites for the ligand. The following equation is applied for this model:

$$2B + A \underset{K_{off1}}{\overset{K_{on1}}{\rightleftharpoons}} BA + B \underset{K_{off2}}{\overset{K_{on2}}{\rightleftharpoons}} B_2A \qquad (9)$$

where K_{on1} and K_{off1} are the first association and dissociation binding constants, while the second association and dissociation binding constants are described as K_{on2} and K_{off2} respectively.

1.9 Antibodies

Antibodies are glycoproteins with high molecular weight in the range of 150 to 1000 kDa. They are produced by the immune system to fight infections and are known as immunoglobulins (Ig). The amount of antibodies in normal serum is about 10^{16} molecules per milliliter[65] .

1.9.1 Antibody structure

Each antibody has a unique structure that allows it to bind specifically to a specific antigen target, but overall, antibody structures are similar. The basic

structure of antibodies consists of four polypeptide chains, two identical heavy chains and two identical light chains that form a Y shape[66]. Each chain of antibody is made of structural domains that are known as immunoglobulin domains. Light chain has two domains, while heavy chain has three to four domains depending on the type of antibody[67]. One heavy chain and one light chain pairs with each other. The chains are held together by noncovalent interactions and covalent disulfide bonds[67].

Each chain consists of two regions: a variable region and a constant region. The variable region (V) is the tip of the arm of the Y-shaped unit of the antibody. The arms of the antibody contain one variable and one constant domain from each chain and is called fragment of antigen-binding (Fab). The tail of the Y-shaped unit is a constant region (C) and does not bind with any antigens. It is named the fragment crystallizable (FC) because it crystallizes during storage under cold temperatures. The FC part is made of heavy chains and is responsible for the antibody's biological activity. For example it can bind to effector proteins such as FC receptors and initiate effector functions[67]. The Fab and Fc part of antibody are linked together by a flexible region called a hinge region.

In the V regions of heavy and light chains there are sequences of amino acids that vary from one antibody to another. These regions are called complementary-determining regions (CDRs) or the hypervariable regions. Moving from the top ends of the Y arms of an antibody to the variable domains, there are three variable regions in the heavy and light chains that are called CDR1

, CDR2 and CDR3 respectively.The amino acid sequences between CDRs are conserved and make up the framework residues. The V regions in Heavy and light chains fold in such a way that the CDRs form a cleft that makes up the antigen-binding sites.

Antibodies can be divided into five groups according to the heavy chain differences and the number of Y units in each antibody: IgG, IgA, IgD, IgE and IgM with heavy chains ɤ, α, δ , ε and μ in Greek letters respectively[68]. According to small differences in polypeptide structure, light chains can be divided into a kappa or lambda type. The structure of IgG will be discussed in more details below, as it is the antibody of choice for this thesis.

1.9.1.1 IgG structure

IgG is the most abundant antibody in serum, comprising about 75% of the antibodies in human serum[69]. IgG has four subclasses based on differences in the length of the hinge region and the number of disulfide bonds in the molecule. IgG subclasses are indicated as IgG1, IgG2a, IgG2b, IgG3 and IgG4 and they have two, four, five and two disulfide respectively that binds the two heavy chains. Their numbering is in accordance to their concentrations in serum. Shown in figure 1.8 the general structure of an IgG1 molecule.

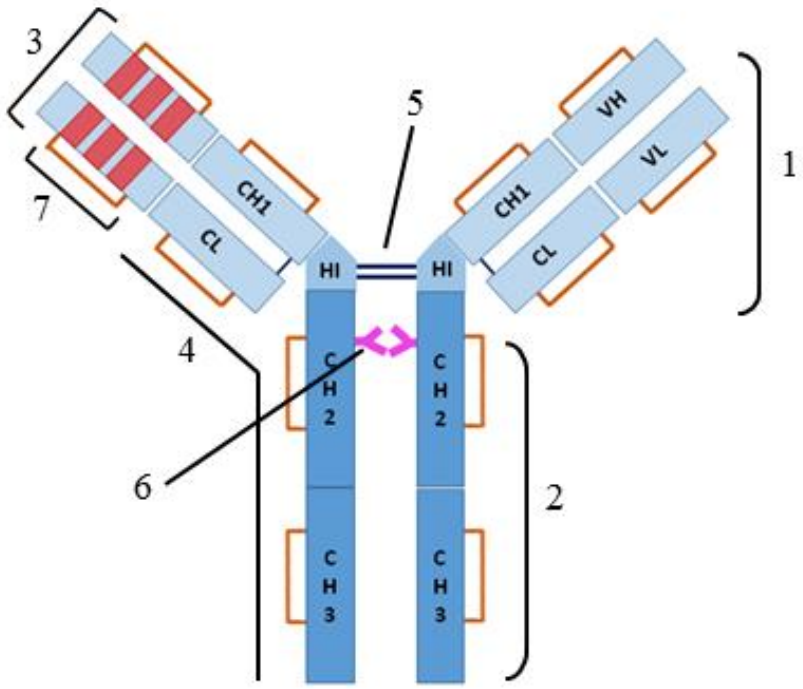

Figure 1.8 Structure of an IgG1 antibody, adapted from reference[70].

1- Fab Region (Antigen binding fragment)

2-Fc Region (Crystalline fargment)

3- Antigen binding site (Variable region)

4- Constant region

5- Hinge regions

6- Glycan

7- CDR

The constant region of the heavy chain of IgG contains three domains (CH1, CH2 and CH3). The hinge parts are located between the first and second constant domain. CH3 domain of each heavy chain is held together through non-covalent bonds[71].

Of the total mass of IgGs, about 2% is related to glycans. These carbohydrates are located at the second domain of each heavy chain (CH2) on Asn^{297} amino acid[72]. In some IgG molecules there is another glycosylation site located at their variable domain[73]. The structure of the glycan on the variable domain is different from those in the constant domain and contains higher amount of sialylated structure and more galactose molecules[74].

1.9.2 Antibody-antigen interaction

The strength of bonding between the Fab portion of antibody and antigen is referred to as affinity. All the bonds that are involved in the formation of the antibody-antigen complex are non-covalent in nature and thus, reversible. These bonding interactions include: van der Waals forces, hydrogen bonds, hydrophobic bonds and electrostatic bonds. However, the initial attraction between antibody and antigen occurs through hydrophobic and ionic forces. Native MS can be used for measuring the binding constants between antibody and its antigen.

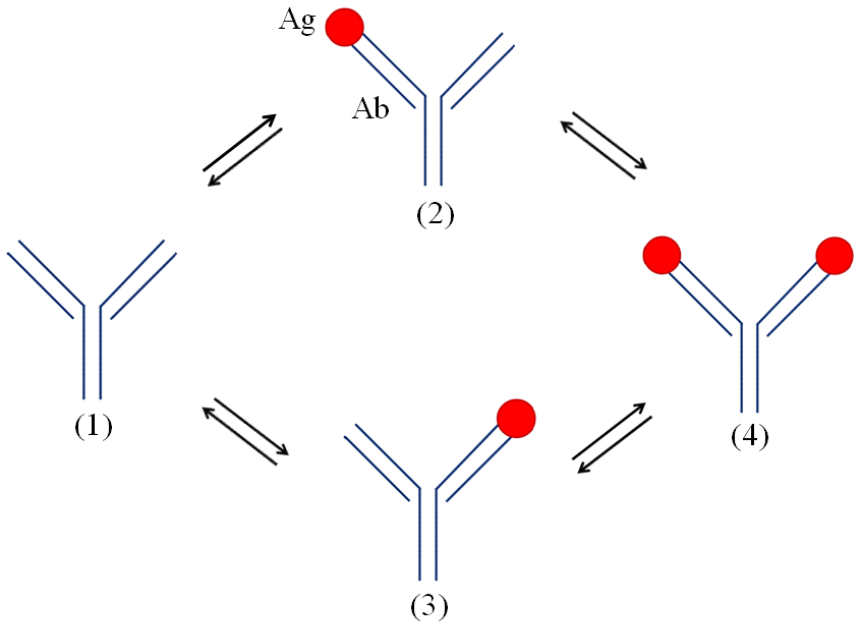

Figure 1.9 Antigen-antibody interaction. The two binding sites are equivalent and Ab (1) can bind to the second Ag molecule through intermediates (2) and (3). The figures depicted in reference[75].

Other techniques such as SPR spectroscopy, size exclusion chromatography (SEC), analytical ultracentrifugation and isothermal calorimetry (ITC) have also been used to determine antibody-antigen interactions. While these techniques provide us with the average binding data, native MS can measure relative abundance of free, singly bound and doubly bound antibodies[71].

Another consideration comes from the fact that the flexibility in the FC part has an effect on antibody-antigen interaction; as such different methods can provide different binding stoichiometry of antibodies depending on the amount of free antibody in solution or immobilized on surface[76].

$$Ab + Ag \rightleftharpoons Ab\text{-}Ag \qquad Ab\text{-}Ag + Ag \rightleftharpoons Ab\text{-}Ag_2 \qquad (10)$$

Affinity between antibody and antigen can be affected by some factors such as pH, temperature and ionic strength.

1.9.3 Polyclonal and monoclonal antibodies

One of the vital responses of the immune system against invading pathogens, viruses and other foreign particles is the production of antibodies. When macrophages, dendritic cells and certain B cells engulf and break down antigens to smaller peptides, these peptides are then displayed on their surfaces by complexing with major histocompatibility complex II (MHC II). T cells then interact and stimulate B cells for antibody production. However activation generally involves multiple B cells presenting different epitope of that specific antigen. As a result, a large number of antibodies are produced with broad range of specificities and epitope affinities. These are known as polyclonal antibodies.

Polyclonal antibodies are extensively used in research and disease diagnosis due to its good detection of multiple epitopes and cost-effective production. Due to its heterogeneity, polyclonal antibodies exhibit a high degree of false positives and cross-reactivity that impede its use[77]. On the other hand, monoclonal antibody which is produced from a single antibody-producing B cell significantly eliminates the pitfalls experience in polyclonal antibodies. These antibodies recognize a specific epitope of an antigen however it is more expensive

due to sophisticated equipment and highly trained personnel required for its production. Monoclonal antibodies are produced by isolating a B cell from spleen and lymph nodes of an immunized animal. Due to the short life span of B cells, they are fused to immortal heteromyleoma cells for long term storage and production. These fused cells are known as hybrodimas[78].

1.9.4 Posttranslational modification

After production of antibodies some posttranslational modifications occurs on the molecules, makes monoclonal antibodies a heterogeneous mixture of isoforms and analysis of the intact antibody challenging. A few examples of these modifications include:

- Glycosylation[79]
- Cleavage of C-terminal lysine residue of the heavy chain[80]
- Conversion of n-terminal glutamine residue to pyroglutamic acid (cyclization) of the heavy chain[81].
- Oxidation
- Deamidation
- Disulfide bond scrambling

1.9.5 Glycans in antibody

One of the most common posttranslational modifications on antibodies is glycosylation. Carbohydrate groups attaches to Fc region of antibody by covalent

binding. While different glycosylation profile on Fc region can lead to different biological activities and influence the structure of antibody[79], glycosylation on the Fab part can have effect on binding affinity of antibody[82]. In biopharma research, characterization of glycans is of utmost importance.

1.9.6 Cross-reactivity

Cross-reactivity is defined to situations in which an antibody binds to antigens that are not specific for the antibody. This occurs when the binding sites of the antigens are similar to each other or low specificity of antibody. Cross-reactivity is an important issue when using antibodies in drug industry. The term cross-species cross-reactivity is applied when human antibody has affinity to antigens from other species.

1.9.7 Studying antibodies by mass spectrometry

The first step in studying antibodies with MS is sample preparation. The type of the prepared sample, intact antibody or fragmented antibody, involves two main approaches:

1.9.7.1 Top-down approach

The top-down method deals with intact or reduced antibody (half antibody fragment) and take advantages of reduced analysis time as it does not require protein digestion[83].Using this method, we can obtain information such as

molecular weight of antibody, charge state distribution, stoichiometry of binding, affinity measurements, specificity, conformation[84] , stability, glycosylation and quality control[85].

In the top-down approach, intact antibody can be characterized either by native or denature conditions depending on the aim of the experiment. In denature condition, information regarding stability[86], different glycoforms[87], covalent dimerisation[88], modification and different isoforms[89] of antibody can be obtained. Native conditions can be used to gain data related to antibody antigen interaction[76], aggregation and oligomerisation status[90] and conformational changes[91] in antibodies.

1.9.7.2 Bottom-up approach

This method requires digestion of protein into small peptides (enzymatically or chemically) before MS or tandem MS analysis. Amino acid sequence[92], covalent interactions in antibody structure such as covalent disulfide linkages and covalently attached oligosaccharide groups [93], analysis of glycosylation profile[94], conformational changes[95] and local dynamics[96] of antibodies are information that can be obtained by this approach. However, it is probable that artifacts are introduced in the antibody sample due to multistep and long preparation protocols.

1.10 Nanodiscs

A wide range of biochemical processes occur via receptors on the surface of cell membrane such as membrane proteins and glycolipids. Many of these interactions require specific lipid composition of the membrane to act efficiently; so finding a model to mimic membrane environment is essential for elucidating these interactions and discovering new pharmaceutical targets. A wide variety of model membranes have been developed such as bicelles and micelles which have their own advantages and limitations.

A new technology for studying biophysical processes and biomolecular interaction on the cell surface is the nanodisc (ND). NDs are composed of non-covalent assembly of phospholipid bilayer confined by two copies of the membrane scaffold protein (MSP) of defined and controllable size; so the size of ND is determined by the length of the MSP and the size distribution is monodisperse and reproducible[97]. The typical diameter of ND is between 9 to 17 nm[98]. The presence of the protein make ND soluble in aqueous solutions (in millimolar range) and stable over time[99]. In addition, by modification of the MSP with various tags, NDs can be immobilized for use in different assays.

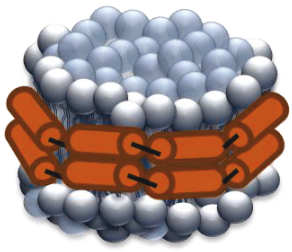

Figure 1.10 Structure of nanodisc

The first attempt for using ND as a membrane model was done in the Sligar lab by incorporating N-terminally anchored cytochrome P450 monoxygenase (P450)[100] and bacteriorhodopsin[101]. Later in 2006, NDs were used for incorporation of bacterial chemoreceptor dimmers to investigate their activities regarding binding ligand and performing transmembrane signaling[102]. Since then, many researchers have performed incorporation of different cell membrane receptors into ND to investigate their biophysical and biochemical activities, including ligand binding behavior[103], influence of surrounding phospholipids in binding activities[104], effect of oligomerization state of incorporated protein in binding activities[105], lipid-protein interactions[106] and proton-coupled electron-transfer reactions[107].

1.10.1 Synthesis of nanodiscs

For making ND, a precise ratio of MSP, phospholipids and a detergent such as sodium cholate are mixed together. The self-assembly process initiates by gentle removal of the detergent by dialysis or using biobeads at the phase transition temperature of the lipid[99]. This creates a discoidal phospholipid bilayer that has its hydrophobic alkyl chains surrounded by the MSP. An optimal lipid to MSP ratio is essential for proper formation of ND. After removing of the detergent, the synthesized NDs are purified by size exclusion chromatography to eliminate any excess proteins or lipids.

1.11 The present work

This thesis focuses on the study of protein-carbohydrate interaction and the application of direct ESI assay and SPR spectroscopy for measuring the noncovalent protein-carbohydrate binding constant.

The work described in chapter two focuses on antibody-antigen interactions and developing a direct ESI-MS binding assay for the protein (anti-GD2 antibody) with two noncovalent binding sites. ESI-MS experiments were performed under both negative and positive ion modes to confirm the consistency of the results in both polarity modes. The effect of cone voltage on the binding constant of antibody-antigen complex was investigated. Immunoglobulin G (IgG) antibodies from healthy human serum and mouse serum was sprayed with soluble GD2 to investigate the existence of the complex. Formation of the complex was identified for both human and mouse IgGs with ESI-MS and tandem mass. The antibody cross- reactivity was tested with a few carbohydrate sugars.

In another experiment CS-35 monoclonal antibody was run against Hexa-Arabinofuranoside (H-Araf) sugar to obtain a binding constant with the new developed assay. However, this antibody was very heterogeneous and formation of the complex was only detectable by tandem mass. Deglycosylation was performed on the antibody to reduce the heterogeneity induced by the glycans. Even deglycosylation did not have significant effect on reducing heterogeneity of the antibody. Probably the source of heterogeneity came from the method and experimental condition used for the expression of the antibody.

Chapter three describes measuring protein-carbohydrate binding constants using SPR and ND as a membrane model to investigate the difference in toxicity between Shiga toxin type 1 and 2. Also incorporation of fatty acids with different carbon chain length into ND was investigated. The aim of this project was to find the best fatty acid for the ND and attach it to the synthetic sugars provided by Bundle group. Using SPR, the interaction between cholera toxin and GM1-ND on the surface of CM5 and NTA sensor chip reproduced the results from the Borch *et al.* paper [108]. The interaction between Gb3-ND and shiga toxin was investigated on the surface of a CM5 sensor chip. Further investigation on Gb3-ND was performed to determine the incorporation of Gb3 into the ND. Also ND with different phospholipids or mixtures of phospholipids was made to incorporate Gb3 into it. In another experiment GM3-ND and GD1b-ND were made; MS was used to confirm incorporation of the gangliosides into ND. Different proteins as analytes were examined in this experiment. GD1b-ND was used as negative control.

1.12 Literature cited

1. Norris, A. J.; Whitelegge, J. P.; Faull, K. F.; Toyokuni, T., Analysis of enzyme kinetics using electrospray ionization mass spectrometry and multiple reaction monitoring: Fucosyltransferase V. *Biochemistry* **2001,** *40* (13), 3774-3779.
2. Kapur, A.; Beck, J. L.; Sheil, M. M., Observation of daunomycin and nogalamycin complexes with duplex DNA using electrospray ionisation mass spectrometry. *Rapid Communications in mMass Spectrometry* **1999,** *13* (24), 2489-2497.
3. De Dominicis, E.; Commissati, I.; Suman, M., Targeted screening of pesticides, veterinary drugs and mycotoxins in bakery ingredients and food commodities by liquid chromatography-high-resolution single-stage Orbitrap mass spectrometry. *Journal of Mass Spectrometry* **2012,** *47* (9), 1232-1241.
4. Trauger, S. A.; Webb, W.; Siuzdak, G., Peptide and protein analysis with mass spectrometry. *Journal of Spectroscopy* **2002,** *16* (1), 15-28.
5. Hernández, F.; Portolés, T.; Pitarch, E.; López, F. J., Gas chromatography coupled to high-resolution time-of-flight mass spectrometry to analyze trace-level organic compounds in the environment, food safety and toxicology. *TrAC Trends in Analytical Chemistry* **2011,** *30* (2), 388-400.
6. Cubrilovic, D.; Biela, A.; Sielaff, F.; Steinmetzer, T.; Klebe, G.; Zenobi, R., Quantifying protein-ligand binding constants using electrospray

ionization mass spectrometry: a systematic binding affinity study of a series of hydrophobically modified trypsin inhibitors. *Journal of the American Society for Mass Spectrometry* **2012,** *23* (10), 1768-1777.

7. Xu, Y.; Falk, I. N.; Hallen, M. A.; Fitzgerald, M. C., Mass spectrometry- and lysine amidination-based protocol for thermodynamic analysis of protein folding and ligand binding interactions. *Analytical Chemistry* **2011,** *83* (9), 3555-3562.

8. Ohtsubo, K.; Marth, J. D., Glycosylation in cellular mechanisms of health and disease. *Cell* **2006,** *126* (5), 855-867.

9. Kakehi, K.; Oda, Y.; Kinoshita, M., Fluorescence polarization: analysis of carbohydrate–protein interaction. *Analytical Biochemistry* **2001,** *297* (2), 111-116.

10. Bundle, D. R.; Sigurskjold, B. W., Determination of accurate thermodynamics of binding by titration microcalorimetry. *Methods in Enzymology* **1994,** *247*, 288.

11. Smith, E. A.; Thomas, W. D.; Kiessling, L. L.; Corn, R. M., Surface plasmon resonance imaging studies of protein-carbohydrate interactions. *Journal of the American Chemical Society* **2003,** *125* (20), 6140-6148.

12. Chiodo, F.; Marradi, M.; Tefsen, B.; Snippe, H.; van Die, I.; Penadés, S., High sensitive detection of carbohydrate binding proteins in an ELISA-solid phase assay based on multivalent glyconanoparticles. *PLoS One* **2013,** *8* (8), e73027.

13. del Carmen Fernández-Alonso, M.; Díaz, D.; Berbis, M. Á.; Marcelo, F.; Cañada, J.; Jiménez-Barbero, J., Protein-carbohydrate interactions studied by NMR: from molecular recognition to drug design. *Current Protein & Peptide Science* **2012,** *13* (8), 816.

14. Wilcox, J. M.; Rempel, D. L.; Gross, M. L., Method of measuring oligonucleotide-metal affinities: Interactions of the thrombin binding aptamer with K+ and Sr2+. *Analytical Chemistry* **2008,** *80* (7), 2365-2371.

15. Oshannessy, D. J.; Brighamburke, M.; Soneson, K.; Hensley, P.; Brooks, I., Determination of rate and equilibrium binding constants for macromolecular interactions using surface plasmon resonance: use of nonlinear least squares analysis methods. *Analytical Biochemistry* **1993,** *212* (2), 457-468.

16. Jecklin, M. C.; Schauer, S.; Dumelin, C. E.; Zenobi, R., Label-free determination of protein–ligand binding constants using mass spectrometry and validation using surface plasmon resonance and isothermal titration calorimetry. *Journal of Molecular Recognition* **2009,** *22* (4), 319-329.

17. Larsen, K.; Thygesen, M. B.; Guillaumie, F.; Willats, W. G.; Jensen, K. J., Solid-phase chemical tools for glycobiology. *Carbohydrate Research* **2006,** *341* (10), 1209-1234.

18. Wishart, D., NMR spectroscopy and protein structure determination: applications to drug discovery and development. *Current Pharmaceutical Piotechnology* **2005,** *6* (2), 105-120.

19. Collie, J. N.; Patterson, H. S., On the Appearance of Helium and Neon in Vacuum Tubes. *Nature* **1913,** *90*, 699.

20. Fenn, J. B.; Mann, M.; Meng, C. K.; Wong, S. F.; Whitehouse, C. M., Electrospray ionization for mass spectrometry of large biomolecules. *Science* **1989,** *246* (4926), 64-71.

21. Kitova, E. N.; Kitov, P. I.; Bundle, D. R.; Klassen, J. S., The observation of multivalent complexes of Shiga-like toxin with globotriaoside and the determination of their stoichiometry by nanoelectrospray Fourier-transform ion cyclotron resonance mass spectrometry. *Glycobiology* **2001,** *11* (7), 605-611.

22. St. Hilaire, P. M.; Boyd, M. K.; Toone, E. J., Interaction of the Shiga-like toxin type 1 B-subunit with its carbohydrate receptor. *Biochemistry* **1994,** *33* (48), 14452-14463.

23. (a) Shoemaker, G. K.; Soya, N.; Palcic, M. M.; Klassen, J. S., Temperature-dependent cooperativity in donor–acceptor substrate binding to the human blood group glycosyltransferases. *Glycobiology* **2008,** *18* (8), 587-592; (b) ávan Dongen, W. D.; Albert, J., Binding of selected carbohydrates to apo-concanavalin A studied by electrospray ionization mass spectrometry. *Analyst* **2000,** *125* (4), 583-589.

24. Zeleny, J., The electrical discharge from liquid points, and a hydrostatic method of measuring the electric intensity at their surfaces. *Physical Review* **1914,** *3* (2), 69.

25. Kebarle, P.; Verkerk, U. H., Electrospray: from ions in solution to ions in the gas phase, what we know now. *Mass Spectrometry Reviews* **2009,** *28* (6), 898-917.

26. Cloupeau, M.; Prunet-Foch, B., Electrostatic spraying of liquids: main functioning modes. *Journal of Electrostatics* **1990,** *25* (2), 165-184.

27. Kebarle, P.; Tang, L., From ions in solution to ions in the gas phase-the mechanism of electrospray mass spectrometry. *Analytical Chemistry* **1993,** *65* (22), 972A-986A.

28. Wilm, M. S.; Mann, M., Electrospray and Taylor-Cone theory, Dole's beam of macromolecules at last? *International Journal of Mass Spectrometry and Ion Processes* **1994,** *136* (2), 167-180.

29. Dole, M.; Mack, L.; Hines, R.; Mobley, R.; Ferguson, L.; Alice, M. d., Molecular beams of macroions. *The Journal of Chemical Physics* **1968,** *49* (5), 2240-2249.

30. Banerjee, S.; Mazumdar, S., Electrospray ionization mass spectrometry: a technique to access the information beyond the molecular weight of the analyte. *International Journal of Analytical Chemistry* **2012,** *2012*.

31. Iribarne, J.; Thomson, B., On the evaporation of small ions from charged droplets. *The Journal of Chemical Physics* **1976,** *64* (6), 2287-2294.

32. Labowsky, M.; Fenn, J.; de la Mora, J. F., A continuum model for ion evaporation from a drop: effect of curvature and charge on ion solvation energy. *Analytica Chimica Acta* **2000,** *406* (1), 105-118.

33. Jecklin, M. C.; Touboul, D.; Bovet, C.; Wortmann, A.; Zenobi, R., Which electrospray-based ionization method best reflects protein-ligand interactions found in solution? A comparison of ESI, nanoESI, and ESSI for the determination of dissociation constants with mass spectrometry. *Journal of the American Society for Mass Spectrometry* **2008,** *19* (3), 332-343.

34. Pacholarz, K. J.; Garlish, R. A.; Taylor, R. J.; Barran, P. E., Mass spectrometry based tools to investigate protein–ligand interactions for drug discovery. *Chemical Society Reviews* **2012,** *41* (11), 4335-4355.

35. Joensson, H. N.; Samuels, M. L.; Brouzes, E. R.; Medkova, M.; Uhlén, M.; Link, D. R.; Andersson-Svahn, H., Detection and Analysis of Low-Abundance Cell-Surface Biomarkers Using Enzymatic Amplification in Microfluidic Droplets. *Angewandte Chemie International Edition* **2009,** *48* (14), 2518-2521.

36. Wilm, M.; Mann, M., Analytical properties of the nanoelectrospray ion source. *Analytical Chemistry* **1996,** *68* (1), 1-8.

37. Bahr, U.; Pfenninger, A.; Karas, M.; Stahl, B., High-sensitivity analysis of neutral underivatized oligosaccharides by nanoelectrospray mass spectrometry. *Analytical Chemistry* **1997,** *69* (22), 4530-4535.

38. Karas, M.; Bahr, U.; Dülcks, T., Nano-electrospray ionization mass spectrometry: addressing analytical problems beyond routine. *Fresenius' Journal of Analytical Chemistry* **2000,** *366* (6-7), 669-676.

39. Gobom, J.; Nordhoff, E.; Mirgorodskaya, E.; Ekman, R.; Roepstorff, P., Sample purification and preparation technique based on nano-scale reversed-phase columns for the sensitive analysis of complex peptide mixtures by matrix-assisted laser desorption/ionization mass spectrometry. *Journal of Mass Spectrometry* **1999,** *34* (2), 105-116.

40. Ho, C.; Lam, C.; Chan, M.; Cheung, R.; Law, L.; Lit, L.; Ng, K.; Suen, M.; Tai, H., Electrospray ionisation mass spectrometry: principles and clinical applications. *The Clinical Biochemist Reviews* **2003,** *24* (1), 3.

41. Watson, J. T.; Sparkman, O. D., *Introduction to mass spectrometry: instrumentation, applications, and strategies for data interpretation*. *John Wiley & Sons*: 2007.

42. Morris, M., Future paths of mass spectrometry in routine clinical chemistry. *Clinica Chimica Acta* **2010,** *411* (11), 905-906.

43. Mamyrin, B.; Shmikk, D., Linear mass reflectron. *Zh. Eksp. Teor. Fiz* **1979,** *76*, 1500-1505.

44. Clauser, K. R.; Baker, P.; Burlingame, A. L., Role of accurate mass measurement (±10 ppm) in protein identification strategies employing MS or MS/MS and database searching. *Analytical Chemistry* **1999,** *71* (14), 2871-2882.

45. Kitova, E. N.; El-Hawiet, A.; Schnier, P. D.; Klassen, J. S., Reliable determinations of protein–ligand interactions by direct ESI-MS measurements. Are we there yet? *Journal of the American Society for Mass Spectrometry* **2012,** *23* (3), 431-441.

46. Ganem, B.; Henion, J. D., Going gently into flight: analyzing noncovalent interactions by mass spectrometry. *Bioorganic & Medicinal Chemistry* **2003,** *11* (3), 311-314.

47. Kitova, E. N.; Kitov, P. I.; Paszkiewicz, E.; Kim, J.; Mulvey, G. L.; Armstrong, G. D.; Bundle, D. R.; Klassen, J. S., Affinities of Shiga toxins 1 and 2 for univalent and oligovalent Pk-trisaccharide analogs measured by electrospray ionization mass spectrometry. *Glycobiology* **2007,** *17* (10), 1127-1137.

48. Gross, J.; Xavier, A.; Gross, M. In *RNA Neomycin Complexes Analyzed by Electrospray and UV-MALDI-MS*, Papers, *49th ASMS Conference on Mass Spectrometry and Allied Topics*, 2001.

49. Gabelica, V.; Galic, N.; Rosu, F.; Houssier, C.; De Pauw, E., Influence of response factors on determining equilibrium association constants of non-covalent complexes by electrospray ionization mass spectrometry. *Journal of Mass Spectrometry* **2003,** *38* (5), 491-501.

50. Gabelica, V.; Rosu, F.; De Pauw, E., A simple method to determine electrospray response factors of noncovalent complexes. *Analytical Chemistry* **2009,** *81* (16), 6708-6715.

51. Sun, J.; Kitova, E. N.; Wang, W.; Klassen, J. S., Method for distinguishing specific from nonspecific protein-ligand complexes in nanoelectrospray ionization mass spectrometry. *Analytical Chemistry* **2006,** *78* (9), 3010-3018.

52. Deng, L.; Sun, N.; Kitova, E. N.; Klassen, J. S., Direct Quantification of Protein− Metal Ion Affinities by Electrospray Ionization Mass Spectrometry. *Analytical Chemistry* **2010,** *82* (6), 2170-2174.

53. Sun, J.; Kitova, E. N.; Klassen, J. S., Method for stabilizing protein-ligand complexes in nanoelectrospray ionization mass spectrometry. *Analytical Chemistry* **2007,** *79* (2), 416-425.

54. Taft, R. W.; Anvia, F.; Taagepera, M.; Catalan, J.; Elguero, J., Electrostatic proximity effects in the relative basicities and acidities of pyrazole, imidazole, pyridazine, and pyrimidine. *Journal of the American Chemical Society* **1986,** *108* (12), 3237-3239.

55. Bagal, D.; Kitova, E. N.; Liu, L.; El-Hawiet, A.; Schnier, P. D.; Klassen, J. S., Gas phase stabilization of noncovalent protein complexes formed by electrospray ionization. *Analytical Chemistry* **2009,** *81* (18), 7801-7806.

56. El-Hawiet, A.; Kitova, E. N.; Liu, L.; Klassen, J. S., Quantifying labile protein–ligand interactions using electrospray ionization mass spectrometry. *Journal of the American Society for Mass Spectrometry* **2010,** *21* (11), 1893-1899.

57. Wang, W.; Kitova, E. N.; Klassen, J. S., Influence of solution and gas phase processes on protein-carbohydrate binding affinities determined by nanoelectrospray Fourier transform ion cyclotron resonance mass spectrometry. *Analytical Chemistry* **2003,** *75* (19), 4945-4955.

58. Salamon, Z.; Macleod, H. A.; Tollin, G., Surface plasmon resonance spectroscopy as a tool for investigating the biochemical and biophysical

properties of membrane protein systems. II: Applications to biological systems. *Biochimica et Biophysica Acta (BBA)-Reviews on Biomembranes* **1997,** *1331* (2), 131-152.

59. Van Der Merwe, P. A., Surface plasmon resonance. *Oxford University Press*: New York, NY, USA: 2001; pp 137-170.

60. Patching, S. G., Surface plasmon resonance spectroscopy for characterisation of membrane protein–ligand interactions and its potential for drug discovery. *Biochimica et Biophysica Acta (BBA)-Biomembranes* **2014,** *1838* (1), 43-55.

61. Cooper, M. A.; Hansson, A.; Löfås, S.; Williams, D. H., A vesicle capture sensor chip for kinetic analysis of interactions with membrane-bound receptors. *Analytical Biochemistry* **2000,** *277* (2), 196-205.

62. Drescher, D. G.; Drescher, M. J.; Ramakrishnan, N. A., Surface plasmon resonance (SPR) analysis of binding interactions of proteins in inner-ear sensory epithelia. In *Auditory and Vestibular Research*, Springer: 2009; pp 323-343.

63. Andersson, K.; Areskoug, D.; Hardenborg, E., Exploring buffer space for molecular interactions. *Journal of Molecular Recognition* **1999,** *12* (5), 310-315.

64. Karlsson, R.; Fält, A., Experimental design for kinetic analysis of protein-protein interactions with surface plasmon resonance biosensors. *Journal of Immunological Methods* **1997,** *200* (1), 121-133.

65. Fahey, J. L., Antibodies and Immunoglobulins: II. Normal Development and Changes in Disease. *JAMA* **1965,** *194* (3), 255-258.

66. Harris, L. J.; Larson, S. B.; Hasel, K. W.; Day, J.; Greenwood, A.; McPherson, A., The three-dimensional structure of an intact monoclonal antibody for canine lymphoma. **1992**.

67. Carter, P. J., Potent antibody therapeutics by design. *Nature Reviews Immunology* **2006,** *6* (5), 343-357.

68. Zhang, Z.; Pan, H.; Chen, X., Mass spectrometry for structural characterization of therapeutic antibodies. *Mass spectrometry Reviews* **2009,** *28* (1), 147-176.

69. Schroeder Jr, H. W.; Cavacini, L., Structure and function of immunoglobulins. *Journal of Allergy and Clinical Immunology* **2010,** *125* (2), S41-S52.

70. Beck, A.; Wurch, T.; Bailly, C.; Corvaia, N., Strategies and challenges for the next generation of therapeutic antibodies. *Nature Reviews Immunology* **2010,** *10* (5), 345-352.

71. Thompson, N. J.; Rosati, S.; Rose, R. J.; Heck, A. J., The impact of mass spectrometry on the study of intact antibodies: from post-translational modifications to structural analysis. *Chemical Communications* **2013,** *49* (6), 538-548.

72. Beck, A.; Wagner-Rousset, E.; Bussat, M.-C.; Lokteff, M.; Klinguer-Hamour, C.; Haeuw, J.-F.; Goetsch, L.; Wurch, T.; Dorsselaer, A. V.; Corvaïa, N., Trends in glycosylation, glycoanalysis and glycoengineering

of therapeutic antibodies and Fc-fusion proteins. *Current Pharmaceutical Biotechnology* **2008,** *9* (6), 482-501.

73. Huang, L.; Biolsi, S.; Bales, K. R.; Kuchibhotla, U., Impact of variable domain glycosylation on antibody clearance: an LC/MS characterization. *Analytical Biochemistry* **2006,** *349* (2), 197-207.

74. Wormald, M. R.; Rudd, P. M.; Harvey, D. J.; Chang, S.-C.; Scragg, I. G.; Dwek, R. A., Variations in oligosaccharide-protein interactions in immunoglobulin G determine the site-specific glycosylation profiles and modulate the dynamic motion of the Fc oligosaccharides. *Biochemistry* **1997,** *36* (6), 1370-1380.

75. Oda, M.; Uchiyama, S.; Robinson, C. V.; Fukui, K.; Kobayashi, Y.; Azuma, T., Regional and segmental flexibility of antibodies in interaction with antigens of different size. *FEBS Journal* **2006,** *273* (7), 1476-1487.

76. Oda, M.; Uchiyama, S.; Noda, M.; Nishi, Y.; Koga, M.; Mayanagi, K.; Robinson, C. V.; Fukui, K.; Kobayashi, Y.; Morikawa, K., Effects of antibody affinity and antigen valence on molecular forms of immune complexes. *Molecular Immunology* **2009,** *47* (2), 357-364.

77. Harlow, E.; Lane, D., *Antibodies: a laboratory manual*. Cold Spring Harbor Laboratory Cold Spring Harbor, NY: 1988; Vol. 559.

78. Yokoyama, W. M.; Christensen, M.; Santos, G. D.; Miller, D.; Ho, J.; Wu, T.; Dziegelewski, M.; Neethling, F. A., Production of monoclonal antibodies. *Current Protocols in Immunology* **2006**, 2.5. 1-2.5. 29.

79. Lund, J.; Takahashi, N.; Pound, J. D.; Goodall, M.; Jefferis, R., Multiple interactions of IgG with its core oligosaccharide can modulate recognition by complement and human Fc gamma receptor I and influence the synthesis of its oligosaccharide chains. *The Journal of Immunology* **1996,** *157* (11), 4963-4969.

80. Dick, L. W.; Qiu, D.; Mahon, D.; Adamo, M.; Cheng, K. C., C-terminal lysine variants in fully human monoclonal antibodies: Investigation of test methods and possible causes. *Biotechnology and Bioengineering* **2008,** *100* (6), 1132-1143.

81. Dick, L. W.; Kim, C.; Qiu, D.; Cheng, K. C., Determination of the origin of the N-terminal pyro-glutamate variation in monoclonal antibodies using model peptides. *Biotechnology and Bioengineering* **2007,** *97* (3), 544-553.

82. Kaneko, Y.; Nimmerjahn, F.; Ravetch, J. V., Anti-inflammatory activity of immunoglobulin G resulting from Fc sialylation. *Science* **2006,** *313* (5787), 670-673.

83. Cui, W.; Rohrs, H. W.; Gross, M. L., Top-down mass spectrometry: recent developments, applications and perspectives. *Analyst* **2011,** *136* (19), 3854-3864.

84. Kaltashov, I. A.; Abzalimov, R. R., Do ionic charges in ESI MS provide useful information on macromolecular structure? *Journal of the American Society for Mass Spectrometry* **2008,** *19* (9), 1239-1246.

85. Zamani, L.; Lindholm, J.; Ilag, L. L.; Jacobsson, S. P., Discrimination among IgG1-κ monoclonal antibodies produced by two cell lines using

charge state distributions in nanoESI-TOF mass spectra. *Journal of the American Society for Mass Spectrometry* **2009,** *20* (6), 1030-1036.

86. Dillon, T. M.; Bondarenko, P. V.; Rehder, D. S.; Pipes, G. D.; Kleemann, G. R.; Ricci, M. S., Optimization of a reversed-phase high-performance liquid chromatography/mass spectrometry method for characterizing recombinant antibody heterogeneity and stability. *Journal of Chromatography A* **2006,** *1120* (1), 112-120.

87. Nallet, S.; Fornelli, L.; Schmitt, S.; Parra, J.; Baldi, L.; Tsybin, Y. O.; Wurm, F. M., Glycan variability on a recombinant IgG antibody transiently produced in HEK-293E cells. *New Biotechnology* **2012,** *29* (4), 471-476.

88. Remmele, R. L.; Callahan, W. J.; Krishnan, S.; Zhou, L.; Bondarenko, P. V.; Nichols, A. C.; Kleemann, G. R.; Pipes, G. D.; Park, S.; Fodor, S., Active dimer of Epratuzumab provides insight into the complex nature of an antibody aggregate. *Journal of Pharmaceutical Sciences* **2006,** *95* (1), 126-145.

89. Johnson, K. A.; Paisley-Flango, K.; Tangarone, B. S.; Porter, T. J.; Rouse, J. C., Cation exchange–HPLC and mass spectrometry reveal C-terminal amidation of an IgG1 heavy chain. *Analytical Biochemistry* **2007,** *360* (1), 75-83.

90. Kükrer, B.; Filipe, V.; van Duijn, E.; Kasper, P. T.; Vreeken, R. J.; Heck, A. J.; Jiskoot, W., Mass spectrometric analysis of intact human

monoclonal antibody aggregates fractionated by size-exclusion chromatography. *Pharmaceutical Research* **2010,** *27* (10), 2197-2204.

91. Atmanene, C. agner-Rousset, E. Malissard, M. Chol, B. Robert, A. Corva a, N. Dorsselaer, A. . Beck, A. Sanglier-Cianf rani, S.-. Extending mass spectrometry contribution to therapeutic monoclonal antibody lead optimization: characterization of immune complexes using noncovalent ESI-MS. *Analytical Chemistry* **2009,** *81* (15), 6364-6373.

92. Kaltashov, I. A.; Bobst, C. E.; Abzalimov, R. R.; Wang, G.; Baykal, B.; Wang, S., Advances and challenges in analytical characterization of biotechnology products: mass spectrometry-based approaches to study properties and behavior of protein therapeutics. *Biotechnology Advances* **2012,** *30* (1), 210-222.

93. Chelius, D.; Xiao, G.; Nichols, A. C.; Vizel, A.; He, B.; Dillon, T. M.; Rehder, D. S.; Pipes, G. D.; Kraft, E.; Oroska, A., Automated tryptic digestion procedure for HPLC/MS/MS peptide mapping of immunoglobulin gamma antibodies in pharmaceutics. *Journal of Pharmaceutical and Biomedical Analysis* **2008,** *47* (2), 285-294.

94. Fornelli, L.; Damoc, E.; Thomas, P. M.; Kelleher, N. L.; Aizikov, K.; Denisov, E.; Makarov, A.; Tsybin, Y. O., Analysis of intact monoclonal antibody IgG1 by electron transfer dissociation Orbitrap FTMS. *Molecular & Cellular Proteomics* **2012,** *11* (12), 1758-1767.

95. Houde, D.; Arndt, J.; Domeier, W.; Berkowitz, S.; Engen, J. R., Characterization of IgG1 conformation and conformational dynamics by

hydrogen/deuterium exchange mass spectrometry. *Analytical Chemistry* **2009,** *81* (7), 2644-2651.

96. Manikwar, P.; Majumdar, R.; Hickey, J. M.; Thakkar, S. V.; Samra, H. S.; Sathish, H. A.; Bishop, S. M.; Middaugh, C. R.; Weis, D. D.; Volkin, D. B., Correlating excipient effects on conformational and storage stability of an IgG1 monoclonal antibody with local dynamics as measured by hydrogen/deuterium-exchange mass spectrometry. *Journal of Pharmaceutical Sciences* **2013,** *102* (7), 2136-2151.

97. Nath, A.; Atkins, W. M.; Sligar, S. G., Applications of phospholipid bilayer nanodiscs in the study of membranes and membrane proteins. *Biochemistry* **2007,** *46* (8), 2059-2069.

98. Numata, M.; Grinkova, Y. V.; Mitchell, J. R.; Chu, H. W.; Sligar, S. G.; Voelker, D. R., Nanodiscs as a therapeutic delivery agent: inhibition of respiratory syncytial virus infection in the lung. *International Journal of Nanomedicine* **2013,** *8*, 1417.

99. Denisov, I.; Grinkova, Y.; Lazarides, A.; Sligar, S., Directed self-assembly of monodisperse phospholipid bilayer Nanodiscs with controlled size. *Journal of the American Chemical Society* **2004,** *126* (11), 3477-3487.

100. Civjan, N. R.; Bayburt, T. H.; Schuler, M. A.; Sligar, S. G., Direct solubilization of heterologously expressed membrane proteins by incorporation into nanoscale lipid bilayers. *Biotechniques* **2003,** *35* (3), 556-563.

101. Bayburt, T. H.; Sligar, S. G., Self-assembly of single integral membrane proteins into soluble nanoscale phospholipid bilayers. *Protein Science* **2003,** *12* (11), 2476-2481.

102. Boldog, T.; Grimme, S.; Li, M.; Sligar, S. G.; Hazelbauer, G. L., Nanodiscs separate chemoreceptor oligomeric states and reveal their signaling properties. *Proceedings of the National Academy of Sciences* **2006,** *103* (31), 11509-11514.

103. Nath, A.; Grinkova, Y. V.; Sligar, S. G.; Atkins, W. M., Ligand Binding to Cytochrome P450 3A4 in Phospholipid Bilayer Nanodiscs THE EFFECT OF MODEL MEMBRANES. *Journal of Biological Chemistry* **2007,** *282* (39), 28309-28320.

104. Alami, M.; Dalal, K.; Lelj-Garolla, B.; Sligar, S. G.; Duong, F., Nanodiscs unravel the interaction between the SecYEG channel and its cytosolic partner SecA. *The EMBO Journal* **2007,** *26* (8), 1995-2004.

105. Bayburt, T. H.; Leitz, A. J.; Xie, G.; Oprian, D. D.; Sligar, S. G., Transducin activation by nanoscale lipid bilayers containing one and two rhodopsins. *Journal of Biological Chemistry* **2007,** *282* (20), 14875-14881.

106. Schuler, M. A.; Denisov, I. G.; Sligar, S. G., Nanodiscs as a new tool to examine lipid–protein interactions. In *Lipid-Protein Interactions*, Springer: 2013; pp 415-433.

107. Öjemyr, L. N.; von Ballmoos, C.; Gennis, R. B.; Sligar, S. G.; Brzezinski, P., Reconstitution of respiratory oxidases in membrane nanodiscs for

investigation of proton-coupled electron transfer. *FEBS Letters* **2012,** *586* (5), 640-645.

108. Borch, J.; Torta, F.; Sligar, S. G.; Roepstorff, P., Nanodiscs for immobilization of lipid bilayers and membrane receptors: kinetic analysis of cholera toxin binding to a glycolipid receptor. *Analytical Chemistry* **2008,** *80* (16), 6245-6252.

Chapter 2

Investigation of antibody-antigen interactions using electrospray ionization mass spectrometry

2.1 Introduction

Many biological processes depend on interaction between molecules; so detailed analysis of these interactions is of considerable importance for understanding these processes. One of the most important interactions takes place in the immune system. Knowledge about the biophysical properties of antibody-antigen interaction helps in the elucidation of the biological mechanisms and design of therapeutic monoclonal antibodies against disorders such as cancer[109]. The binding constant is an important quantity that governs protein-ligand interactions and is one of the most important factors in optimization of therapeutic antibodies. Different techniques have been developed to obtain binding constants of antibody-antigen interaction. Here, the two common methods are briefly described.

Equilibrium dialysis is one of the most common methods. In this technique a known concentration of an antibody solution is placed in a dialysis bag with a known concentration of a radiolabeled antigen outside the bag. The antigen should be small enough to be able to pass across the semipermeable dialysis membrane. After equilibrium the concentration of free antigen and antibody-antigen complex is measured[110]. This method is simple and the Ka value

is easy to obtain but is only appropriate for small antigen molecules that are able to diffuse across the dialysis membrane. It also requires the antigen to be labeled with a radioactive isotope.

SPR is another method. In this assay one species (antibody or antigen) is immobilized on the surface of a sensor chip and the other one is flowed over the surface. The change in the mass of the chemicals on the surface of the sensor chip is recorded in real time and from the resultant curves the binding data can be obtained[111]. However in this method, one reactant must be immobilized and this may alter binding affinities. In addition equilibrium dialysis and SPR do not supply detailed information of the relative abundance of unbound and bound antibody. There is a necessity for an alternative method to measure Ka as the current available methods have their limits and shortcomings.

In recent years mass spectrometry (MS) has emerged as a powerful technique for the characterization of therapeutic monoclonal antibody due to development of new MS-based methods. In the past, MS was appropriate only for the study of small molecules. After the introduction of ionization techniques such as matrix-assisted laser desorption ionization (MALDI) and electrospray ionization (ESI), MS has become a complementary approach for studying large, complex biomolecules. Using MS the relative abundance of bound antigen to antibody can be determined; as well as their Ka. In this chapter, we present the use of MS to obtain antibody-antigen interaction Ka values.

Working with antibody molecules for the assay led us to think of MS as a

diagnostic tool for multiple sclerosis by detection of anti-GD2 antibody from multiple sclerosis patients' sera. Multiple sclerosis is a complex disease of the central nervous system (CNS) where the myelin sheaths surrounding the axons are damaged[112]. This leads to a disruption in the nerve cell communication which inherently affects the patient physically, mentally and at times psychologically. Even though there is no cure for multiple sclerosis yet, early diagnosis of the disease can aid in delaying multiple sclerosis progression by consumption of specific drugs[113].

Multiple sclerosis is a difficult disease to diagnose. Neurologists diagnose patients with MS only after various tests along with an in-depth review of the patient's medical history[112]. A single test is not enough of a proof for detecting multiple sclerosis as there are many nerve disorders that share the same symptoms. The most prevalent tests for multiple sclerosis currently are, magnetic resonance imaging (MRI), the spinal tap and evoked potential tests[114]. Using MRI, the damaged inflamed area in the brain or spinal cord can be visualized. 90% of patients that show these neural patterns can be said to have a high chance of being diagnosed with multiple sclerosis. More tests are required in order to truly confirm this diagnosis. Unfortunately, not all people with MS disease are detectable by MRI[114]. In evoked potential tests, wires are placed on the scalp in certain areas of the brain to measure electrical activity and to detect problems along the nerve pathway caused by MS[115]. In spinal tap, a small amount of spinal fluid is removed to test for multiple sclerosis. This test detects glucose levels, the

levels of other different proteins[116] and types of white blood cells or abnormal cells. This test is not specific for multiple sclerosis [117]. Stoop *et al.* used MALDI-TOF mass spectrometer to analyze proteins in the spinal fluid sample using tryptic digestion[112]. Also Noga *et al.* used animal model for multiple sclerosis to investigate the change in metabolism of spinal fluid by LC-MS and GC-MS[118]. Jia *et al.* used LC-MS to detect surrogate peptides in spinal fluid of patients with neurological disorders[119].

It is known that anti-GD2 antibodies exist in the sera of 30% of multiple sclerosis patients[120]. These antibodies are produced during the demyelination process in multiple sclerosis and may contribute to axonal injury by impediment of axonal conductivity and outgrowth and obstruction of axon- myelin interaction[121]. Regrettably, our preliminary results for detection of anti-GD2 antibody from human sera were not promising enough for us to move forward. This would be further discussed later in the chapter (Figure 2.14).

2.1.1 Mass spectrometry and antibody-antigen interaction

Studying of antibodies and noncovalent antibody-antigen interaction was originally limited to the characterization of antibody fragments[122], denatured, but intact antibody[123] and antigen complex with the antibody fragment[124]. With the introduction of ESI-TOF technology, access to high m/z values even for protein complexes with the molecular weight in mega Dalton range has become possible[125]. As a result, antibodies in native form could be analysed[126]. In native

MS spectra, because of the folded structure of the protein, the spectrum is distributed only over a few charge states which yields higher intensity peaks with reduced signal dilution. Moreover the distributed ions signal has a narrower m/z range; as such it reduces the probability that overlapping with other ion peaks generated by other protein in the mixture. In native MS the protein samples are generally retained in a volatile buffer solution at neutral pH so that the native structure is preserved; so noncovalent interactions such as antibody-antigen interaction can be measured[127]. Tito *et al.* were one of the first to use native MS to determine antibody to antigen stoichiometry[127]. In another research study, Oda *et al.* investigated the effect of antigen size on the antibody to antigen stoichiometry [75]. Recently Rosati *et al.* employed native MS to analyze a complex mixture of monoclonal antibodies[128]. As well, Rose *et al.* quantified the noncovalent interactions in homodimerization of hinge deleted human IgG4 half molecules (HL)[129]. Here, we developed a quantitative and direct MS assay for antibody-antigen interaction where we have demonstrated how native MS can be used as an efficient method.

2.2 Experimental section

2.2.1 General reagents

Mouse anti-human disialoganglioside GD2 monoclonal antibody (anti-GD2 mAb) was purchased from Millipore (Cat. # 2379328) and used without further purification. Bovine serum albumin (BSA) was purchased from Sigma

Aldrich (Cat. # A7030) and used as a reference protein (P_{ref}). IgG from mouse serum (Sigma-Aldrich, Cat. # I8765) and IgG from healthy human serum (Sigma-Aldrich, Cat. # I2511) were used against different carbohydrates. For deglycosylation, a monoclonal anti-mycobacterium tuberculosis LAM was used. This mAb, designated as CS-35, was expressed by the Alberta Glycomics Center Biological Laboratory at the University of Alberta. The cell line expressing this mAb was provided by Dr. John S. Spencer from Colorado State University. Remove-iT Endo S enzyme from New England Biolabs (Cat. # P0741S) was used for the antibody deglycosylation. Different concentrations of GD2 oligosaccharide (Sigma-Aldrich), GM1 oligosaccharide (Sigma-Aldrich), Maltotriose (Elicityl), asialo-GM2 oligosaccharide (Sigma-Aldrich) and H-Araf oligosaccharide (obtained from Dr. Lowary, University of Alberta) were prepared from their stock solutions in water and used for the experiment.

2.2.2 Sample preparation

Prior to analysis of antibodies by native MS, samples should be prepared appropriately via two steps:

2.2.2.1 Buffer exchange

Whether antibodies are ordered from a company or expressed and purified in your own lab, the buffer of the antibody is different from that which is suitable for MS. As such, a buffer exchange step is necessary. The buffer should be

volatile and should not change the native conformation of the Abs. If the buffer exchange is not efficient, adducts will form because of high concentration of salts and thus the antibody peak will broaden on the spectra[128]. An aqueous ammonium acetate solution is a suitable buffer as most proteins preserve their activities and native structure in this solution[128]. As such in the present work 200 mM ammonium acetate pH 6.8 was used for all solutions to maintain the antibody native structure.

There are two common ways for buffer exchange. A centrifugal-filter concentrator is an efficient way to complete buffer exchange and sample concentration simultaneously. The method is fast; however recovery is low. Another method is to dialyze the sample. This method is slow and causes sample dilution but, the benefits are a higher recovery[128].

For the ESI-MS experiments, the antibodies buffer was exchanged to 200 mM ammonium acetate (pH 6.8) using ultracentrifugation microconcentrators (Millipore Corp., Bedford,MA) with a 10 kDa molecular weight cut-off (MWCO) and stored at 4°C if not used immediately. The protein concentration was 1μM for ESI-MS binding measurements. Bovine serum albumin (BSA) buffer were exchanged the same way as the antibody.

2.2.2.2 Enzymatic deglycosylation:

Glycosylation is a post translational modification in proteins which holds particular importance for antibodies. This makes monoclonal antibodies a

heterogeneous mixture of different isoforms. As a result, the MS spectrum of the antibody is broadened and consists of different peaks related to the different isoforms. If the aim of the research is not related to the glycans on the antibodies, deglycosylation is a helpful step to increase signal intensity and simplify the spectra[130]. Glycosylation in antibodies predominantly occur in the CH2 domain at each heavy chain. The glycosylation has an effect on the binding of antibody to the related Fc receptor and also influence the half-life of the antibody in serum[131]. It is important to note that glycosylation occurs rarely in the variable domain of the antibody but if this situation does arise binding affinity of the antibody will be affected[82].

There are a few enzymes that are able to remove the carbohydrates from a specific amino acid residue of the antibody such as PNGase F that cleaves most optimally under denaturing conditions between the asparagine 297 residue of the IgG and the attached N-acetylglucosamine (GlcNAc). Remove-iT Endo S (New England BioLabs) is another appropriate deglycosylation enzyme that is more robust and completely cleaves the glycan moiety at asparagine 297 of IgG under native conditions. This particular enzyme is expressed and purified from *E. coli*. It is also tagged with chitin binding domain (CBD) to effectively remove the enzyme after the deglycosylation reaction if it is necessary[132].

Remove-iT Endo S enzyme was used for the deglycosylation of the CS-35 anti-sugar antibody. The enzyme is tagged with a chitin binding domain (CBD) for easy removal from the reaction mixture.

For the deglycosylation experiment, CS-35 antibody was dialyzed against Tris buffer (20 mM Tris, 50 mM NaCl, 5mM Disodium EDTA at pH 7.4) using 12-14 kDa MWCO dialysis tubing from Fisher Scientific (Cat. # 21-152-14) for 10 hours and concentrated with Amicon ultra centrifugal filter, (15 mL, 10 kDa MWCO). The final concentration was 0.85 mg/mL obtained via nanodrop spectrometer (ND-1000, NanoDrop Technologies, US). 60 µL of the antibody was mixed with 3µL of Remove-iT Endo S enzyme and incubated at 37°C for 7 hours. Then the enzyme was removed by chitin magnetic beads from New England Biolabs (Cat. # E8036S) according to the protocol provided by the company. The deglycosylated antibody was dialyzed against 200 mM ammonium acetate buffer (pH 6.8) using a dialysis cassette with a 10 kDa MWCO from Thermo Scientific (Cat. # 66380) for 10 hours and then concentrated via Vivaspin Turbo centrifugal concentrators (10kDa MWCO) from Sartorius Stedim Biotech. The final concentration of 2 µM was obtained by nanodrop.

2.3 Mass spectrometry measurements

ESI-MS measurements were performed on a Synapt G2S quadrupole-ion mobility separation-time-of-flight (Q-IMS-TOF) mass spectrometer (Waters UK Ltd., Manchester, UK). For all experiments, nanoESI was used as the ionization technique and borosilicate glass capillaries (1.0 mm o.d., 0.78 mm i.d.) were pulled using a P-1000 micropipette puller (Sutter instruments, Novato, CA) to

make nanoESI tips. The experiments were completed in either positive or negative ion modes and cesium iodide (concentration 1mg/mL) was used for calibration. Some experimental conditions for the positive ion mode are listed here: A capillary voltage of 1 kV was applied for nanoESI. Different cone voltages including 30, 50, 75, 100, 125 and 150 V were used for binding measurement experiments. The source temperature was set at 60°C. The injection voltages into the trap and transfer ion guides were maintained at 5 V and 2 V respectively. Argon gas was used in the trap and transfer ion guides at a pressure of 8.51×10^{-3} mbar and 8.56×10^{-3} mbar respectively. For collision induced dissociation (CID) experiments, the injection voltages into the trap and transfer ion guides were kept at 150 V and 2 V respectively. LM resolution was set at 12. Data analysis were performed using Mass Lynx (v 4.1).

2.4 Results and discussion

NanoESI mass spectra were measured in both positive and negative ion modes for a mixture of antiGD2 antibody, GD2 and BSA, in which BSA acts as a reference protein, in 200 mM ammonium acetate buffer (pH 6.8) at six different cone voltages. Interestingly, increasing the cone voltage (from 50 to 100 V) did not have any effect on breaking the antibody-antigen complexes. At higher cone voltages of 125 and 150 V very small amounts of the antigen was released. This is contradictory to the previous observations for other protein–ligand complexes. In the latter case mild energy conditions are recommended to

avoid breaking the protein-ligand complexes or risk underestimation of the Ka values[45].

Rupturing a bond requires sufficient vibrational energy. In CID, using high collision energy results in excitation of internal electronic modes. This energy redistributes to vibrational internal energy and finally leads to bond cleavage. In large molecules such as antibodies, many vibrational modes exist, hence; the energy redistributed in these modes is miniscule for large molecules compared to small molecules with fewer vibrational modes. As a result antibody-antigen complexes can better withstand high energy conditions without breaking. Even though this can be a reason for the stability of large protein-ligand complexes, there are examples of protein complexes as high as 1MDa that release their ligand upon induction of high cone voltages.

Another possible explanation for the stability of the antibody-antigen complexes is the occurrence of hydrogen bonding between antibody and ligand in the gas phase. The hydrogen bond is one of the most important intermolecular forces responsible for noncovalent binding of the antigen to antibody. It is shown that the number of hydrogen bonds in the gas phase is greater than in the solution because of the solvation of the OH groups in aqueous solutions[133]. Considering GD2 as a large oligosaccharide ligand with several -OH functional groups (18 – OH group), a significant number of hydrogen bonding interactions can occur between GD2 oligosaccharide and the antibody in the gas phase. This leads to the increased stability of the antibody complex.

Figure 2.1 shows the acquired mass spectra of the antibody-antigen complexes at different cone voltages. The related lower m/z area of the antibody-antigen complexes are shown in Figure 2.2. Figure 2.3 shows the acquired mass spectra of the antibody-antigen complexes in negative ion mode at different cone voltages.

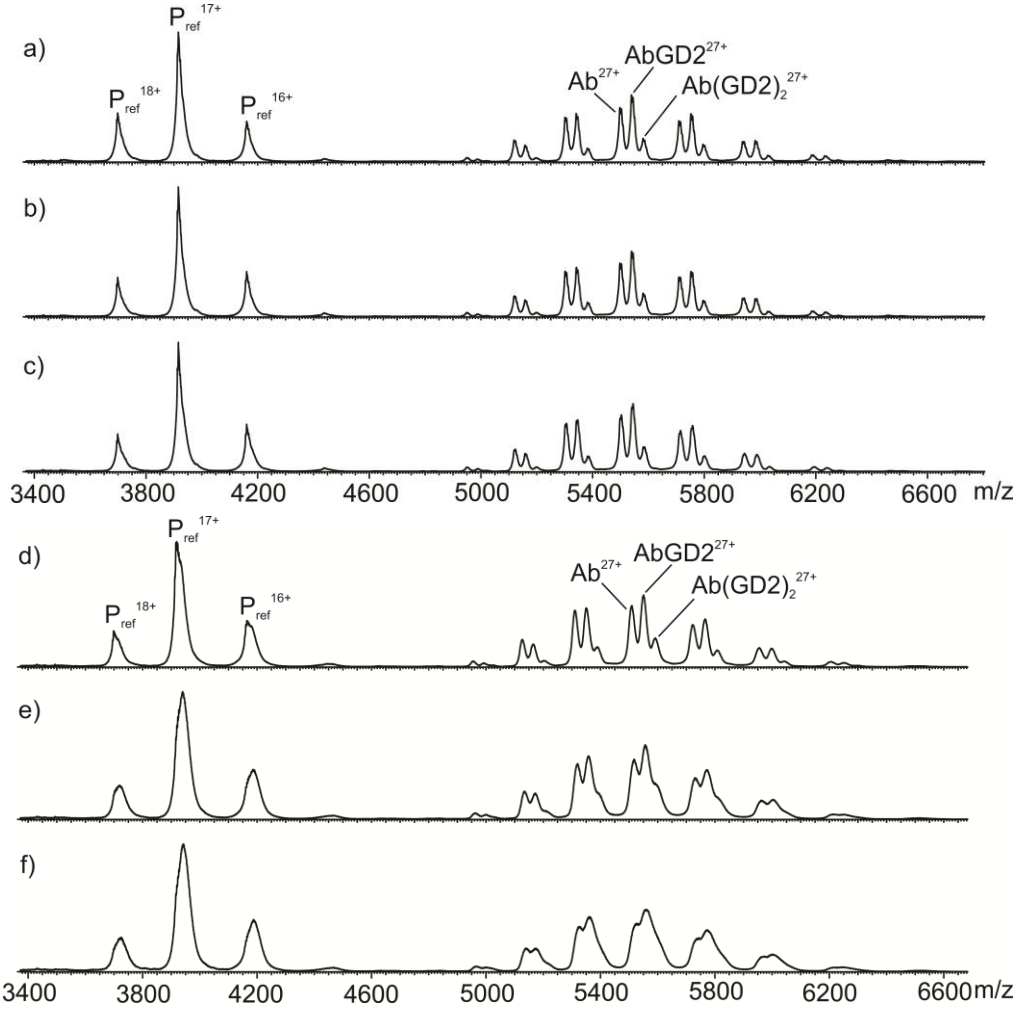

Figure 2.1 NanoESI mass spectra acquired for antiGD2 antibody (1.7 μM) and GD2 (20 μM) in 200 mM ammonium acetate buffer (pH 6.8). To quantify the extent of nonspecific antibody-antigen binding, BSA (1 μM) was added as reference protein. The measurements were done in positive ion mode at different cone voltages: a) 150, b) 125, c) 100, d) 75, e) 50 and f) 30 V.

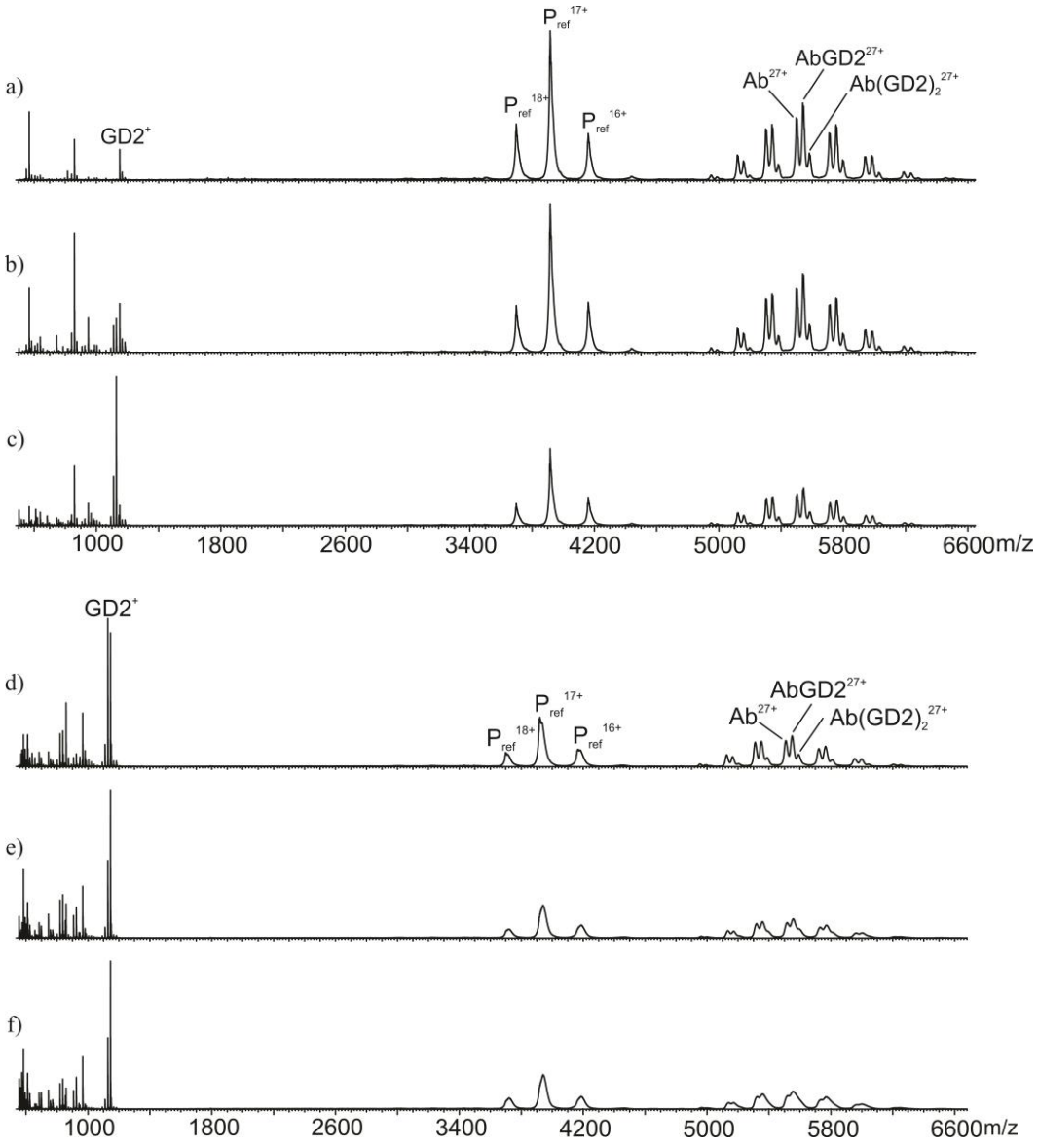

Figure 2.2 NanoESI mass spectra showing the lower m/z area acquired for anti-GD2 antibody (1.7 μM) and GD2 (20 μM) in 200 mM ammonium acetate buffer (pH 6.8). To quantify the extent of nonspecific antibody-antigen binding, BSA (1 μM) was added as reference protein. The measurements were done in positive ion mode at different cone voltages: a) 150, b) 125, c) 100, d) 75, e) 50 and f) 30 V.

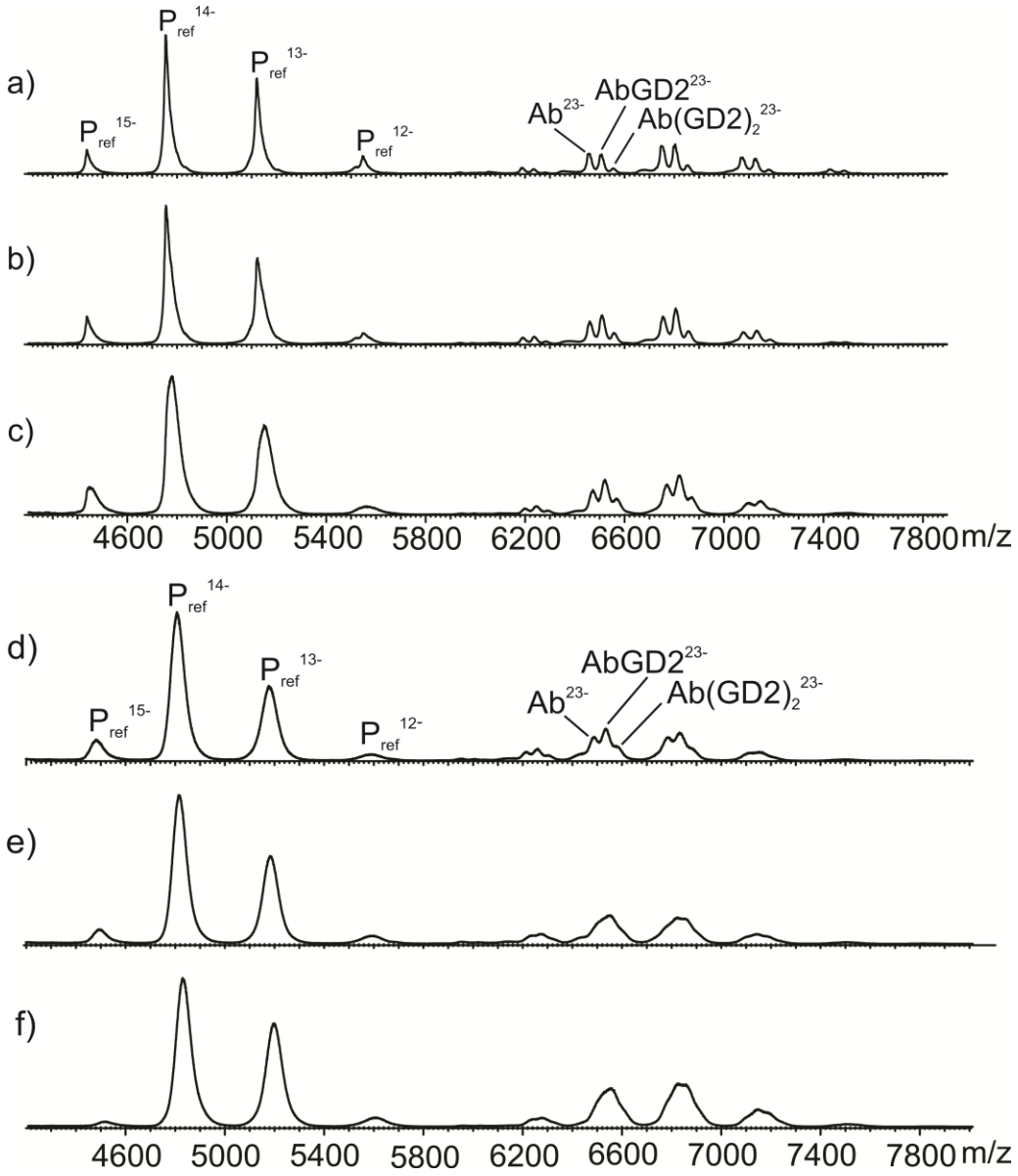

Figure 2.3 NanoESI mass spectra acquired for anti-GD2 antibody (1 μM) and GD2 (20 μM) in 200 mM ammonium acetate buffer (pH 6.8). To quantify the extent of nonspecific antibody-antigen binding, BSA (1 μM) was added as reference protein. The measurements were done in negative ion mode at different cone voltages: a) 150, b) 125, c) 100, d) 75, e) 50 and f) 30 V.

2.4.1 Direct ESI-MS binding assay

Considering the antibody as a molecule with two identical binding sites, a direct ESI-MS assay was developed for quantifying the interaction of an antibody with its cognate antigen. In developing the assay two situations were taken into account: one in which nonspecific binding occurs in high concentration of antigen and the other without occurrence of nonspecific binding due to low antigen concentration.

2.4.1.1 Calculation of K_a for a protein with two binding sites without considering P_{ref} correction

This assay is based on direct detection and analysis of the free protein (P) and protein-ligand complexes (PL and PL_2) by ESI-MS in the gas phase. Known concentration of the ligand ($[L_0]$) and the protein ($[P_0]$) is used. As the protein has two binding sites, two reactions are considered:

$$P + L \underset{k_{off}}{\overset{k_{on}}{\rightleftharpoons}} PL$$

$$PL + L \underset{k_{off}}{\overset{k_{on}}{\rightleftharpoons}} PL_2$$

Equations (1), (2), (3) and (4) show the corresponding apparent association constants ($K_{a\ app}$). R_1 is ratio of total abundance of all one ligand-bound to free protein ions. R_2 is ratio of total abundance of all two ligand-bond to free protein ions:

$$K_{a\ app1} = \frac{[PL]}{[P][L]} = 2K_{a\ int} \qquad R_1 = \frac{PL}{P} \tag{1}$$

$$K_{a\ app2} = \frac{[PL_2]}{[PL][L]} = \frac{1}{2}K_{a\ int} \qquad R_2 = \frac{PL_2}{P} \tag{2}$$

$$K_{a\ app1} = \frac{R_1}{L} = 2K_{a\ int} \tag{3}$$

$$K_{a\ app2} = \frac{R_2}{R_1 L} = \frac{1}{2}K_{a\ int} \tag{4}$$

$$R_2 = \tag{5}$$

$$\frac{(L_o - 2P_o - 1/K_{a\ int})^2 + 2L_o/K_{a\ int} + (L_o - 2P_o -)\sqrt{(L_o - 2P_o - 1/K_{a\ int})^2 + 4L_o/K_{a\ int}}}{2/K_{a\ int}{}^2}$$

$$R_1 = 2\sqrt{R_2} \tag{6}$$

$$= \frac{(L_o - 2P_o - 1/K_{a\ int}) + \sqrt{(1/K_{a\ int} - L_o + 2P_o)^2 + 4L_o/K_{a\ int}}}{1/K_{a\ int}}$$

$$K_{a\ int} = \frac{2R_2(1 + R_1 + R_2)}{R_1[(L_o - P_o)R_1 + (L_o - 2P_o)R_2 + L_o]} \tag{7}$$

2.4.1.2 Calculation of K_a for a protein with two binding sites with considering P_{ref} correction

The basic assumption of the reference protein (P_{ref}) method is that nonspecific binding occurs independently regardless of the nature of the proteins present, as long as the sizes of the proteins are comparable. Considering f_xP is the fractional abundance of P that is bound to x molecule of L, apparent abundance of the proteins and the complexes are defined in equations (8) to (13):

$$P_{app} = f_o P \tag{8}$$

$$PL_{app} = f_o PL + f_1 P \tag{9}$$

$$PL_{2app} = f_o PL_2 + f_1 PL + f_2 P \tag{10}$$

$$P_{ref,\mathrm{app}} = f_o P_{ref} \tag{11}$$

$$P_{ref} L_{app} = f_1 P_{ref} \tag{12}$$

$$P_{ref} L_{2app} = f_2 P_{ref} \tag{13}$$

$$R_1 = \frac{PL_{app}}{P_{app}} - \frac{P_{ref} L_{app}}{P_{ref,app}} \tag{14}$$

$$R_2 = \frac{PL_{2app}}{P_{app}} - \frac{P_{ref} L_{2app}}{P_{ref,app}} - \frac{P_{ref} L_{app}}{P_{ref,app}} R_1 \tag{15}$$

$$K_{a\,int} = \frac{1}{2}\left(\frac{L_o R_1 (1 + R_1 + R_2)}{{R_1}^2 (1 + R_1 + R_2) - P_o L_o (R_1 + 2R_2)}\right) \tag{16}$$

2.4.1.3 Calculation of $K_{a,int}$ for data fitting

To determine the Ka value, different concentrations of the ligand is used against single concentration of the protein to obtain a titration curve. The value of Ka can be computed using nonlinear regression analysis of the fraction of protein-ligand complex to total binding site (*f*) at different ligand concentrations.

$$f = \frac{R_1 + 2R_2}{2(1 + R_1 + R_2)} \tag{17}$$

$$K_{a,\text{int}} = \frac{f}{(1-f)(L_0 - 2fP_0)} = \frac{1}{(\frac{1}{f} - 1)(L_0 - 2fP_0)} \tag{18}$$

$$f = \frac{(1 + L_0K_{a,\text{int}} + 2P_0K_{a,\text{int}}) - \sqrt{(1 - L_0K_{a,\text{int}} + 2P_0K_{a,\text{int}})^2 + 4L_0K_{a,\text{int}}}}{4P_0K_{a,\text{int}}} \tag{19}$$

2.4.2 Validation of the developed binding assay

To validate the accuracy of this antibody binding assay, an antibody-antigen system with a well-established binding constant is required as a control. For this purpose, anti-lipoarabinomannan (LAM) CS-35 mAb was chosen. CS-35 is a mAb against the hexa arabinofuranoside termini of the *Mycobacterium leprae*[134]**.** This mAb has served as reference antibody for characterization of new mAbs against LAMs and as a recognition motif for a variety of assays developed for Tuberculosis (TB)[135].

CS-35 antibody was buffer exchanged to 200mM ammonium acetate (pH 6.8) and sprayed into the MS. The mass spectra were acquired at different cone

voltages in both negative and positive ion modes (Figure 2.4b). The broad antibody peaks is related to heterogeneity of the antibody that occurs during its expression and its post translational modification during the purification process. In addition, the antibody peaks begin to split at cone voltages of 75 V and higher. These two aspects make direct recognition of the CS-35 and H-Araf complex impossible (Figure 2.4a). Figure 2.4 shows a comparison between nanoESI mass spectra obtained for CS-35 antibody and the one acquired for incubated CS-35 with H-Araf. The antibody-antigen peak appears at the same m/z value as the split antibody peak making the measurement of the relative amount of antibody complexes inaccurate. To prove the formation of CS-35 antibody- H-Araf complex, tandem MS was performed at different m/z of the CS-35 antibody-H-Ara6 spectra (Figure 2.5). To show the occurrence of overlap between the antibody peak and the antibody-antigen complex a deconvolution software, Massign (from Oxford University), was used. Figure 2.6 and 2.7 depicts the deconvoluted peaks for the antibody and the antibody-antigen respectively. The masses acquired by Massign software was 150838, 150103 and 149233 Da for the split antibody peak and 150946, 150104 and 149224 Da for the split antibody-antigen peak. The small difference between the masses of the split peaks it is evident that overlapping is occurring.

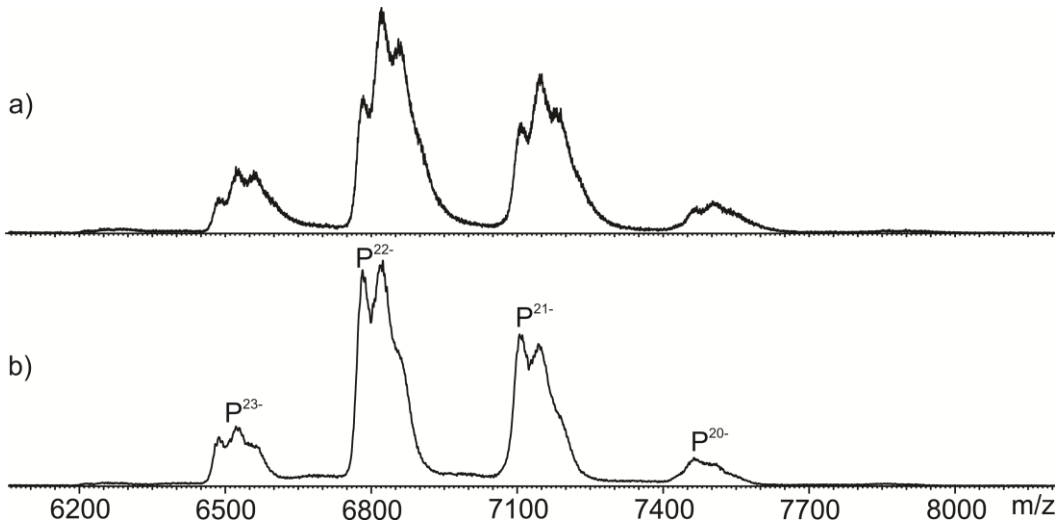

Figure 2.4 NanoESI mass spectra acquired for a) 1 μM CS-35 antibody incubated with 16 uM arabinose, b) 1.5 μM CS-35 antibody in 200 mM ammonium acetate (pH 6.8).

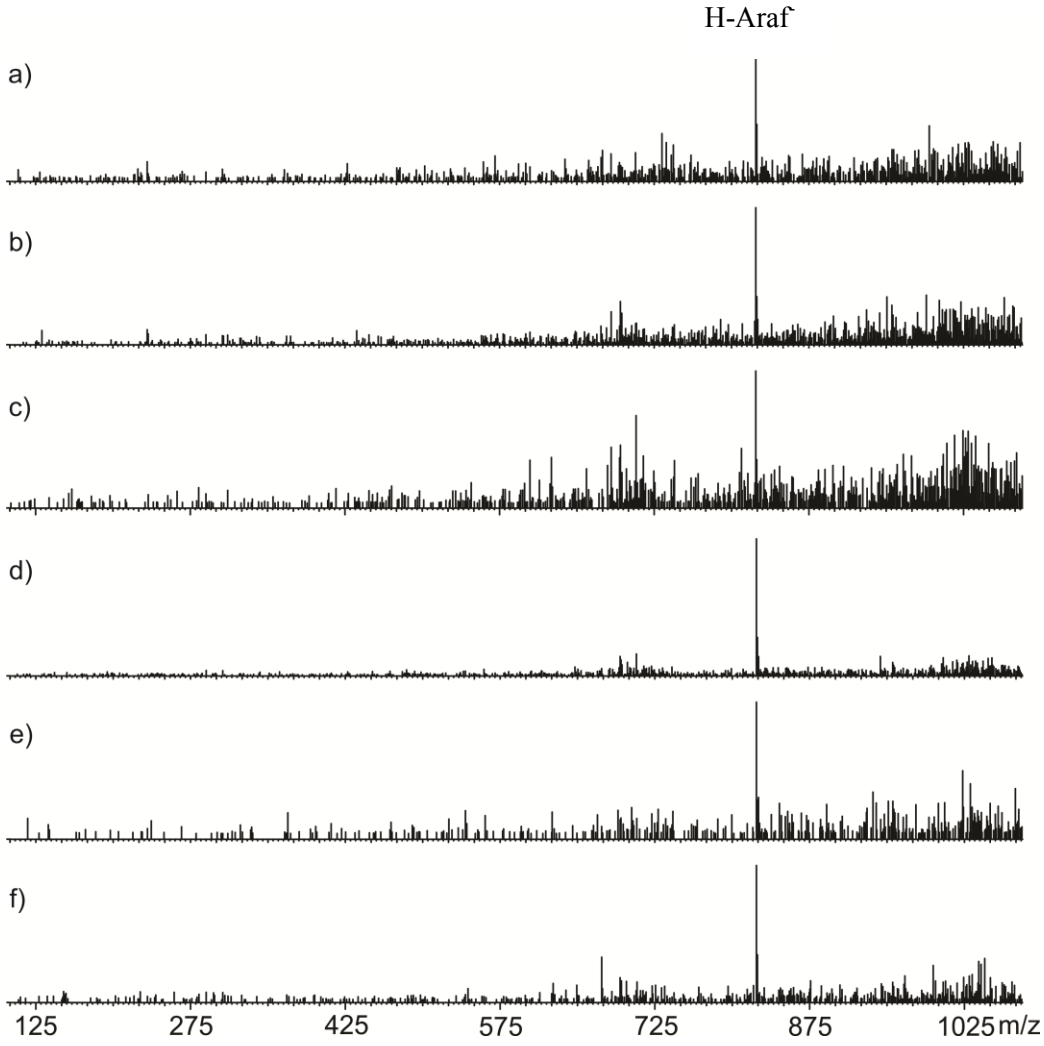

Figure2.5 Tandem MS spectra acquired for 1 μM CS-35 antibody incubated with 16 μM H-Araf at different m/z of: a) 6895, b) 6860, c) 6820, d) 7260, e) 6980 and f) 6940.

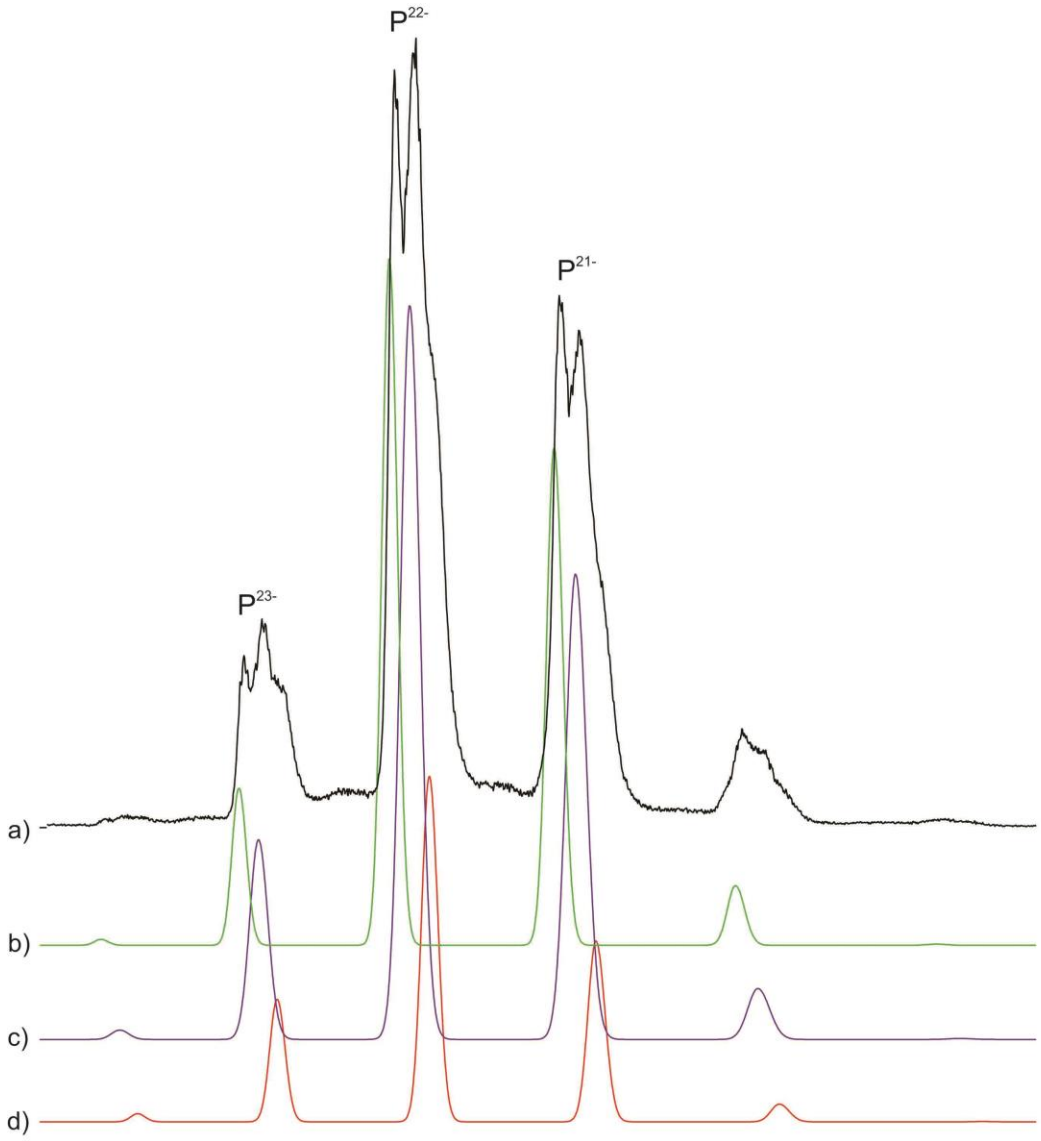

Figure 2.6 NanoESI mass spectra acquired for 1.5 μM CS-35 antibody in 200 mM ammonium acetate (pH 6.8), b), c) and d) The deconvoluted mass spectra related to the split antibody peak.

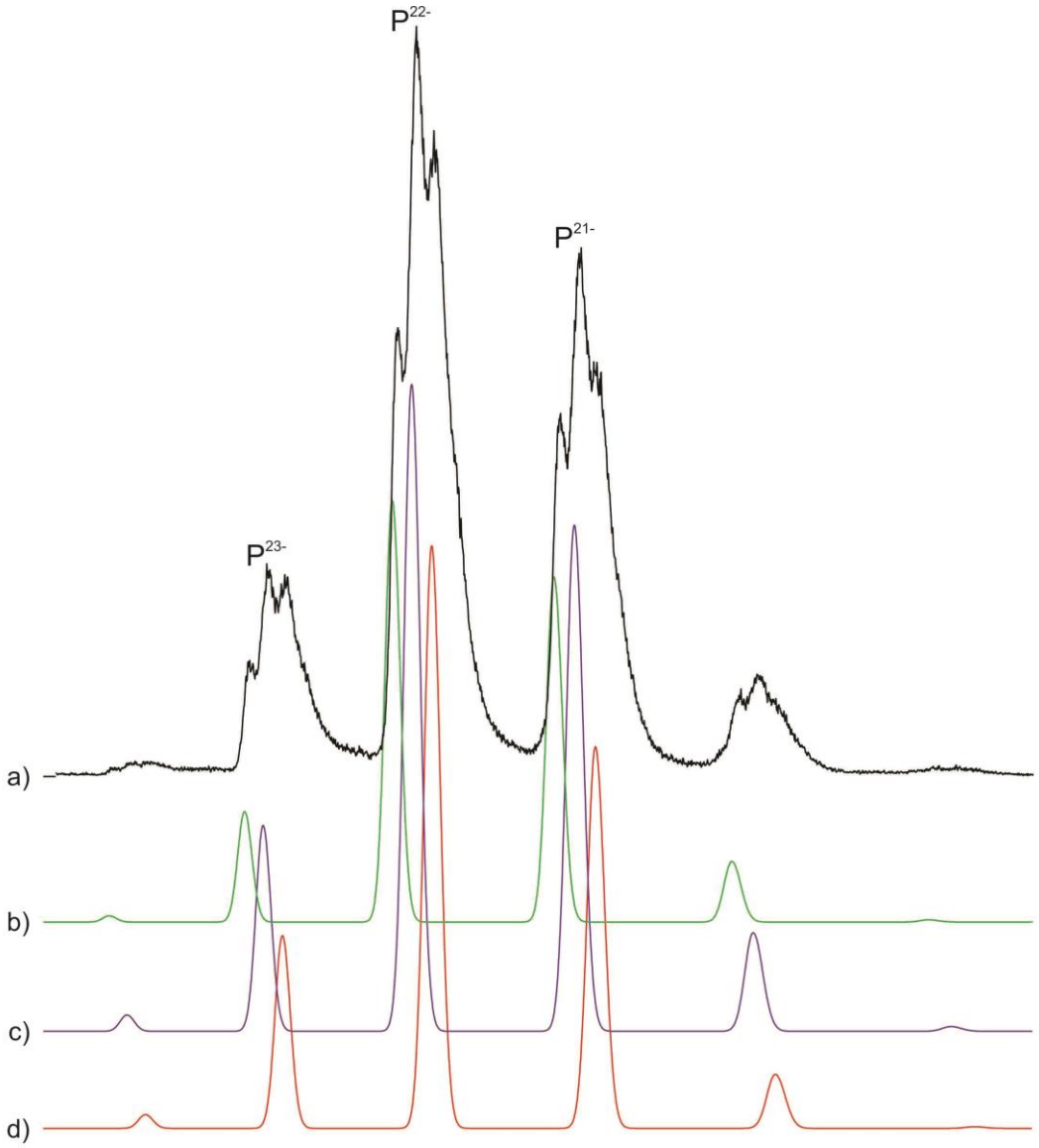

Figure 2.7 NanoESI mass spectra acquired for a) 1 µM CS-35 antibody incubated with 16 µM arabinose in 200 mM ammonium acetate (pH 6.8), b), c) and d) The deconvoluted mass spectra related to the split antibody peak.

To solve the problem related to direct measurement of binding constants for CS-35 antibody, the antibody was deglycosylated in order to decrease the heterogeneity caused by glycans and reduce the broadness of the antibody spectrum. For this purpose Remove-iT Endo S enzyme was used since it is suitable for deglycosylation of antibodies in nature conditions. Different experiments were done to optimize the experimental condition for deglycosilation of CS-35 antibody. At first CS-35 Ab dialysed against Tris buffer (20 mM Tris, 50mMNaCl and 5mM sodium-EDTA, pH 7.4). The Ab then concentrated using 15 mL Amicon centrifugal filter (M CO. 10 kDa). Finally 60µL of the concentrated CS-35 antibody (0.85 mg/mL) was mixed with 3 µL of Endo S enzyme and incubated for 7 hours at 37°C. As the molecular weight of the enzyme is 136 kDa, it should be removed from the solution before spraying the Ab into the MS. Endo S enzyme was removed by Chitin magnetic beads according to the protocol from NewEngland BioLabs. After buffer exchange to 200 mM ammonium acetate, the deglycosylated antibody was sprayed into MS. The MS results showed no concluding evidence that CS-35 was deglycosylated (Figure 2.8). The peaks for this antibody were so broad compared to the commercially prepared one (Figure 2.1) that deglycosylated species were not resolved in MS. As control, the deglycosylated CS-35 was incubated with 30 µM H-Araf. Tandem MS at the different m/z released H-Araf from its complex with CS-35 antibody (Figure 2.9). Thus, with these results, direct measurement of binding constant of the deglycosylated antibody with its antigen is highly improbable.

The broad characteristic of CS-35 MS signals could be due to poor antibody expression, purification and storage protocols or could be attributed to the effects of the extent of posttranslational modifications on the antibody. Despite the unsuccessful attempt to validate our assay, our research group has a broad background in developing different assays to measure protein-ligand binding constants. As such, we decided to continue further to measure the binding constant between GD2 oligosaccharide and anti-GD2 antibody using this assay.

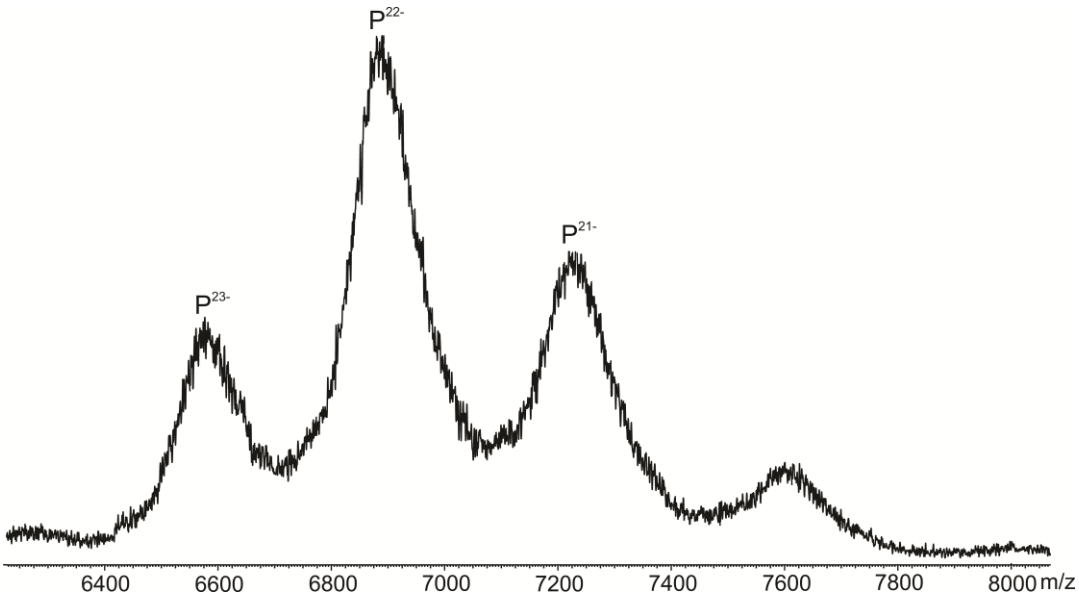

Figure 2.8 NanoESI mass spectra acquired for a) 1 μM CS-35 antibody incubated with 3 μL Endo S enzyme for deglycosylation in 200 mM ammonium acetate (pH 6.8).

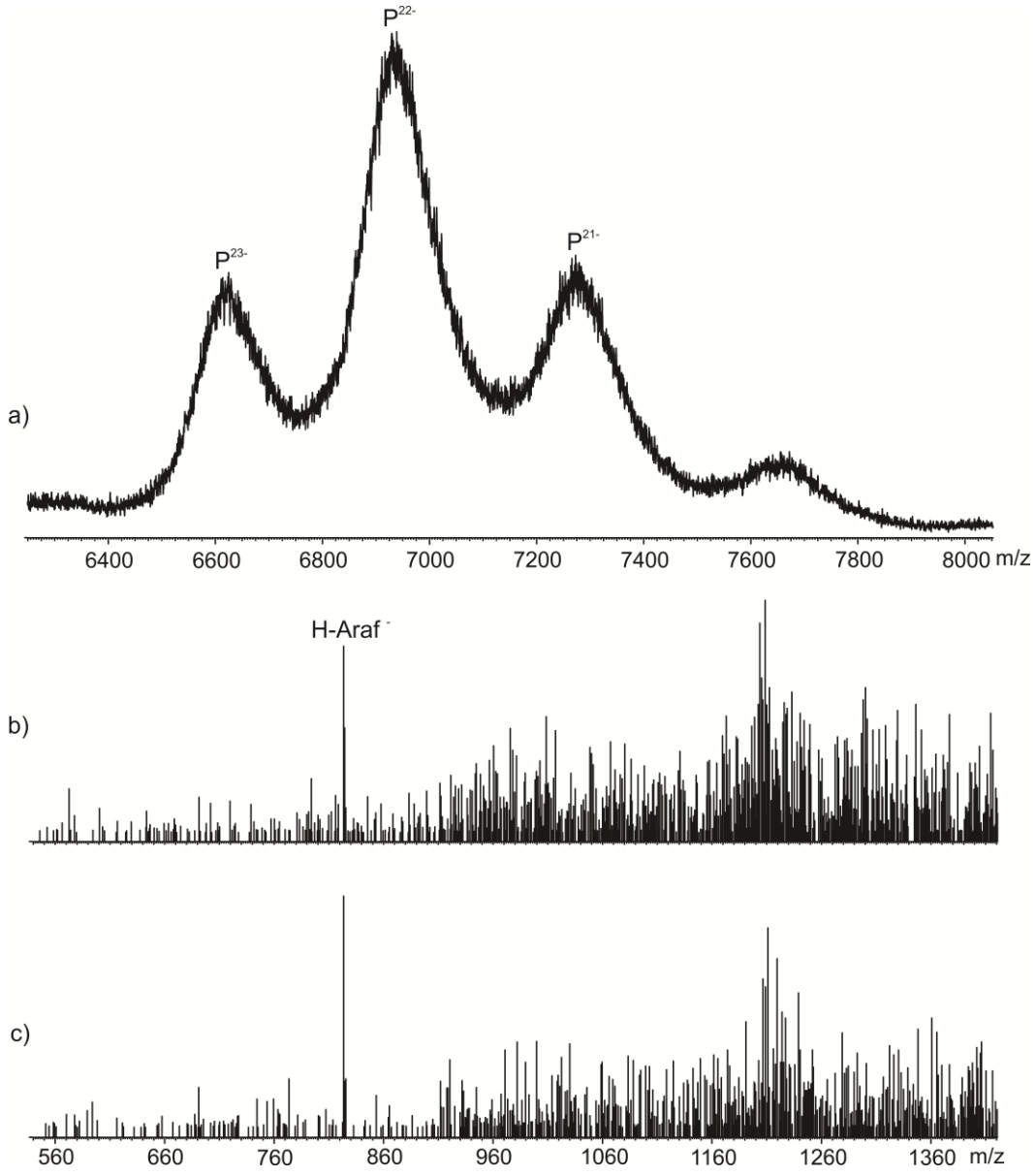

Figure 2.9 a) NanoESI mass spectra acquired for a) 1 μM CS-35 antibody incubated with 3 μL Endo S enzyme for deglycosylation and 30 μM H-Araf in 200 mM ammonium acetate (pH 6.8). Related tandem MS spectra acquired at different m/z of b) 6960 and c) 7000.

2.4.3 Quantifying the interaction between anti-GD2 antibody and GD2 oligosaccharide

To obtain a titration curve for measuring binding data, different concentration of GD2 were run against fixed concentration of anti-GD2 antibody in the presence of BSA as the reference protein. The measurements were run two times. To validate the consistency of the binding data, the experiments were run in both positive and negative ion modes. Also investigation of different cone voltages was applied to monitor the effect on the antibody-antigen binding. Nonspecific binding of GD2 to the P_{ref} and the antibody was detected at GD2 concentrations of 30 μM and higher. Figure 2.10 shows occurrence of nonspecific binding at 50 μM of GD2 at different cone voltages.

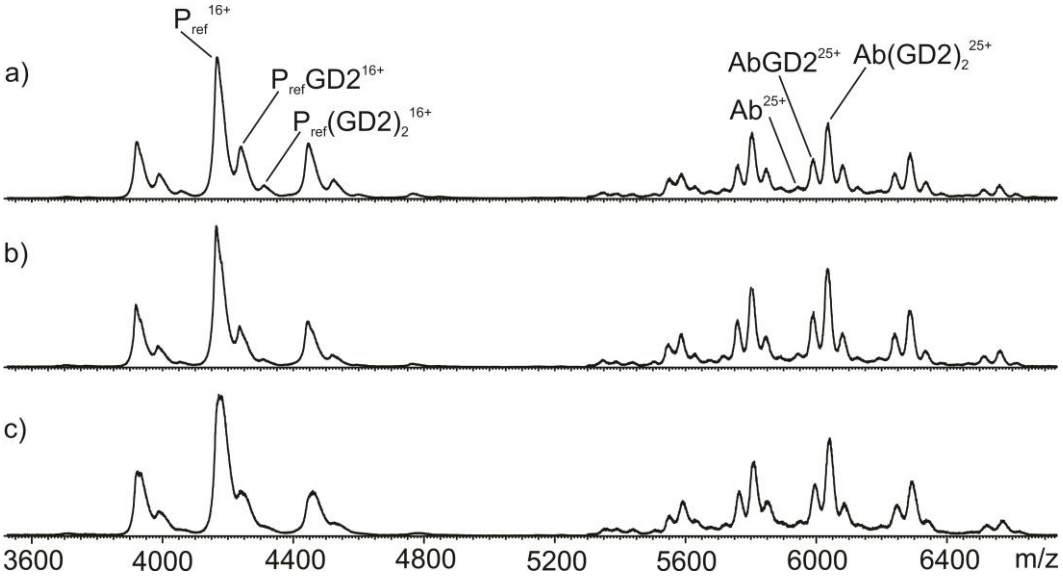

Figure 2.10 NanoESI mass spectra acquired for 50 μM of GD2 at different cone voltages of: a) 125, b) 100 and c) 75 V at positive ion mode. The occurrence of nonspecific binding is shown by attachment of one and two molecules of GD2 to P_{ref}.

As shown in Figure 2.1, increasing the cone voltage improves the resolution of the mass spectra of the antibody and its complexes. To ensure the correct measurement of the intensities obtained at lower cone voltages or lower concentrations from the mass spectra, Massign software was used to assign and identify the complexes. The results for deconvolution of the spectra are shown in Figure 2.11. The percent of signal acquired by Massign software was 49.64, 36.77 and 13.59 for the antibody, the antibody + GD2 and the antibody + 2GD2 respectively. Inserting these values in the formula for calculation of the $K_{a,int}$, gave a $K_{a,int}$ value of 3.4×10^4 M^{-1}. The $K_{a,int}$ value acquired by direct measurement of

intensities from the mass spectrum was 3.4×10^4 M^{-1} which is the same as the result obtained by Massign.

As the results from Massign were found to be similar to the results obtained by direct measurement of intensities from the mass spectra, it was not necessary to continue deconvolution with Massign. Instead, intensities can be retrieved from the mass spectra and inputted into the formulas directly.

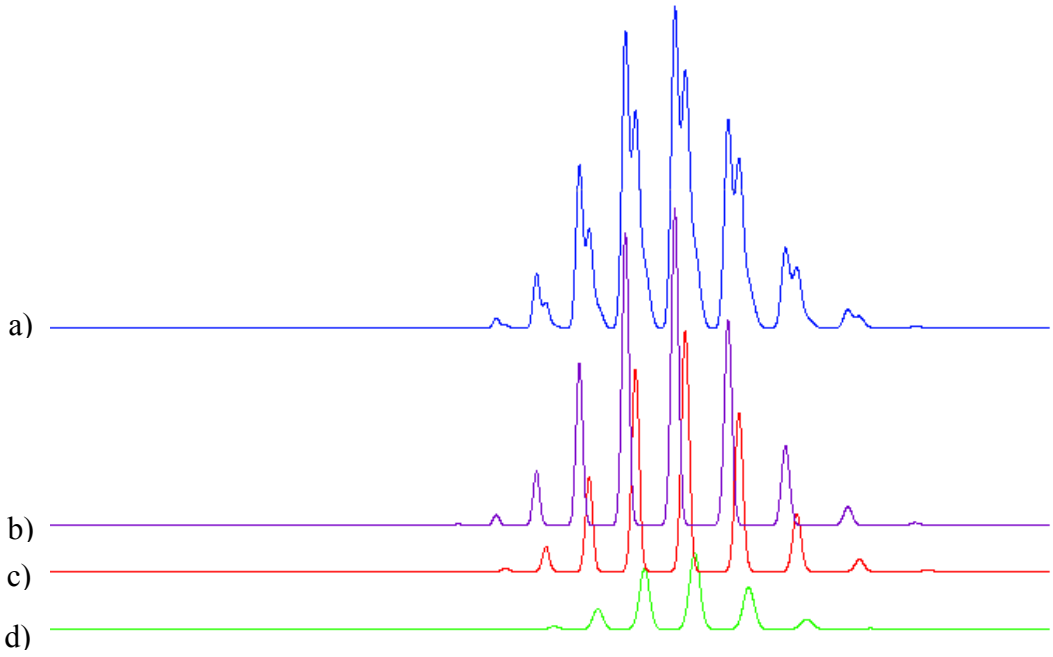

Figure 2.11 a) NanoESI mass spectra acquired for 15 µM GD2 incubated with 1 µM anti-GD2 antibody at cone voltage of 50 V in positive ion mode. The deconvoluted mass spectra related to b) AntiGD2 antibody, c) Anti-GD2 antibody + GD2 d) Anti-GD2 antibody + 2GD2.

The results acquired from the mass spectra are computed via the equation (19) to yield four titration curves which were obtained in both positive and negative ion modes for an average of two measurements (Figures 2.12 and 2.13).

Only in the first titration curve (Figure 2.12a) is the 30 μM GD2 concentration shown. At 30 μM on the mass spectra a nonspecific binding complex peak of P_{ref} was detected via tandem MS in negative ion mode (Figure 2.14). As such, this concentration does not give accurate R1 and R2 values and results in an inaccurate fitting. Thus the 30 μM concentration was omitted from the following titration curves (Figure 2.12b, Figure 2.13a, b). The results for fitting data for the $K_{a,int}$ value are summarized in Table 2.1. In order to compare the values of Ka at different cone voltages, similar measurements were completed at cone voltages of 50, 125 and 150 V in negative and positive ion modes (Table 2.1). The results suggest consistency between the Ka obtained at different cone voltages.

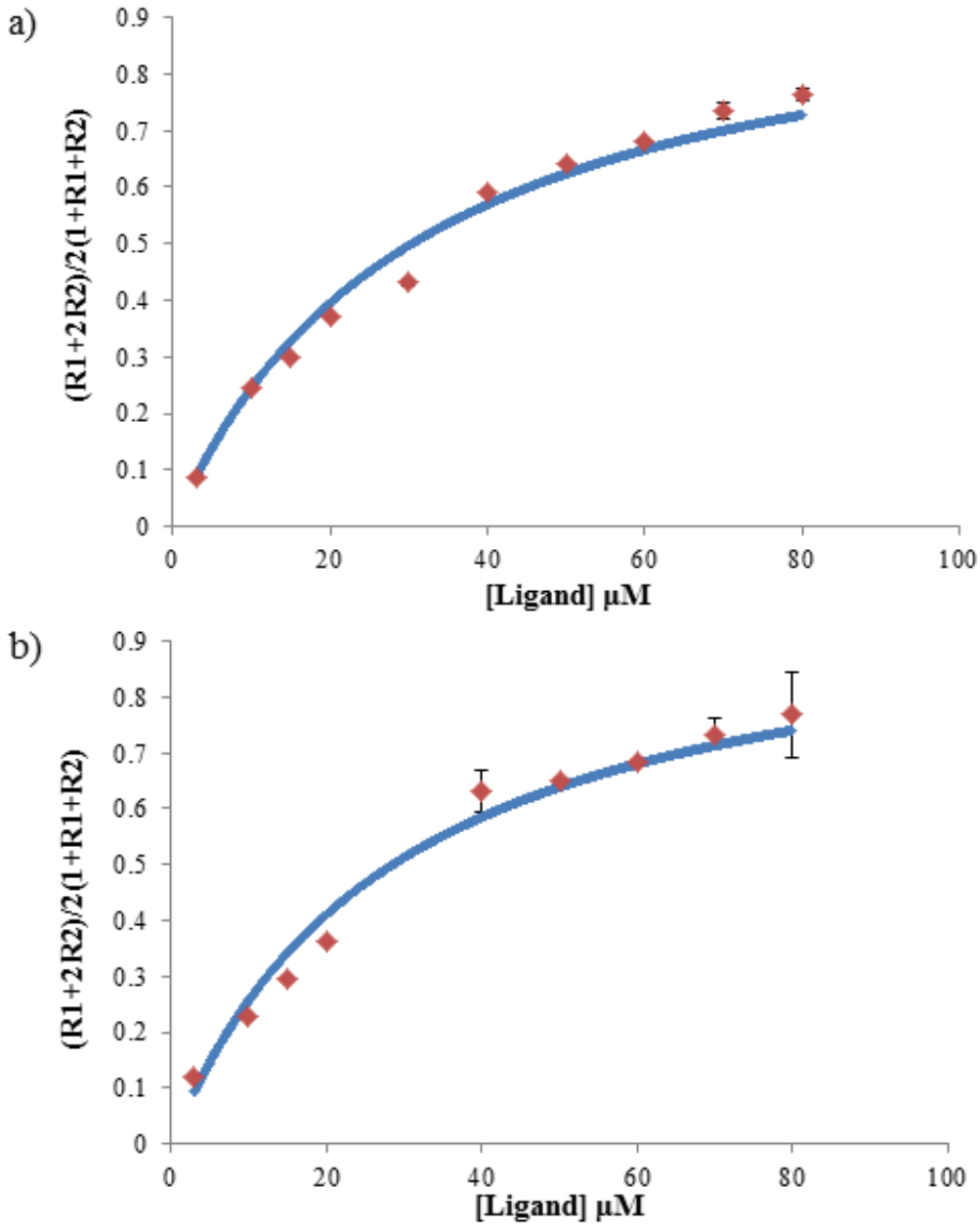

Figure 2.12 Titration curves in positive ion mode for 1.7 µM anti-GD2 antibody in the presence of different concentrations of GD2 of a) 3 µM, 10 µM, 15 µM, 20 µM, 30 µM, 40 µM, 50 µM, 60 µM, 70 µM and 80 µM, b) same concentrations as (a) with exception of 30 µM, in cone voltages of 75 V and 100 V respectively. The solid curves are the best fit acquired by Origin 9.1 software using nonlinear curve fit model (Equation19).

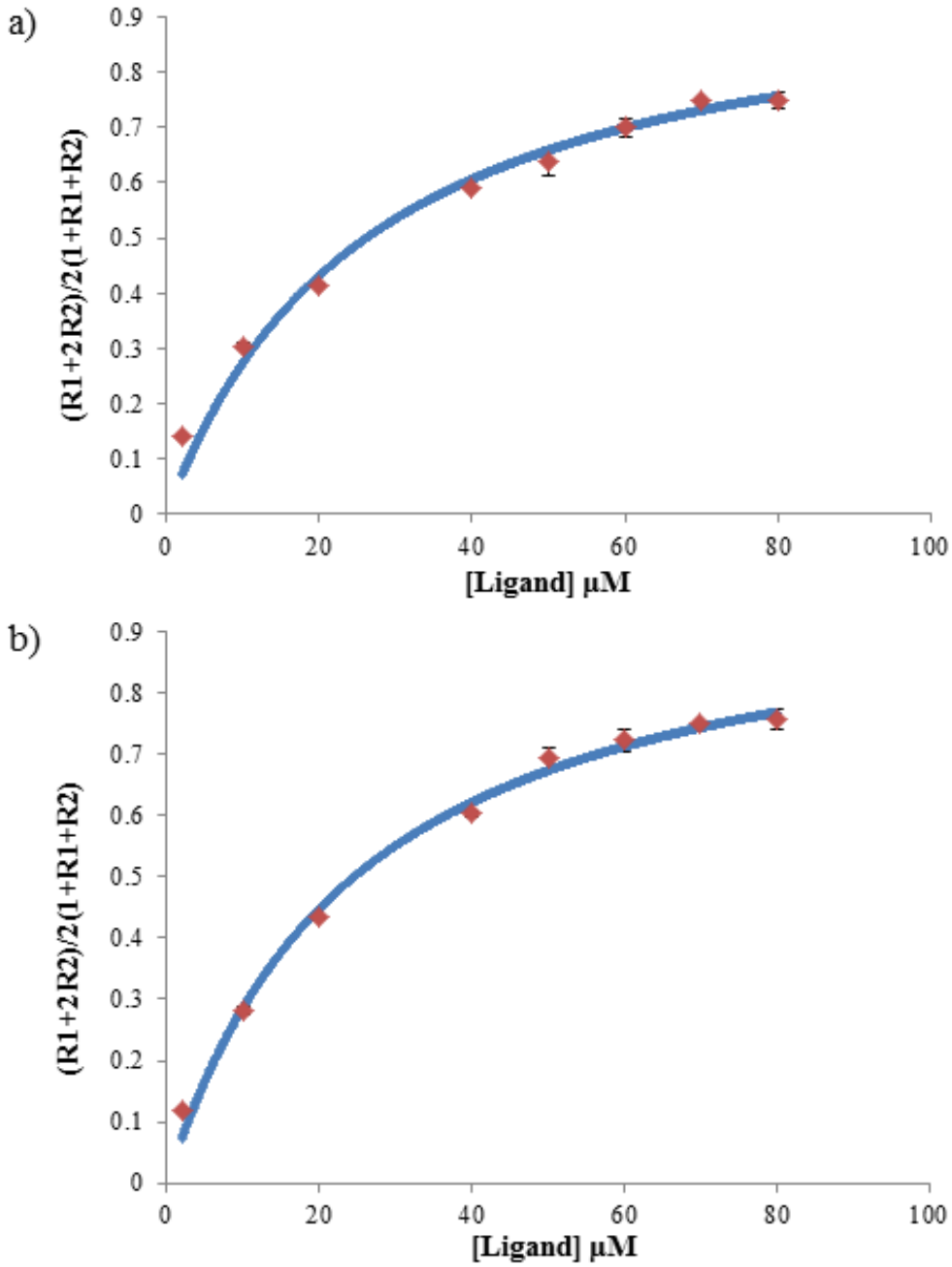

Figure 2.13 Titration curves in negative ion mode for 1 µM anti-GD2 antibody in the presence of different concentrations of GD2 of a), b) 3 µM, 10 µM, 15 µM, 20 µM, 40 µM, 50 µM, 60 µM, 70 µM and 80 µM, in cone voltages of 75 V and 100 V respectively. The solid curves are the best fit acquired by Origin 9.1 software using a nonlinear curve fit model (Equation 19).

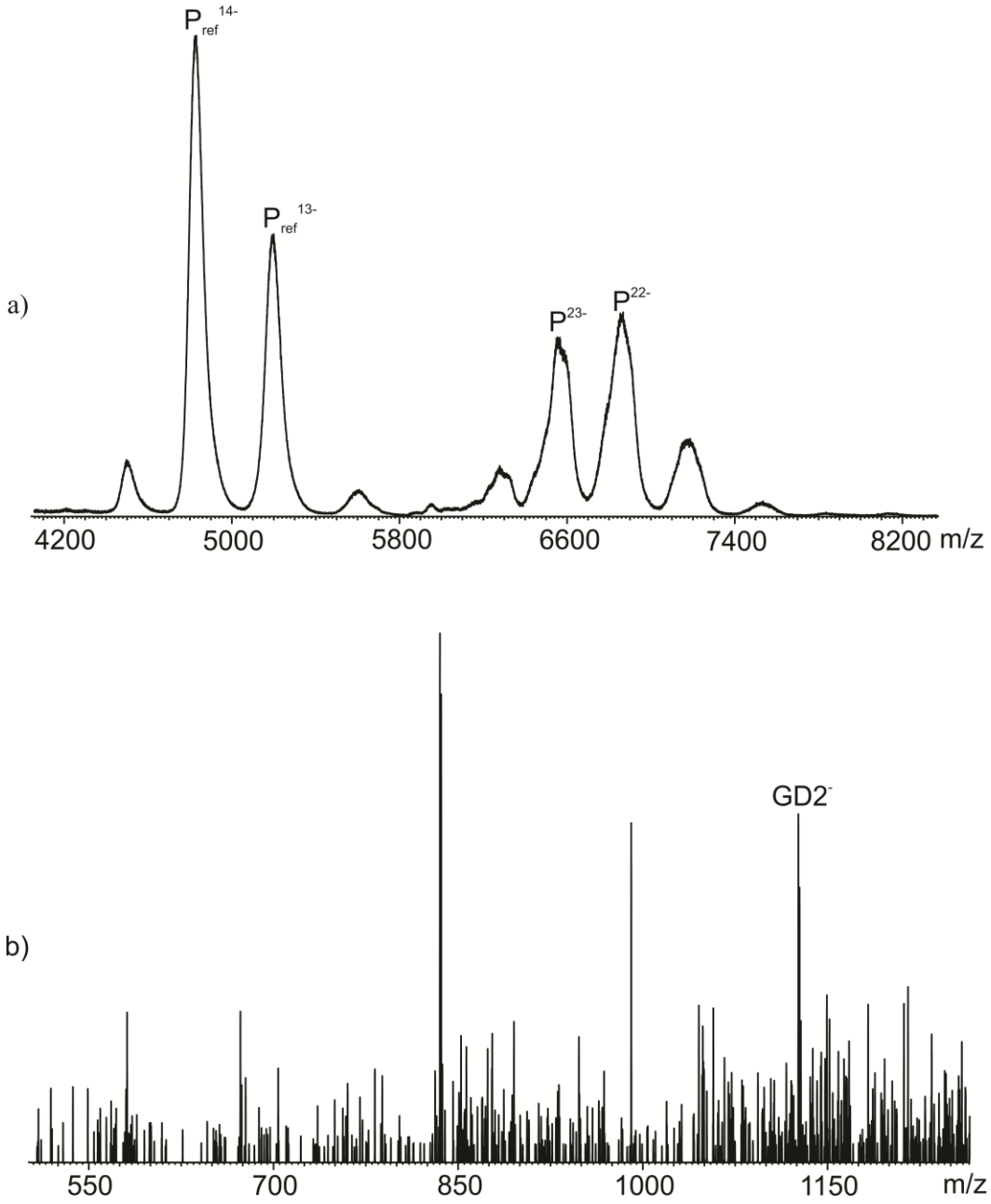

Figure 2.14 a) Mass spectra acquired in negative ion mode for binding of 30 μM GD2 to anti-GD2 antibody, b) the related tandem MS spectra acquired for m/z 4860. The release of GD2 oligosaccharide was observed from P_{ref}.

Table 2.1 The results for $K_{a,int}$ obtained from nonlinear curve fit by Origin software at 50, 75, 100, 125 and 150 cone voltages acquired in positive and negative ion modes.

Cone Voltage (V)	**Ion Mode**	**$K_{a,int\ M}^{-1}$**	**Adj.R-Square**
50	Positive	$(3.7\pm0.1)\times10^4$	0.99
50	Negative	$(3.7\pm0.1)\times10^4$	0.99
75	Positive	$(3.4\pm0.3)\times10^4$	0.95
75	Negative	$(4.0\pm0.2)\times10^4$	0.98
100	Positive	$(3.6\pm0.3)\times10^4$	0.96
100	Negative	$(4.2\pm0.2)\times10^4$	0.99
125	Positive	$(3.8\pm0.3)\times10^4$	0.97
125	Negative	$(3.8\pm0.1)\times10^4$	0.99
150	Positive	$(3.7\pm0.3)\times10^4$	0.97
150	Negative	$(2.8\pm0.1)\times10^4$	0.99

To further verify antibody-antigen complex stability, the plots of *f* against different cone voltages are shown at different concentrations of the ligand in negative and positive ion modes (Figure 2.15). According to these results, the *f* is the same with negligible reduction at higher cone voltages.

To discover the lowest concentration of anti-GD2 antibody required to give a detectable complex with GD2 for our assay, nanoESI-MS experiments were performed in positive ion mode. Overall, the greater the strength of the bond between an antibody and antigen, the higher its association constant will be. This means that a lower concentration of the antibody can produce a detectable signal of the antibody-antigen complex. A GD2 concentration of 20 μM was used and sprayed against different concentrations of the antibody which were 0.5 μM, 0.25 μM, and 0.1 μM. At 0.1 μM the complex was not detectable. The spectra were acquired for 7 min. This equals to 207 scans, considering a scan time of two seconds. Beginning at 0.25 μM the complex was detectable. e can conclude that 0.25 μM is the lower limit of detection for our assay. The results are shown in Figure 2.16.

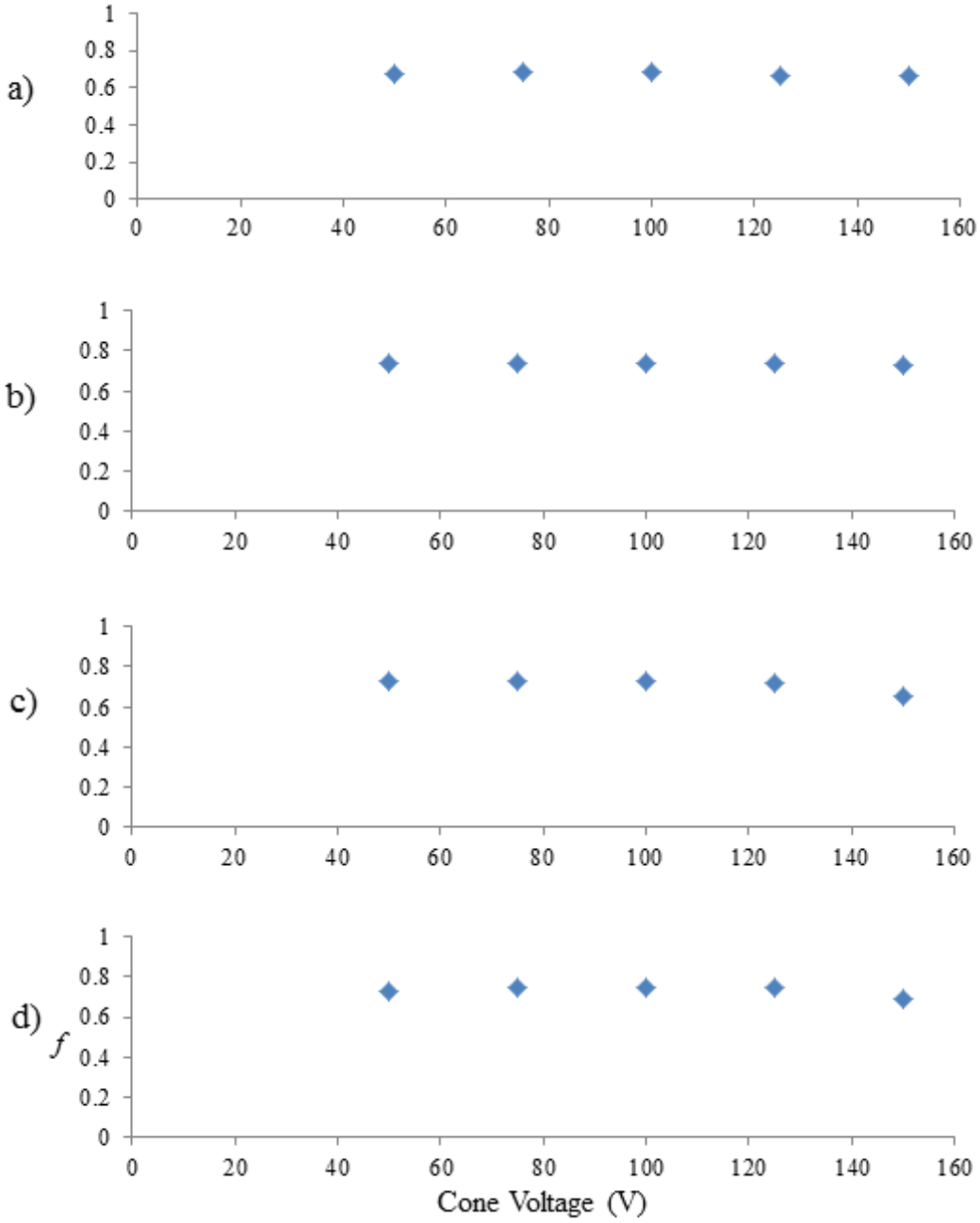

Figure 2.15 Plot of *f* against different cone voltages acquired at positive ion mode of a) 60 µM, b) 70 µM GD2 ligand and negative ion mode of c) 70 µM and d) 80 µM GD2.

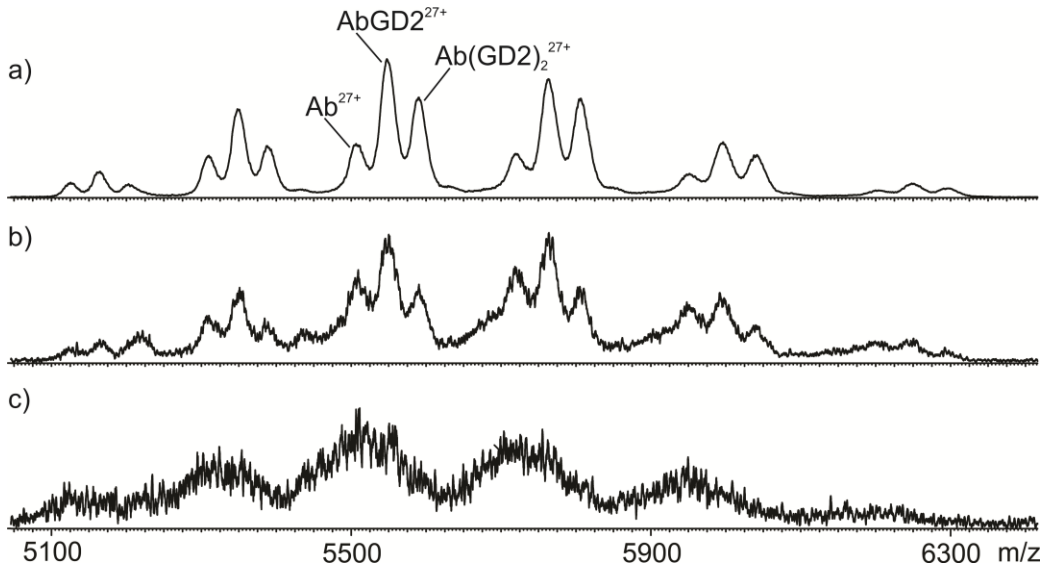

Figure 2.16 NanoESI mass spectra of 20 μM GD2 against different concentrations of anti-GD2 antibody of a) 0.5 μM, b) 0.25 μM and c) 0.1 μM in positive mode.

The second aim of the present work was to develop a new diagnostic method for Multiple Sclerosis disease; IgGs from healthy human serum and IgGs from Mouse serum were used as a negative control test. We expect no complex formation of IgGs with GD2. Different concentrations of GD2 (5 μM and 2 μM) were run against IgGs (3.6 μM) from human serum and followed by tandem MS to release the GD2 sugars from the complex, if any have formed (Figure 2.17). The results show release of GD2 by tandem MS. The experiment was run for Mouse IgGs against GD2 and the results were similar to that of human IgGs.

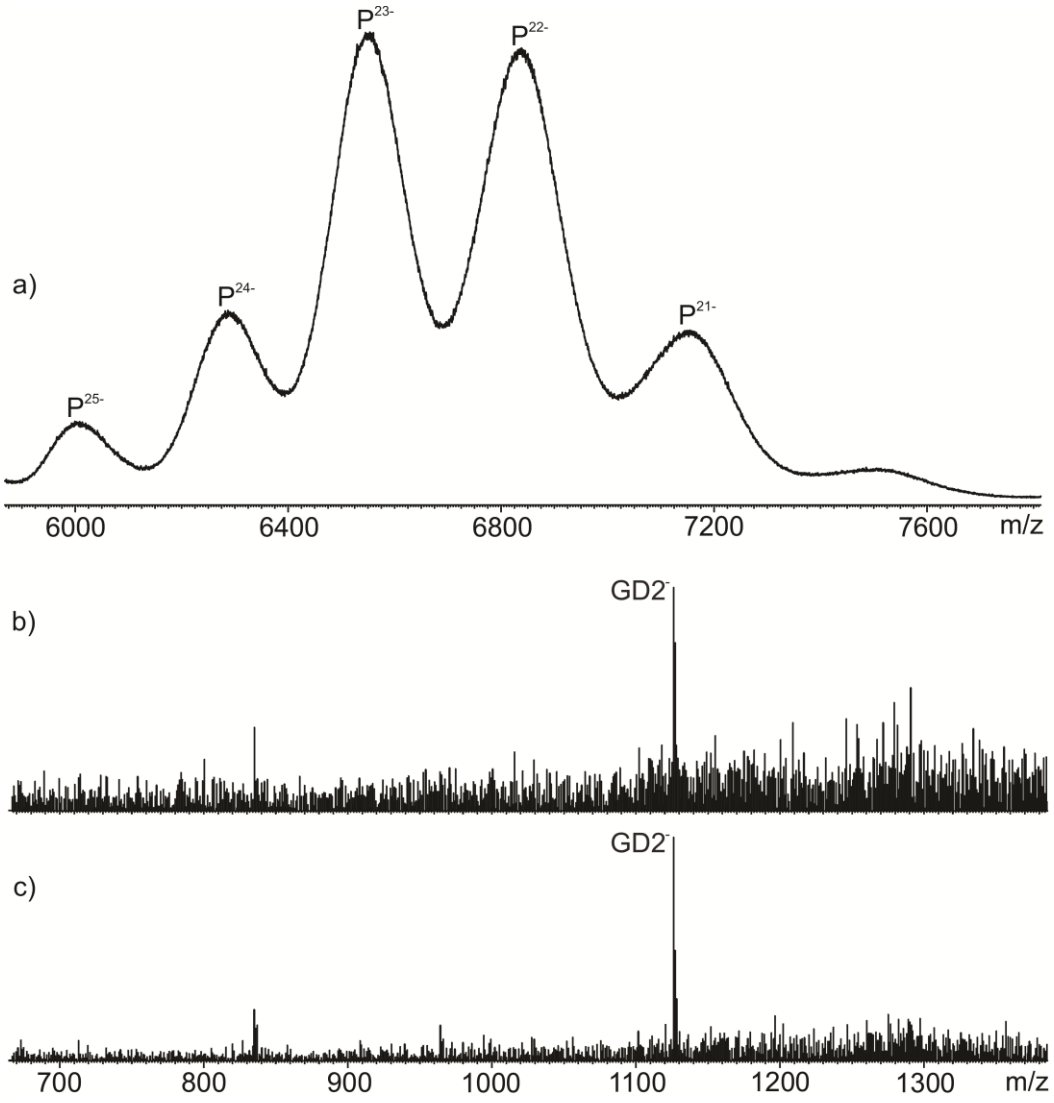

Figure 2.17 a) NanoESI acquired for human IgGs (3.6 μM) against GD2 (2 μM). GD2 released by tandem MS at m/z of 6620 for b) Incubation of 3.6 μM human IgGs with 5 μM GD2 and c) Incubation of 3.6 μM human IgGs with 2 μM GD2.

At this point, our hopes for creating a multiple sclerosis assay were abandoned. Occurrence of the complex between GD2 and the IgGs led to the further investigation of the cross-reactivity of antibodies. Although antibodies

show high degree of specificity for a single antigen, there are cases that antibody can cross-react and bind to an unrelated antigen. This happens when two different antigens have a similar epitope[136].

To probe the occurrence of the cross-reactivity, the possible complex formation of human serum IgGs and GM1 ganglioside was investigated. In order to mimic the native environment of the GM1 ganglioside in cells, this glycolipid was inserted into a ND. As such, 10% GM1 ganglioside was incorporated into the ND according to the protocol explained in chapter three. GM1-ND was run against IgGs from human serum. The peak for the GM1-ND overlapped with the peak for the IgGs (Figure 2.18).

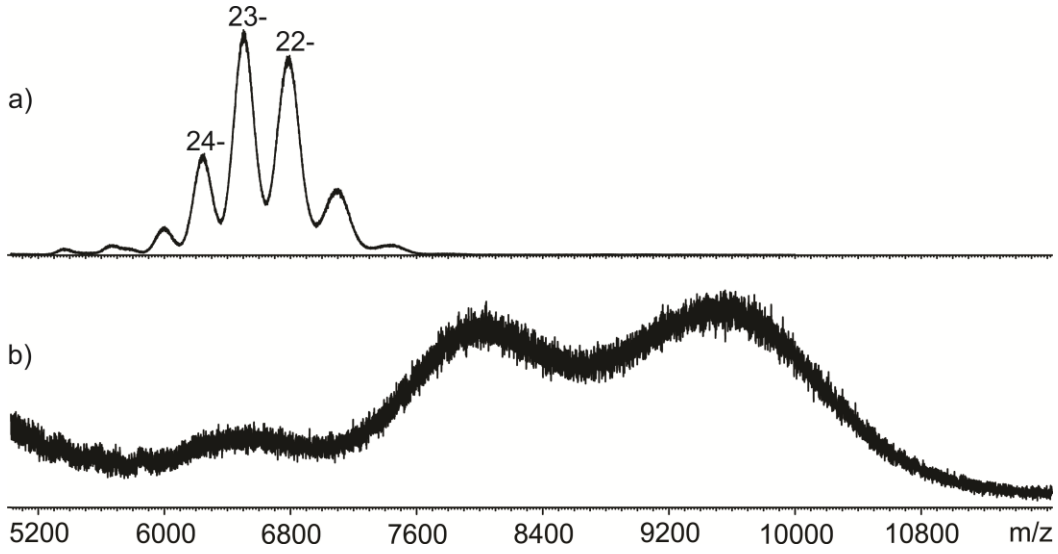

Figure 2.18 NanoESI mass spectra acquired for a) 1.7 μM Human IgGs in 200 mM and b) 3 μM 10%GM1-ND in ammonium acetate (pH 6.8) in negative ion mode. The mass spectra of human IgGs overlap with the GM1-ND peak.

To investigate further if the overlapping prevents detection of GM1 from its probable GM1-IgGs complex, tandem MS experiments were run. In one experiment 10% GM1-ND were incubated with human IgGs and tandem MS was performed on 6300 and 5700 m/z. These are the expected m/z if any complex exists. Results showed GM1 release (Figure 2.19 a,b). In a second experiment tandem MS was performed only on 10% GM1-ND at the same m/z of the first experiment. The results also show that GM1 is released (Figure 2.19 c,d). Therefore, running of the tandem MS experiment did not clarify whether GM1 was released from the probable GM1-IgGs complexes or from the GM1-ND.

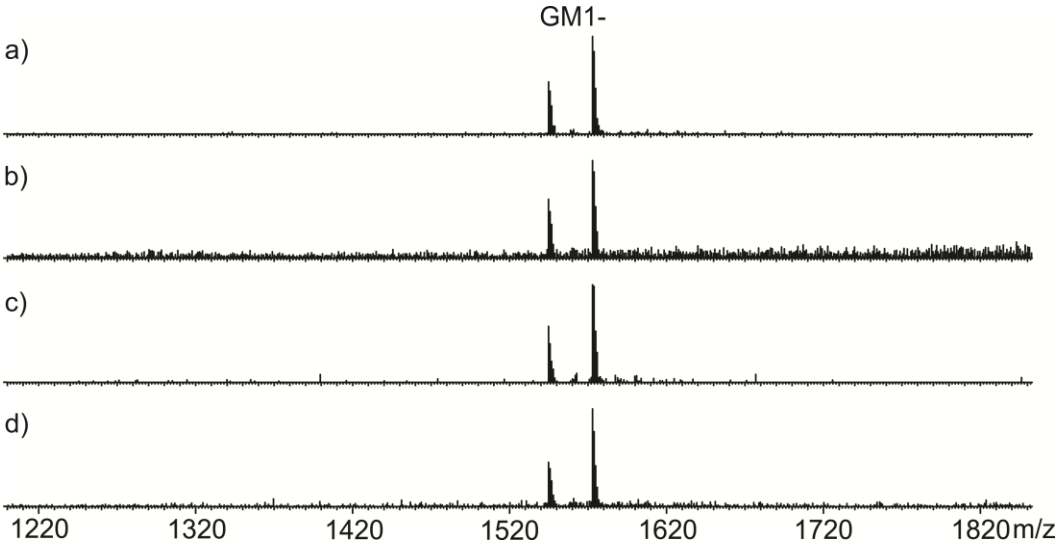

Figure 2.19 Tandem MS experiment for a mixture of 10% GM1-ND (3 μM) and Human IgGs (1.7 μM) at m/z: a) 6300, b) 5700 and for 10% GM1-ND (3 μM) at m/z: c) 6300 and d) 5700. GM1 gangliosides were released in both cases.

To avoid the overlapping problem, GM1 sugar alone was run against human IgGs. In one experiment 40 μM GM1 were run against 2 μM Human IgGs in the presence of BSA as a P_{ref}. The tandem MS experiment showed the release of GM1 from both human IgGs and the P_{ref} (Figure 2.20).

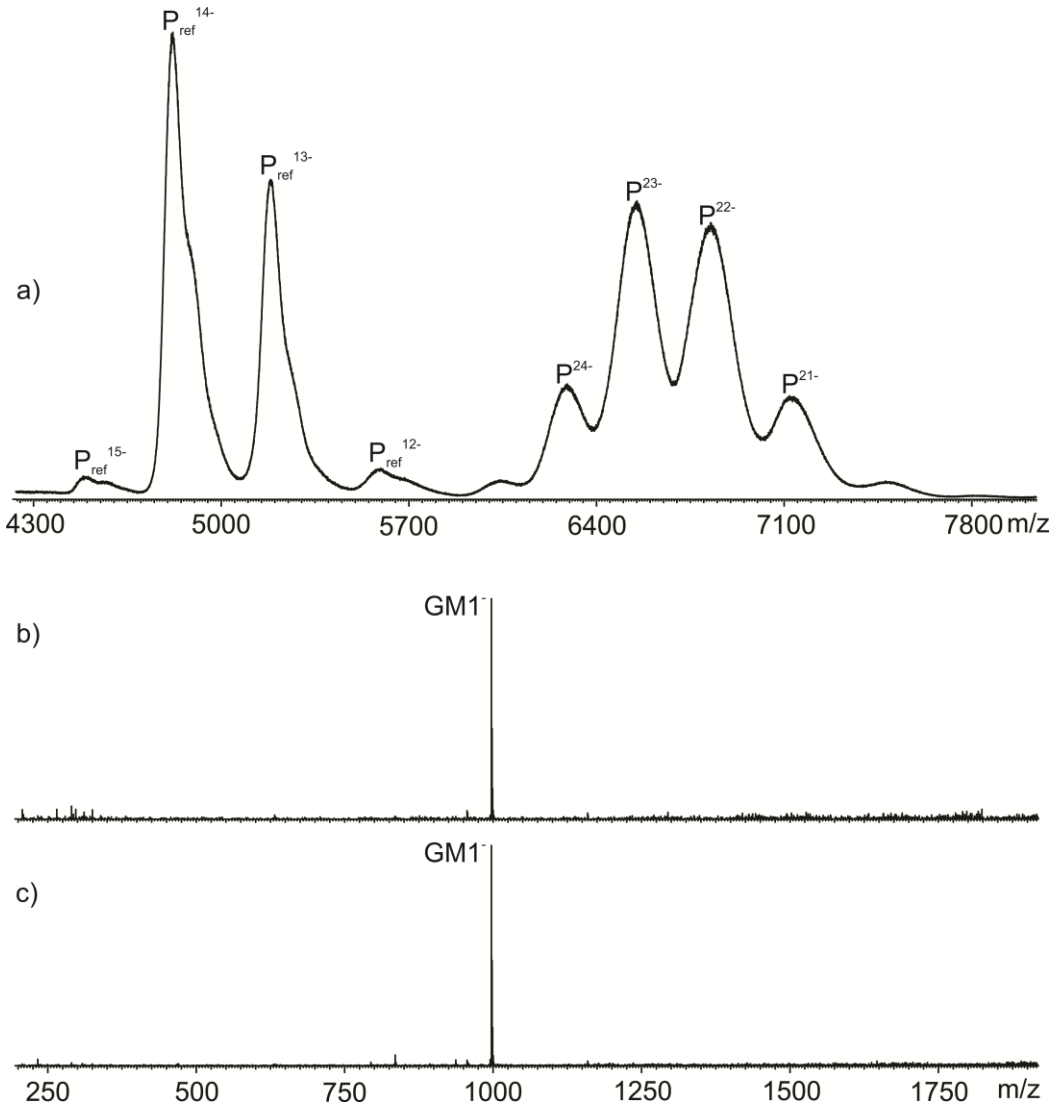

Figure 2.20 a) NanoESI mass spectra acquired for 2 μM human IgGs and 40 μM of GM1 in the presence of BSA as P_{ref}. Release of GM1 by tandem MS at m/z: b) 4890 and c) 6880.

To reduce the probability of nonspecific binding, lower concentrations of GM1 were used. Then tandem MS was performed on different parts of the IgGs and P_{ref} spectra. GM1 was still released from P_{ref} and IgGs (Figure 2.21).

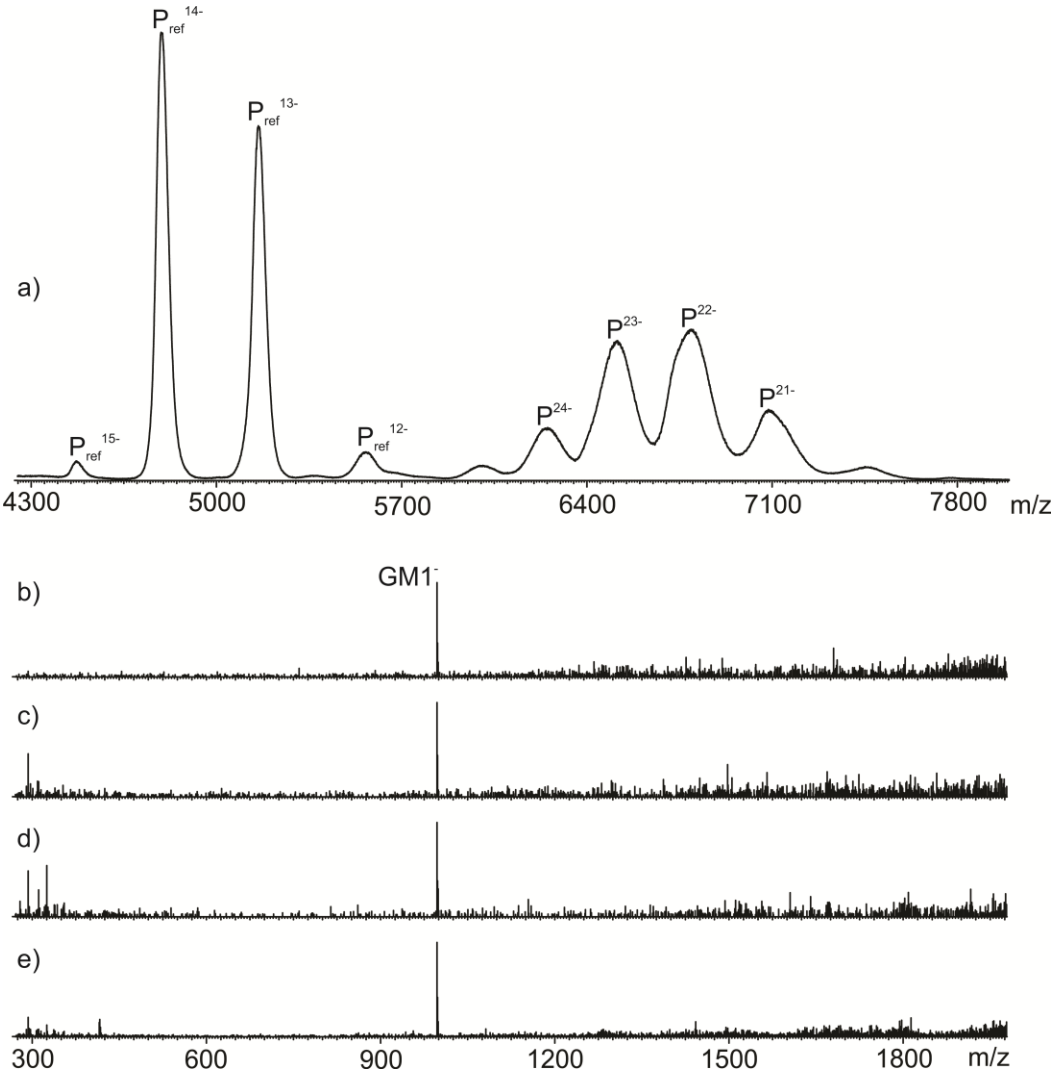

Figure 2.21 a) NanoESI mass spectra acquired from 2 μM Human IgGs and 3 μM of GM1 in negative ion mode in the presence of BSA as P_{ref}. GM1 released by tandem MS at m/z of b) 6580, c) 7150, d) 5260 and e) 4890.

In a similar experiment, to examine the occurrence of cross-reactivity between anti-GD2 antibody and GM1, 2 μM of anti-GD2 antibody was incubated with 3 μM of GM1 and the mass spectra were acquired in negative ion mode. Then tandem MS experiments were run to examine if any complexes occurred between GM1 and the antibody (Figure 2.22).

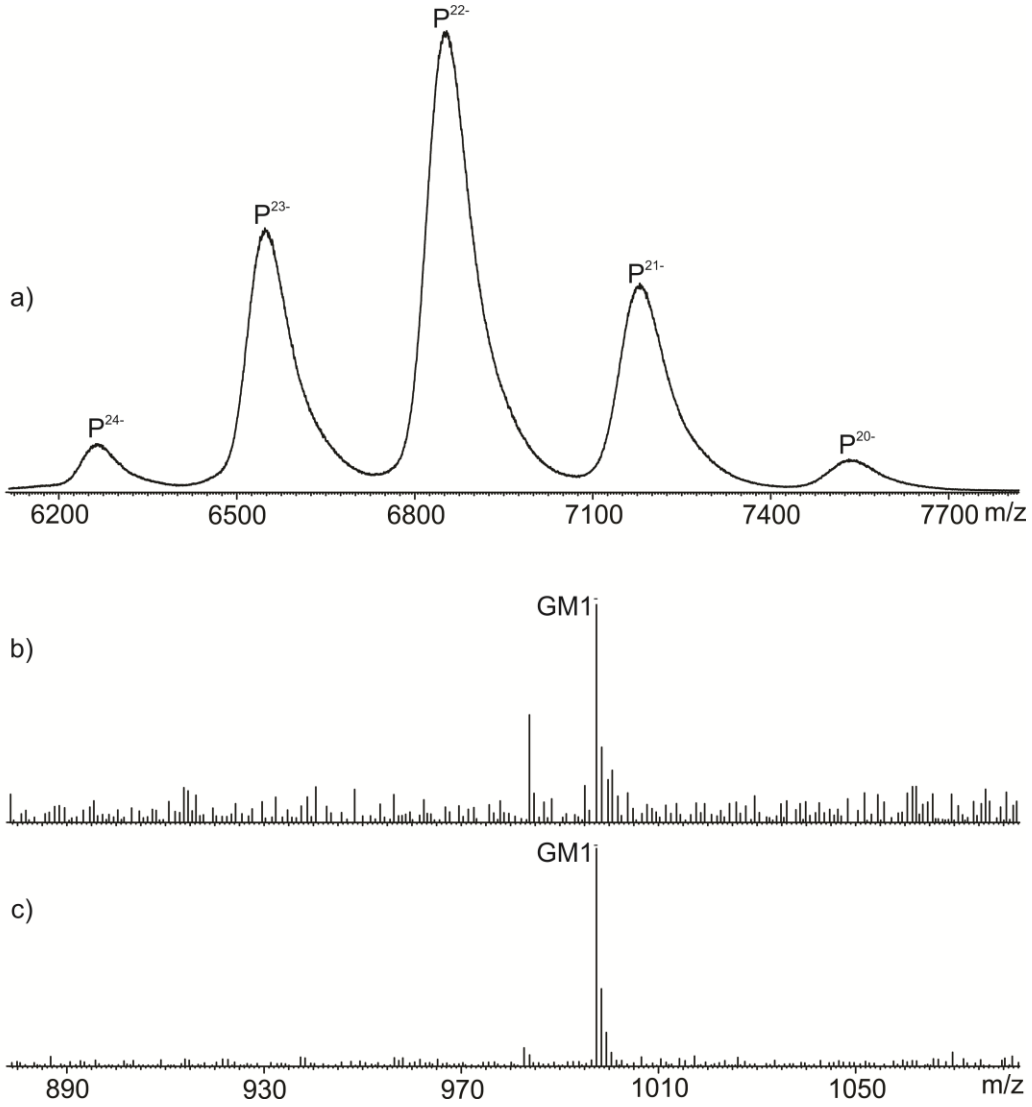

Figure 2.22 a) NanoESI experiment for 2 μM anti-GD2 antibody and 3 μM GM1 in negative ion mode. Tandem MS at m/z of b) 6890 and c) 6640 released GM1 and confirmed the formation of the complex.

Using different antibodies, another experiment was run. In this case 1.7 μM anti-his antibody was used and run against 4 μM GD2. Tandem MS at the different m/z, released GD2 from its complex with anti-his antibody (Figure 2.23).

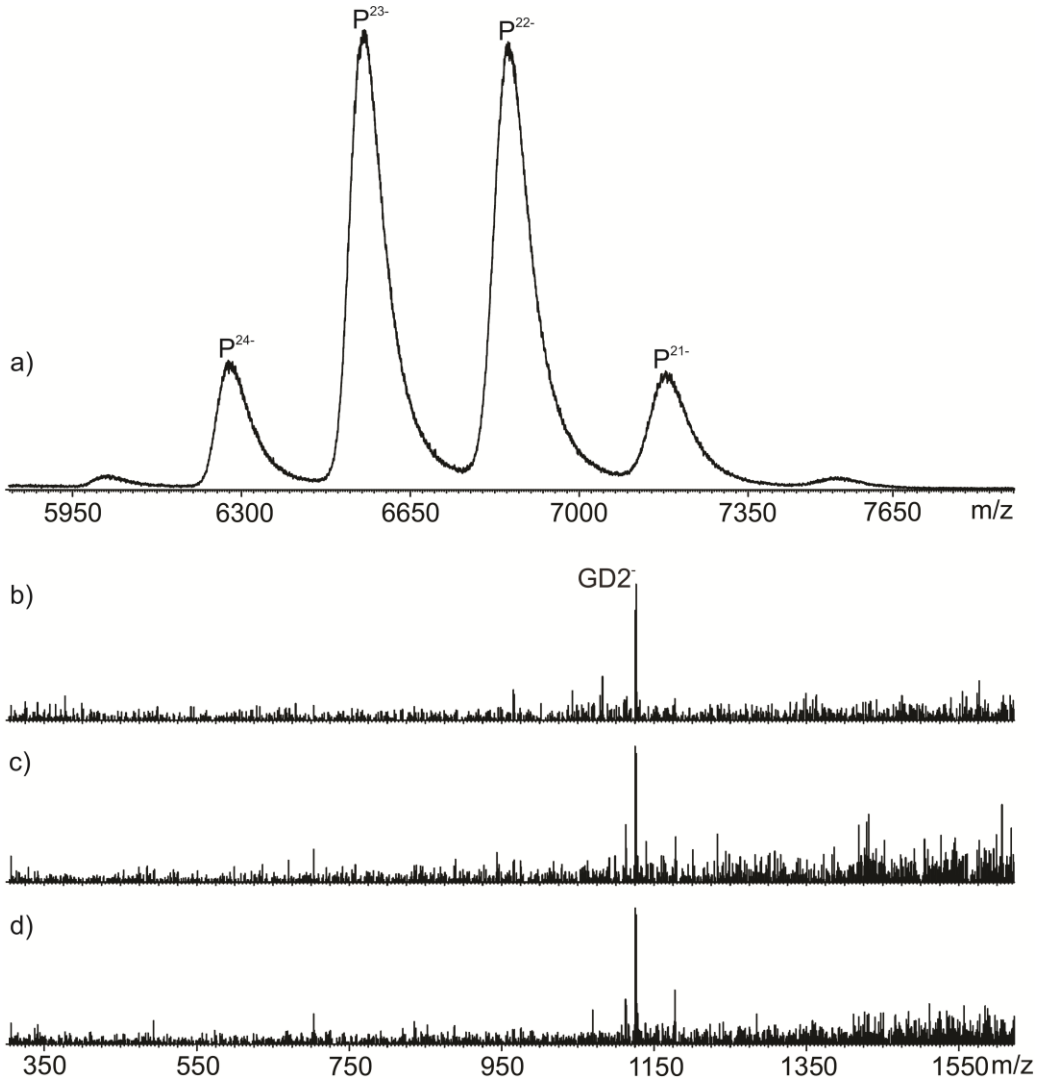

Figure 2.23 a) NanoESI mass spectra acquired for 1.7 μM anti-his antibody incubated with 4 μM GD2. Related tandem MS spectra obtained at different m/z of b) 7232, c) 6600 and d) 6907.

In another experiment maltotriose, a trisaccharide sugar incubated against human IgGs and anti-GD2 antibody in high and low concentrations. BSA was used as P_{ref}. In higher concentration of the sugar, formation of the complex was observed for both the antibodies but not for P_{ref}. (Figure 2.24). As the tandem MS was performed on the antibody-antigen complex, the source of other peaks in Figure 2.24 c) comes from fragmentation of the antibody. However, binding was detected at low concentrations for only human IgGs but not for anti-GD2 antibody (Figure 2.25).

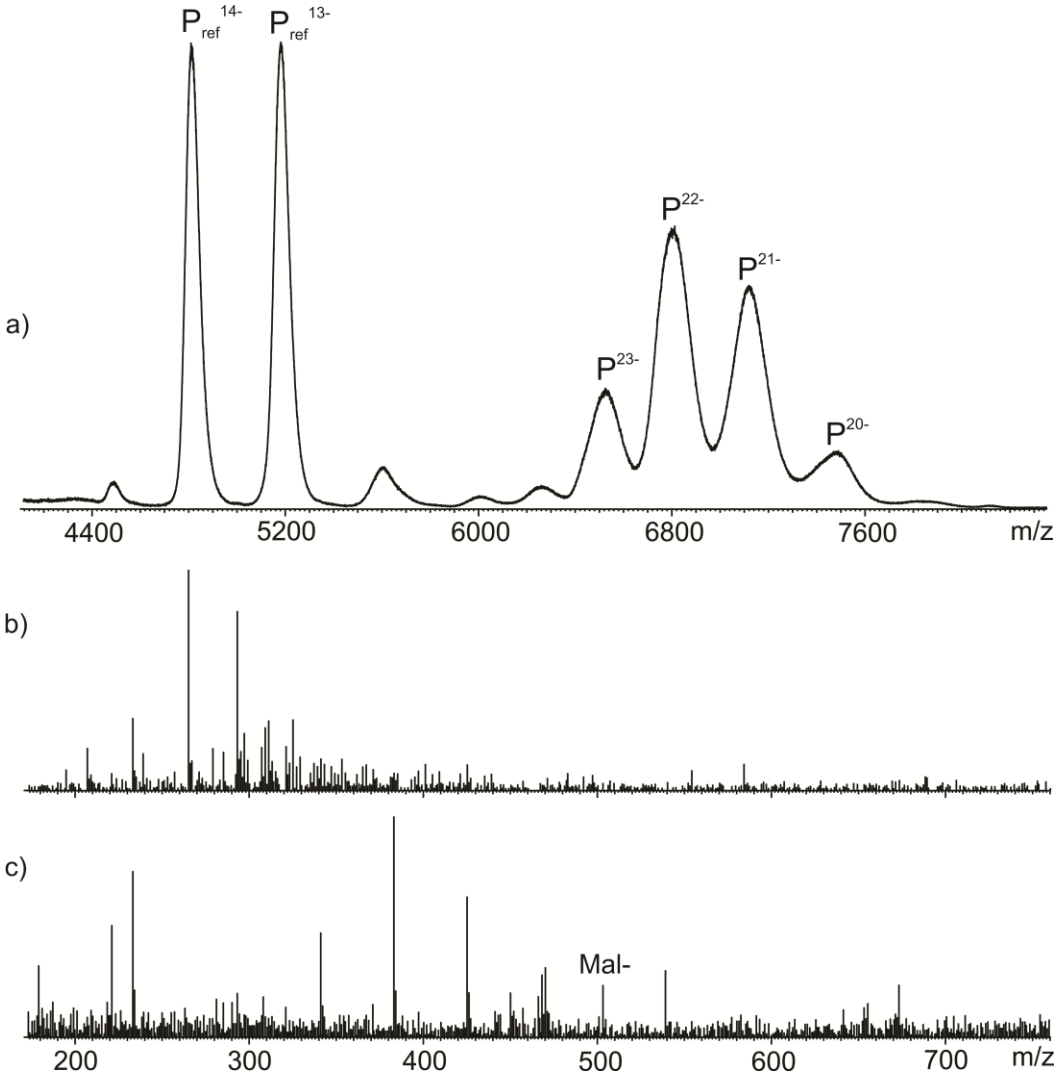

Figure 2.24 a) NanoESI mass spectra acquired in negative ion mode for 1.7 μM human IgGs against 30 μM of Maltotriose and 1 μM BSA as P_{ref}. Tandem MS acquired at m/z of b) 5220 and c) 6740. Release of Maltotriose was detected by tandem MS on the antibody peak.

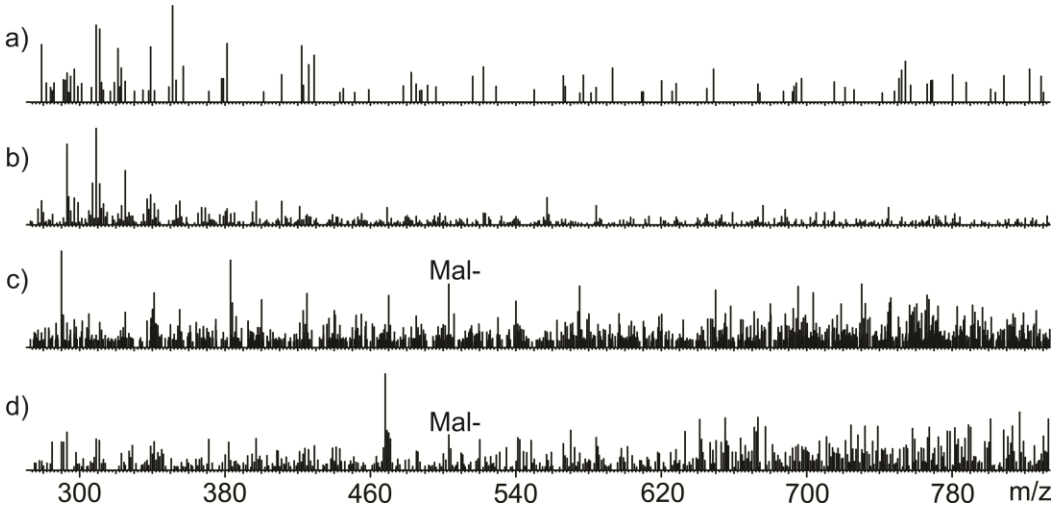

Figure 2.25 Tandem MS acquired in negative ion mode for 1.7 μM human IgGs against 3 μM of Maltotriose and 1 μM BSA at m/z of a) 5641, b) 5214 for P_{ref} and c) 7172, d) 7148 for the antibody.

From this cross-reactivity investigation, the interaction of different antibodies with different oligosaccharides was examined. In the experiment with GM1, using BSA as P_{ref} was not a good choice as it is known that GM1 binds specifically to BSA. Even at low GM1 concentration, the GM1-BSA binding was observed making it difficult to distinguish the observed GM1-antibody complexes that may arise due to occurrence of specific or nonspecific binding. In the case of incubating GD2 sugar at low concentration with anti-his antibody, the antibody-GD2 complex was detected. This suggests the occurrence of cross-reactivity.

Finally maltotriose with high and low concentrations was incubated with human IgGs and anti-GD2 antibody. No binding was observed between BSA and maltitriose in low and high concentrations. However, human IgGs-maltotriose complex was detected by tandem MS in high and low concentrations of

maltotriose suggesting the occurrence of cross-reactivity of human IgGs and maltotriose. While using anti-GD2 antibody, the complex of anti-GD2 antibody with maltotriose was only detected at high concentrations of the sugar, implying the probable occurrence of nonspecific binding. Overall, cross-reactivities can be due to nonspecific hydrophobic interaction or as a result of specific contacts through strong electrostatic interaction between antibody and antigen. Although use of a low concentration of antigen is a way to reduce the occurrence of nonspecific binding, exact determination between specific cross-reactivity or nonspecific cross-reactivity is a matter of further investigations by other techniques such as computational methods[137].

To examine the effect of the glycans on antibody-antigen interaction, anti-GD2 antibody was deglycosylated. For this purpose PNGase F enzyme was used. This enzyme is more suitable for working on denatured antibody. The aim of this experiment was to examine if deglycosylation had any adverse effect on the stability of the antibody-antigen complex at high cone voltages. Hence, it was necessary to keep the antibody in its folded state. So according to the recommendation of the enzyme company (New England Biolabs), the amount of enzyme and incubation time was increased for working on the folded antibody. For the experiment 20 μL antiGD2 antibody (1mg/mL) was mixed with 4 μL of PNGase F, 4 μL reaction buffer (0.5 M sodium acetate, 50 mM $CaCl_2$, pH 5.5) and 12 μL of milliQ water and incubated for 20 hours at 37°C.

After buffer exchange with 200 mM ammonium acetate, the sample was sprayed into the MS. The results show that the antibody is not completely deglycosylated. Three antibodies species were detected; intact antibody, partially deglycosylated antibody and deglycosylated antibody (Figure 2.26,a). In the next step 1.5 μM of the antibody was incubated with 40 μM GD2 and sprayed into the MS (Figure 2.26,b). A complex mass spectrum related to attachment of one and two molecules of GD2 to each species of antibody was obtained.

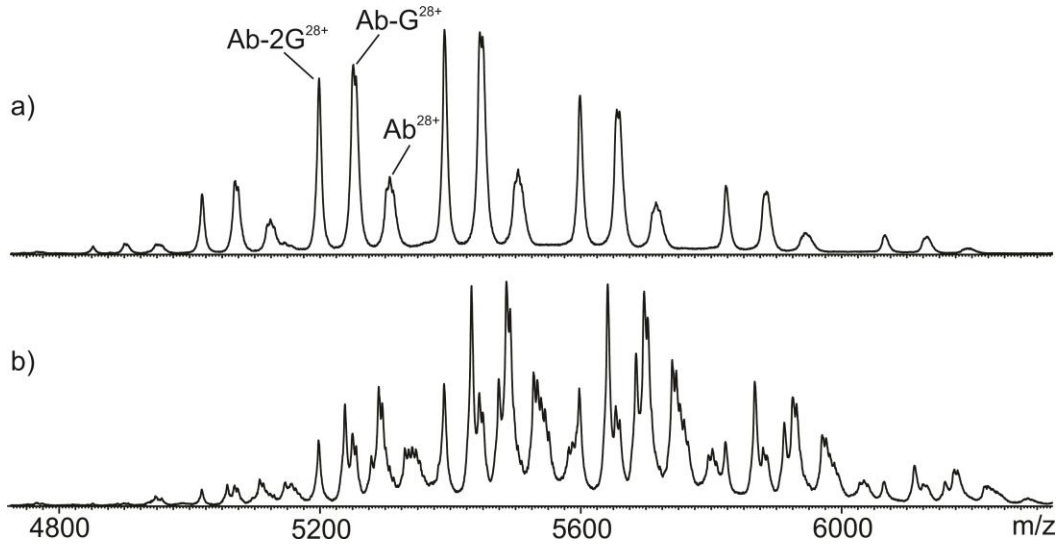

Figure 2.26 NanoESI mass spectra acquired for a) 1.5 μM deglycosylated anti-GD2 antibody sprayed in 200 mM ammonium acetate buffer (pH 6.8). Three species of the antibody were detected, (G: Glycan) b) deglycosylated antibody incubated with 40 μM GD2. Mixtures of different antibody- antigen complexes were obtained.

Figure 2.27 shows a closer look at the 26+ charge state. Identification of the peaks was further confirmed by tandem MS and the release of the GD2 molecules. A rough estimation from the appearance of the spectrum suggest that deglycosylation of the antibody did not have effect on the antibody's ability to bind to its antigen. However, as the antibody was not completely deglycosylated, the whole spectrum is a complicated mixture of different complexes of the antibody with different charge states. Some peaks being hidden under the other peak complexes make quantitative measurement of the interaction inaccurate.

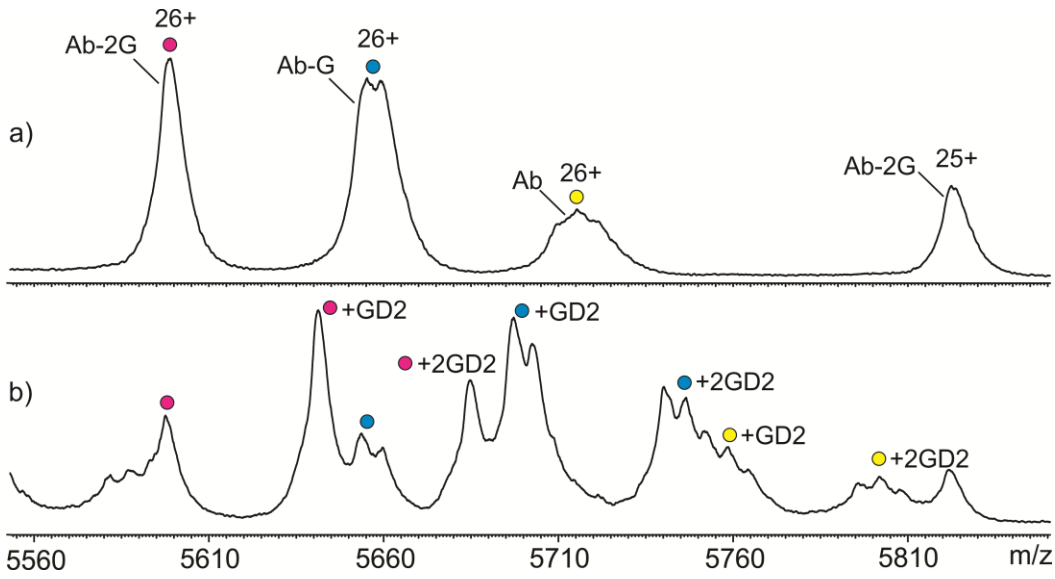

Figure 2.27 a) A closer look at Figure 2.18 b) mass spectra at 26+ charge state. ● : Ab-2G (deglycosylated antibody), ● : Ab-G (Partially deglycosylated antibody), ○: Ab (Intact antibody).

2.5 Conclusion

The present work introduced the first direct quantitative assay for measuring antibody-antigen interaction using nanoESI-MS. In this assay, two conditions were taken into account: the existence of nonspecific binding and the lack of nonspecific binding. The binding constants of anti-GD2 mAb/GD2 sugar complex obtained from titration curves were consistent in both negative and positive ion mode, and in different cone voltages. Unfortunately, we were not successful on validating our method with a well-established CS-35 mAb/H-Araf complex due to purity, heterogeneity and stability issues of CS-35.

In addition, cross-reactivity of different antibodies have been examined qualitatively by MS. It has been known that antibodies are specific for their cognate antigen. However, the results here suggested that antibodies can have cross-reactivity to a certain extent. The present work needs further analysis on more antibody samples against a variety of target antigens for a more detailed cross-reactivity profiling. With our new assay, another antibody-antigen system with known binding data must be used to further weigh the reliability of the assay.

Conditions such as temperature, pH and ionic strength have direct effect on antibody‘s behavior, stability and interaction towards its antigen. To be able to efficiently evaluate the effects of these conditions and quantify changes on binding interactions, our newly developed strategy should be validated by using an antibody-antigen complex with a known binding constant. This is of great use in therapeutic monoclonal antibody development and antibody research.

2.6 Literature cited

109. Mould, D. R.; Sweeney, K. R., The pharmacokinetics and pharmacodynamics of monoclonal antibodies-mechanistic modeling applied to drug development. *Current Opinion in Drug Discovery and Development* **2007,** *10* (1), 84.

110. Nimmo, I.; Atkins, G. L.; Strange, R. C.; Percy-Robb, I. W., An evaluation of ways of using equilibrium dialysis to quantify the binding of ligand to macromolecule. *Biochem. J* **1977,** *165*, 107-110.

111. Bee, C.; Abdiche, Y. N.; Pons, J.; Rajpal, A., Determining the Binding Affinity of Therapeutic Monoclonal Antibodies towards Their Native Unpurified Antigens in Human Serum. *PLoS One* **2013,** *8* (11), e80501.

112. Stoop, M. P.; Dekker, L. J.; Titulaer, M. K.; Burgers, P. C.; Sillevis Smitt, P. A.; Luider, T. M.; Hintzen, R. Q., Multiple sclerosis-related proteins identified in cerebrospinal fluid by advanced mass spectrometry. *Proteomics* **2008,** *8* (8), 1576-1585.

113. Thamilarasan, M.; Hecker, M.; Goertsches, R. H.; Paap, B. K.; Schröder, I.; Koczan, D.; Thiesen, H.-J.; Zettl, U. K., Glatiramer acetate treatment effects on gene expression in monocytes of multiple sclerosis patients. *Journal of Neuroinflammation* **2013,** *10* (1), 126.

114. Rolak, L. A.; Fleming, J. O., The differential diagnosis of multiple sclerosis. *The Neurologist* **2007,** *13* (2), 57-72.

115. Fuhr, P.; Borggrefe-Chappuis, A.; Schindler, C.; Kappos, L., Visual and motor evoked potentials in the course of multiple sclerosis. *Brain* **2001,** *124* (11), 2162-2168.

116. Seehusen, D. A.; Reeves, M. M.; Fomin, D. A., Cerebrospinal fluid analysis. *American Family Physician* **2003,** *68* (6), 1103-1108.

117. de Graaf, M. T.; de Jongste, A. H.; Kraan, J.; Boonstra, J. G.; Smitt, P. A.; Gratama, J. W., Flow cytometric characterization of cerebrospinal fluid cells. *Cytometry Part B: Clinical Cytometry* **2011,** *80* (5), 271-281.

118. Noga, M. J.; Dane, A.; Shi, S.; Attali, A.; van Aken, H.; Suidgeest, E.; Tuinstra, T.; Muilwijk, B.; Coulier, L.; Luider, T., Metabolomics of cerebrospinal fluid reveals changes in the central nervous system metabolism in a rat model of multiple sclerosis. *Metabolomics* **2012,** *8* (2), 253-263.

119. Jia, Y.; Wu, T.; Jelinek, C. A.; Bielekova, B.; Chang, L.; Newsome, S.; Gnanapavan, S.; Giovannoni, G.; Chen, D.; Calabresi, P. A., Development of protein biomarkers in cerebrospinal fluid for secondary progressive multiple sclerosis using selected reaction monitoring mass spectrometry (SRM-MS). *Clin Proteomics* **2012,** *9* (9).

120. Kanda, T.; Iwasaki, T.; Yamawaki, M.; Tai, T.; Mizusawa, H., Anti-GM1 antibody facilitates leakage in an in vitro blood–nerve barrier model. *Neurology* **2000,** *55* (4), 585-587.

121. Vyshkina, T.; Kalman, B., Autoantibodies and neurodegeneration in multiple sclerosis. *Laboratory Investigation* **2008,** *88* (8), 796-807.

122. Krebs, J. F.; Siuzdak, G.; Dyson, H. J.; Stewart, J. D.; Benkovic, S. J., Detection of a catalytic antibody species acylated at the active site by electrospray mass spectrometry. *Biochemistry* **1995,** *34* (3), 720-723.

123. Bennett, K. L.; Smith, S. V.; Lambrecht, R. M.; Truscott, R. J.; Sheil, M. M., Rapid characterization of chemically-modified proteins by electrospray mass spectrometry. *Bioconjugate Chemistry* **1996,** *7* (1), 16-22.

124. Siuzdak, G.; Krebs, J. F.; Benkovic, S. J.; Dyson, H. J., Binding of hapten to a single-chain catalytic antibody demonstrated by electrospray mass spectrometry. *Journal of the American Chemical Society* **1994,** *116* (17), 7937-7938.

125. Uetrecht, C.; Heck, A. J., Modern biomolecular mass spectrometry and its role in studying virus structure, dynamics, and assembly. *Angewandte Chemie International Edition* **2011,** *50* (36), 8248-8262.

126. Rostom, A. A.; Robinson, C. V., Detection of the intact GroEL chaperonin assembly by mass spectrometry. *Journal of the American Chemical Society* **1999,** *121* (19), 4718-4719.

127. Tito, M. A.; Miller, J.; Walker, N.; Griffin, K. F.; Williamson, E. D.; Despeyroux-Hill, D.; Titball, R. W.; Robinson, C. V., Probing molecular interactions in intact antibody: antigen complexes, an electrospray time-of-flight mass spectrometry approach. *Biophysical Journal* **2001,** *81* (6), 3503-3509.

128. Rosati, S.; Yang, Y.; Barendregt, A.; Heck, A. J., Detailed mass analysis of structural heterogeneity in monoclonal antibodies using native mass spectrometry. *Nature Protocols* **2014,** *9* (4), 967-976.

129. Rose, R. J.; Labrijn, A. F.; van den Bremer, E. T.; Loverix, S.; Lasters, I.; van Berkel, P. H.; van de Winkel, J. G.; Schuurman, J.; Parren, P. W.; Heck, A. J., Quantitative analysis of the interaction strength and dynamics of human IgG4 half molecules by native mass spectrometry. *Structure* **2011,** *19* (9), 1274-1282.

130. Thompson, N. J.; Rosati, S.; Heck, A. J., Performing native mass spectrometry analysis on therapeutic antibodies. *Methods* **2014,** *65* (1), 11-17.

131. Houde, D.; Peng, Y.; Berkowitz, S. A.; Engen, J. R., Post-translational modifications differentially affect IgG1 conformation and receptor binding. *Molecular & Cellular Proteomics* **2010,** *9* (8), 1716-1728.

132. Collin, M.; Olsén, A., EndoS, a novel secreted protein from Streptococcus pyogenes with endoglycosidase activity on human IgG. *The EMBO Journal* **2001,** *20* (12), 3046-3055.

133. Kitova, E. N.; Bundle, D. R.; Klassen, J. S., Thermal dissociation of protein-oligosaccharide complexes in the gas phase: Mapping the intrinsic intermolecular interactions. *Journal of the American Chemical Society* **2002,** *124* (20), 5902-5913.

134. Kaur, D.; Lowary, T. L.; Vissa, V. D.; Crick, D. C.; Brennan, P. J., Characterization of the epitope of anti-lipoarabinomannan antibodies as

the terminal hexaarabinofuranosyl motif of mycobacterial arabinans. *Microbiology* **2002,** *148* (10), 3049-3057.

135. Sarkar, S.; Tang, X. L.; Das, D.; Spencer, J. S.; Lowary, T. L.; Suresh, M. R., A bispecific antibody based assay shows potential for detecting tuberculosis in resource constrained laboratory settings. *PLoS One* **2012,** *7* (2), e32340.

136. Klinman, D.; Banks, S.; Hartman, A.; Steinberg, A., Natural murine autoantibodies and conventional antibodies exhibit similar degrees of antigenic cross-reactivity. *Journal of Clinical Investigation* **1988,** *82* (2), 652.

137. James, L. C.; Tawfik, D. S., The specificity of cross-reactivity: promiscuous antibody binding involves specific hydrogen bonds rather than nonspecific hydrophobic stickiness. *Protein Science* **2003,** *12* (10), 2183-2193.

Chapter3

Using Nanodisc for characterization of Protein Ligand Interaction by Surface Plasmon resonance and Mass spectrometry

3.1 Introduction

Interactions of membrane associated biomolecules with their ligands play a crucial role in biological regulations as well as in viral and pathogen invasion. Interactions of toxins with membrane proteins and cell-surface glycans are critical for progression of infectious diseases. Study of these interactions gives us deeper insights on their mechanisms, leading to better drug designs and therapeutic strategies.

In recent years, studies on interactions of membrane related macromolecules such as proteins are rapidly increasing. However, maintaining these macromolecules in their native conformation or evaluating their interactions at physiological conditions continues to be a challenge for researchers due to their instability in aqueous media. ND technology, first introduced by the Sligar lab[138], has greatly facilitated research, because of their ability to mimic a cell membrane. ND is a self-assembled synthetic membrane model, as such, it can be used to study membrane proteins and other membrane associated biomolecules. In 2008, an attempt of using ND with SPR measurement was demonstrated by Borch *et. al* [108]. They immobilized GM1-ND on a CM5 sensor chip and obtained kinetic data for the interaction between GM1 and cholera toxin B subunit (CTB). In 2011, the

same group succeeded in applying ND technology to MS[139]. Since then, different research groups have used MS to investigate biological interactions with ND as a membrane model. In 2012, for the first time GM1-ND was used in our lab to investigate its interaction with cholera toxin using ESI-MS [140].

In this chapter, we describe our efforts in applying ND as a membrane model for incorporation and solubilization of different fatty acids and gangliosides. We will use SPR and MS measurements to analyze them. Here, we attempted to investigate the effects of fatty acid chain lengths to its degree of incorporation into ND using MS. The results can be used for synthesis purposes where biologically important carbohydrates require a carbon chain to incorporate into ND. We have also attempted to use ND as a ganglioside scaffold for investigating kinetics and affinity interactions of ganglioside-NDs and their target receptor using SPR.

3.2 Incorporating different fatty acids into nanodiscs

3.2.1 Experimental section

1,2-dimyristoyl-*sn*-glycero-3-phosphocholine (DMPC) was purchased from Avanti Polar Lipids. Globotriaosylceramide (Gal(α1-4)Gal(β-4)Glc(β1)-ceramide, Gb3-Cer) was purchased from Abcam. All the fatty acids were purchased from Sigma Aldrich. Other chemicals and detergents were purchased from Sigma Aldrich or Thermo Fisher Scientific Inc.

3.2.1.2 Sample preparation

3.2.1.2.1 Expression and purification of membrane scaffold protein

Membrane scaffold protein MSP1E1 (MW 29 494Da) was prepared from plasmid pMSP1E1 with pET 28a system (Novagen) backbone requested from Addgene (Cambridge, MA). Expression and purification of this protein was carried out using the protocol described at http://sligarlab.life.uiuc.edu/nanodisc.html with some modifications. PMSP1E1 was transformed chemically to E. coli BL21 (DE3) codon plus, plated and incubated overnight at 37^{o}C. A colony was picked and inoculated for another day in lysogeny broth (LB) media containing 30 μg/mL kanamycin and 40 mL of this subculture was transferred to 1 L terrific broth (TB) media containing 30 μg/mL kanamycin and incubated at 37^{o}C under 250 rpm rotary shaking until OD_{600} reached 0.6 - 0.8. Protein expression was induced by adding 1mM of Isopropyl β-D-1-thiogalactopyranoside (IPTG) and further incubated for another 3 hours. Cells were harvested by centrifugation (Beckman) at 8000 x g for 20 min., resuspended in 20mM phosphate buffer (pH 7.4) with 1% Triton X-100 and lysed using a homogenizer (Expression Constant Ltd) under 20 kpsi. The resulting mixture was cleared by centrifugation at 8000 x g for 20 min. to separate proteins from cell debris. Supernatant solution containing soluble fraction of MSP1E1 was mixed with Ni-NTA agarose resin (Qiagen) and shaked at 4^{o}C for 1 hour. The protein-resin mixture was washed with 20 mM phosphate buffer (pH 8.0) with 20

mM imidazole to remove impurities and eluted with 20 mM phosphate buffer (pH 7.4) with 200 mM imidazole. The purity of MSP1E1 was evaluated using sodium dodecyl sulfate-polyacrylamide gel electrophoresis (SDS-PAGE) and MS. Finally, purified MSP1E1 was dialyzed with ND buffer (20 mM Tris, 0.1 M NaCl, 0.5 mM EDTA, pH 7.4), 8 hours x 3 and stored at -80ºC. The MSP1E1 concentration was determined by absorbance at 280 nm using literature extinction coefficient.

3.2.1.2.2 Nanodiscs synthesis

For the present work three different types of NDs were prepared which included ND with DMPC alone, ND with gangliosides incorporated into DMPC bilayer and ND with fatty acids incorporated into the DMPC bilayer. Empty discs containing MSP1E1 and DMPC were prepared at a protein to lipid molar ratio of 1:100. At first the desired amount of DMPC was dried in a glass tube under a gentle stream of nitrogen gas to remove the chloroform solvent, the dried lipid was then kept in a desiccator overnight. To prepare NDs containing gangliosides or fatty acids, different percentages of gangliosides or fatty acids according to each experiment were added to the DMPC solution and dried as above. The dried lipids were solubilized into Tris buffer (20 mM Tris, 0.1 M NaCl and 0.5 mM EDTA, pH 7.4) containing 25 mM sodium cholate (cholate concentration is twice the concentration of lipid) and sonicated for 20 min at 35°C. Then an amount of MSP1E1 was added in accordance with the abovementioned ratio, to cholate

solubilized lipids and the solution was incubated for 30 min at room temperature. The NDs underwent self-assembly when equal volume of biobeads SM-2 (Bio-Rad) was added into the solution. The suspension was gently agitated at 25°C for 3 hours. Then the biobeads were removed and the supernatant was injected into a Superdex 200 HR 10/300 GL column (GE Healthcare). ND fractions were collected, concentrated and the buffer exchanged into a proper buffer according to their next use in MS or SPR then stored at -80°C. In a similar procedure, four different fatty acids were incorporated into NDs. This includes: palmitic acid ($C_{16}H_{32}O_{2,}$ MW 256.24), stearic acid ($C_{18}H_{36}O_{2,}$ MW 284.27), arachidic acid ($C_{20}H_{40}O_{2,}$ MW 312.30) and behenic acid ($C_{22}H_{44}O_{2,}$ MW 340.33). It is noteworthy that fatty acids have only one carbon chain. Every DMPC molecule contains two carbon chains, two fatty acid molecules are required in order to be replaced by one DMPC molecule. This should be taken into account to successfully incorporate fatty acids into NDs.

3.2.2 Mass spectrometry measurements

The present work was performed using a Synapt G2-S quadrupole-ion mobility separation time-of-flight (Q-IMS-TOF) mass spectrometer (Waters, UK) and a nanoflow ESI source. Tips made of borosilicate capillaries produced by and pulled to 0.5 μm using a P-1000 micropipette puller for nanoESI experiment. A platinum wire was inserted into the tip, and a capillary voltage of 0.8−1.0 k was applied to perform nanoESI. NanoESI mass spectra were measured in negative

ion mode in 200mM ammonium acetate buffer solution (pH 6.8). To confirm the incorporation of the fatty acids into the ND, quadrupole mass filter was used to isolate ions at different parts of the ND peak. Then the collision energy in the Trap ion guide was increased from 5 V to 150 V to release the fatty acids from the ND. The released fatty acids were then subjected to mass analysis for identification.

3.2.2.1 Results and discussion

To study the effect of fatty acid chain length on their incorporation into NDs, different NDs with fatty acids were used including: 1% stearic acid ND, 1% palmitic acid ND, 1% archidic acid ND, 1% behimitic acid ND, ND made with four different fatty acids (1% palmitic acid, 1% stearic acid, 1% arachidic acid, 1% behenic acid) and (1.5% palmitic acid, 1.5% stearic acid, 1.5% arachidic acid, 1.5% behenic acid). Empty ND was used as control.

At the first step NDs containing only DMPC were sprayed into MS as control and tandem mass was performed at different m/z on the broad peak corresponding to the gaseous ions of intact NDs (Figure 3.1). As shown in Figure 3.1, there are some ion peaks in the lower m/z area of the nanoESI mass spectrum and the tandem mass spectrum, their molecular weight matches with those of the chosen fatty acids which will be applied in further experiments.

In order to confirm the source of the ion peaks, MSP and DMPC, of which an empty ND is made from was individually sprayed. It became clear that DMPC

is the source. The DMPC molecule consists of two fatty acid hydrocarbon chain. In our case the DMPC had 14 carbon atoms in every chain. This is the dominant species of DMPC molecules; however the length of the carbon chain can differ. This diversity is observable by the release of different fatty acid anions with different molar mass. Next, the four fatty acids were incorporated into their individual NDs with 1% molar ratio of fatty acid to lipid. The final concentration of each fatty acid NDs in the final solution is 6.4 μM. The mass spectrum and the results for tandem mass at different areas of the ND peak are depicted in Figure 3.2.

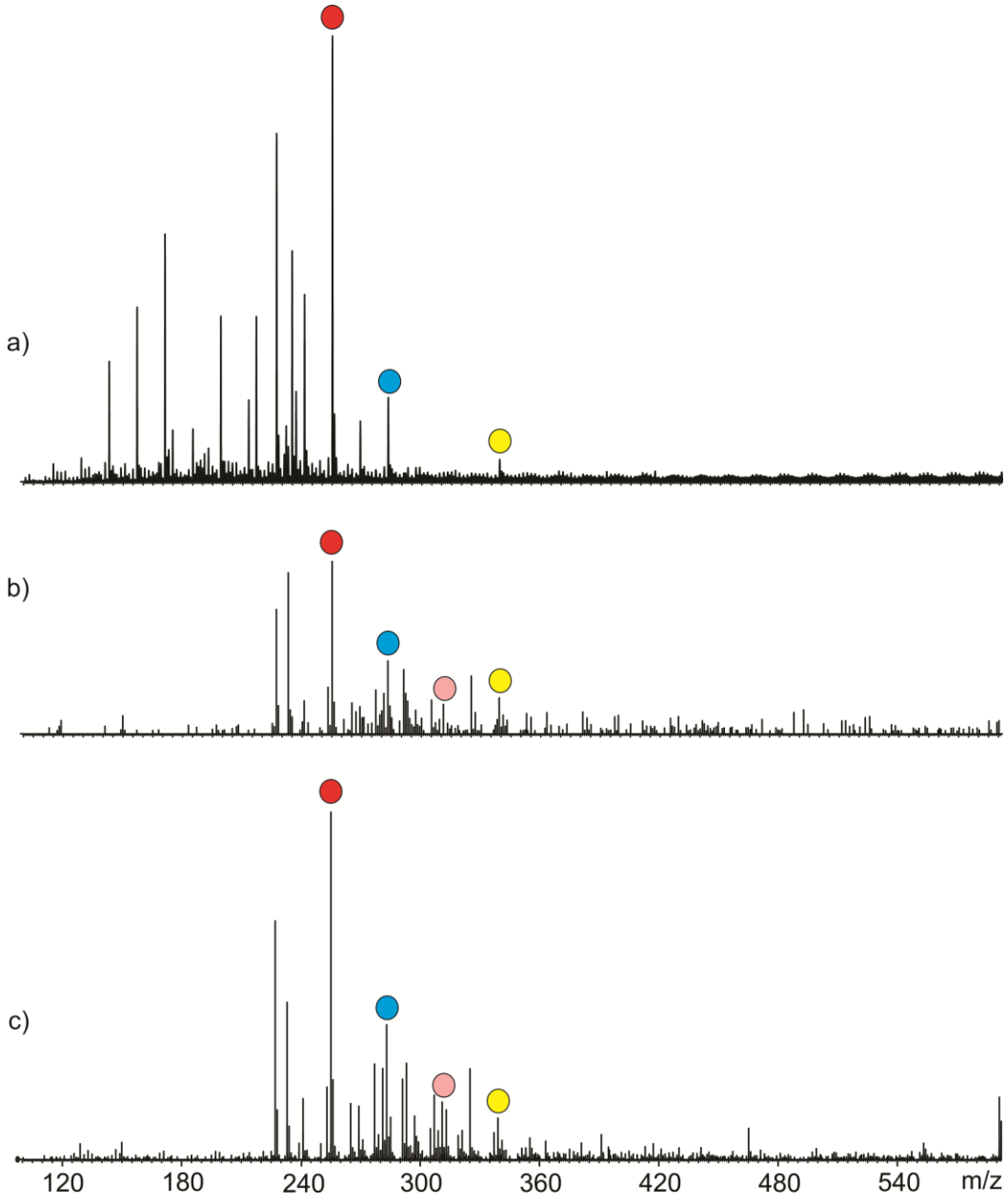

Figure 3.1 a) NanoESI mass spectra acquired in negative ion mode for empty ND, and tandem mass spectra acquired using isolation window centered at m/z of: b) 11000 c) 12000. Some ion species were released at the same m/z value of the fatty acids: palmitic acid, stearic acid, arachidic acid and behenic acid.

According to the results and comparison of the intensities, the amount of behenic acid incorporation into the ND was more than that of the other fatty acids. This fatty acid has the longest carbon chain (22 carbon). Following behenic acid is arachidic acid (20 carbon), stearic acid (18 carbon) and palmitic acid (16 carbon). Considering that the DMPC is a phospholipid molecule with 14 Carbon and that ND consist of two layers of DMPC molecules, a probable explanation is that behenic acid has more carbon in its chain which allows greater hydrophobic interaction with the carbon chain of the DMPC and as a result incorporates more efficiently into the ND.

In another experiment the four different fatty acids were incorporated together into ND with equal molar ratio of 1% for each fatty acid. The NDs were sprayed into MS and tandem mass were performed at different m/z on the ND peak. By increasing energy in the trap region the incorporated fatty acid was released. The results for the experiments were consistent with the previous result in Figure 3.2 where the four different NDs were mixed with each other and sprayed (Figure 3.4). The spectra are quite similar. To prove the reliability and reproducibility of the experiment, the NDs were prepared by incorporating the four fatty acids in them, this time with a molar ratio of 1.5% for each fatty acid.

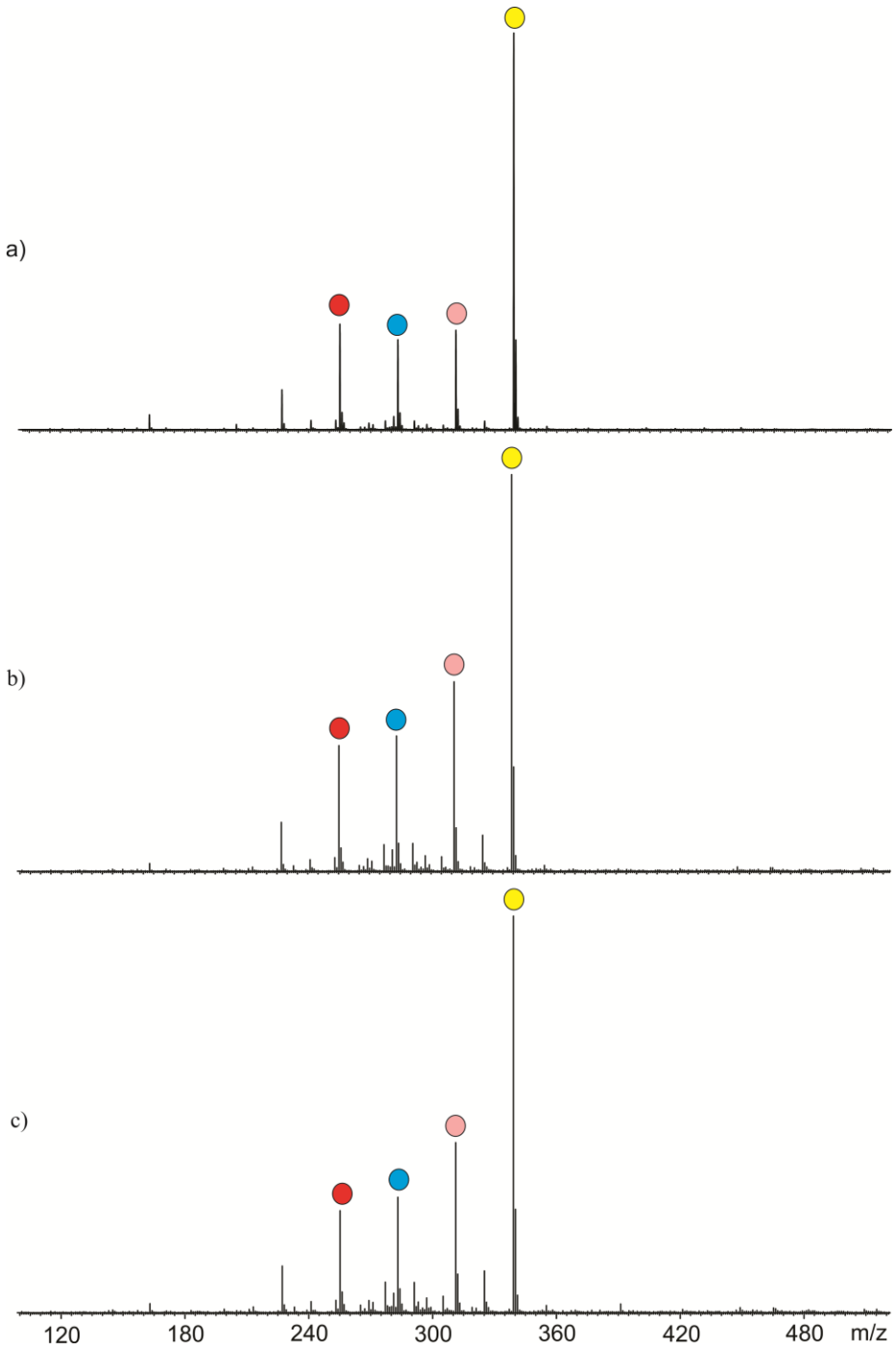

Figure 3.2 a) nanoESI mass spectra acquired in negative ion mode for a mixture of different NDs containing ● 1% Palmitic acid-ND, ● 1% Stearic acid-ND, ● 1% arachidic acid-ND and ● a1% Behenic acid-ND and Tandem mass spectra of the ND mixture at m/z of: b) 13000 and c) 11000.

The reason of using this percentage is that, the four fatty acids together are not solubilized further than this in the ND solution. Higher percentages produce a cloudy solution of ND that creates an improper self-assembly process. The acquired nanoESI mass spectra are shown in Figure 3.5. The result is consistent with the previous ones suggesting that the fatty acid with a longer carbon chain incorporates more efficiently into ND.

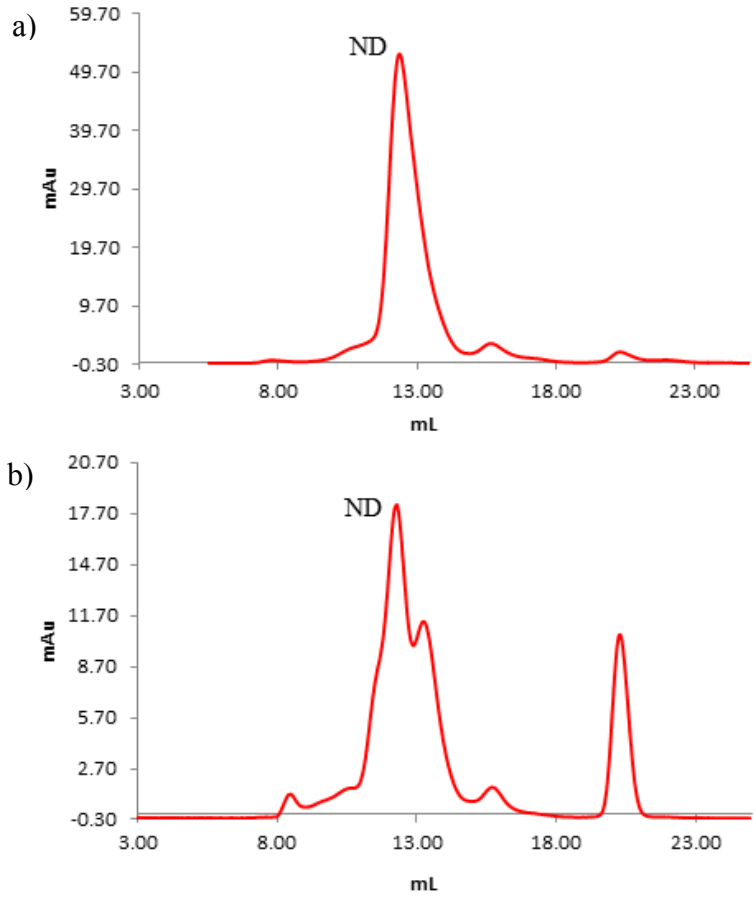

Figure 3.3 Separation of NDs by FPLC using Superdex 200 HR 10/300 GL column (Running buffer 200 mM ammonium acetate, pH 6.8). ND containing of a) 1.5% and b) 3% of each of the fatty acid: Palmitic acid, Stearic acid, Arachidic acid and Behenic acid.

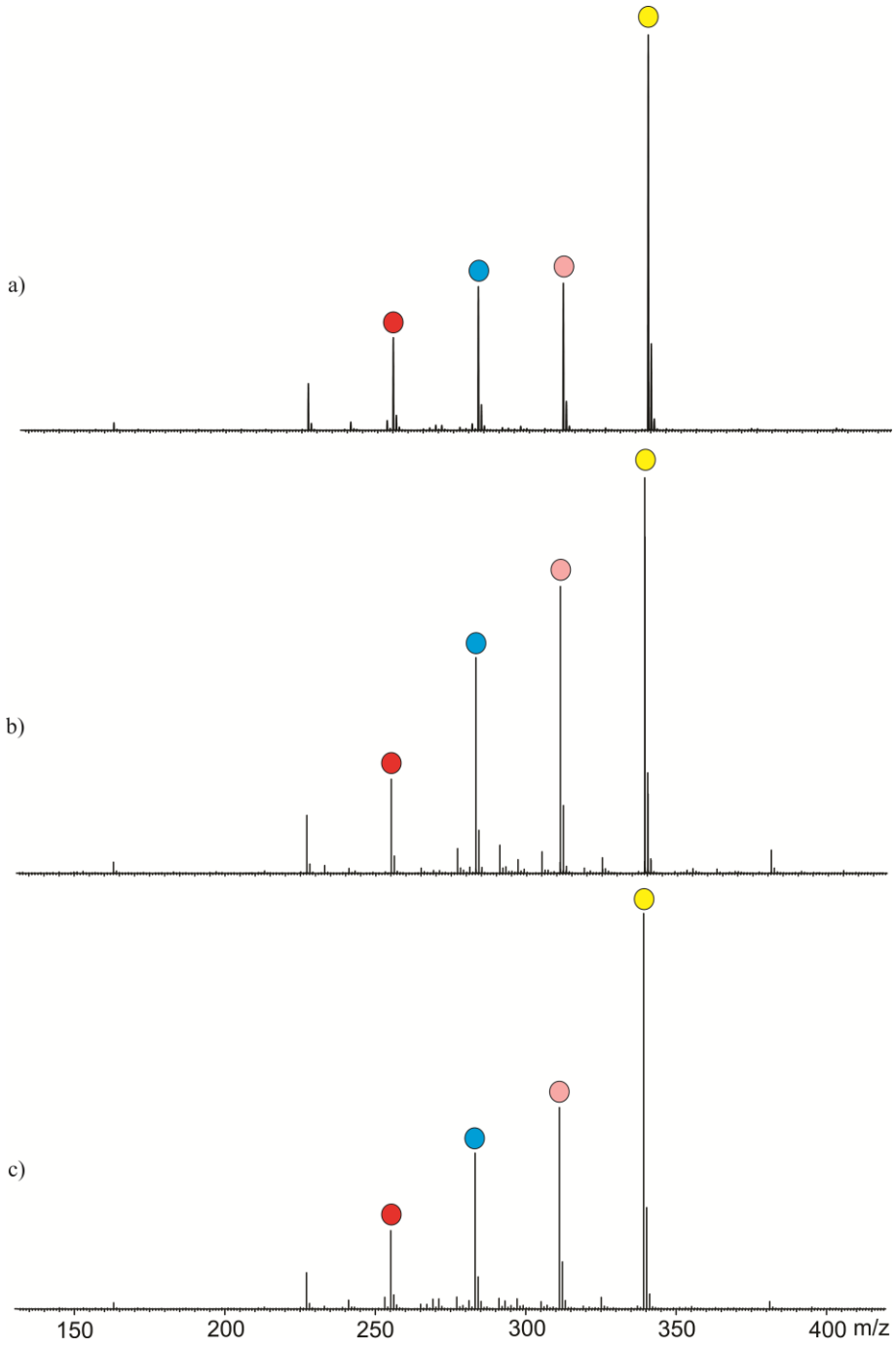

Figure 3.4 a) nanoESI mass spectra acquired in negative ion mode for ND containing ● 1%Palmitic acid, ● 1% Stearic, ● 1% arachidic acid and ● 1%Behenic acid and tandem mass spectra acquired at m/z of b) 11000 and c) 12500.

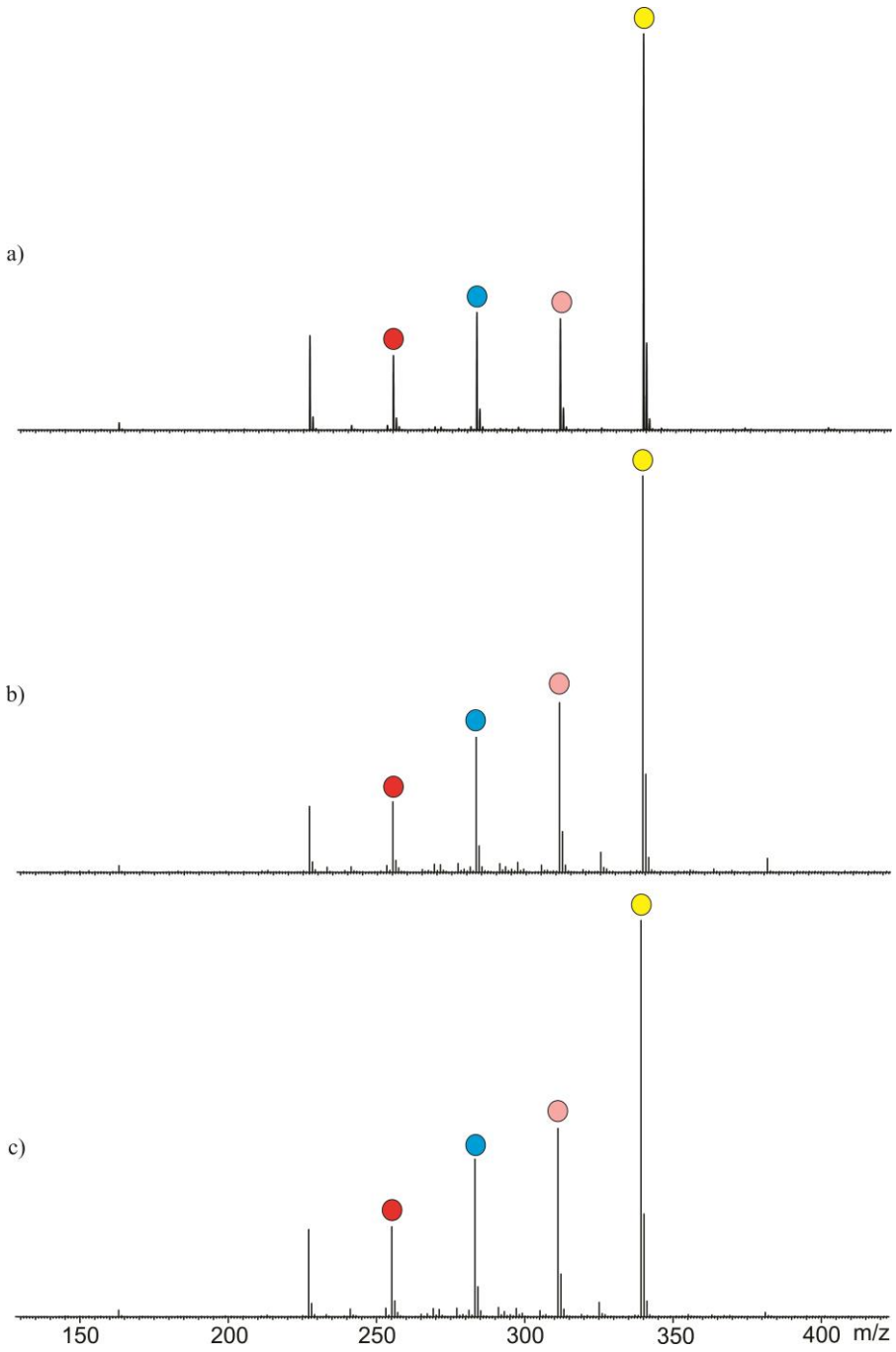

Figure 3.5 a) NanoESI mass spectra acquired in negative ion mode for ND containing ● 1.5% Palmitic acid, ● 1.5% Stearic, ● 1.5% arachidic acid and ● 1.5% Behenic acid and tandem mass spectra acquired at different m/z of b) 11000 and c) 13000.

3.2.2.2 Conclusions

The present work focused on the efficiency of incorporation of fatty acids with different carbon chain lengths into ND. The efficiency of incorporation can be obtained according to the released fatty acids relative abundance from ND. The aim was to choose the best incorporated fatty acid and then attach it to complex sugar molecules. After, we wanted to integrate them into ND for further investigations of the interactions between the biologically important sugars and their cognate receptors. A comparison was made between four fatty acids with carbon chain lengths of 16, 18, 20 and 22. The reason being, we wanted to mimic the natural gangliosides carbon chain length on the surface of a cell membrane. ND made with only DMPC was used as control. Even though the latter ND could release the ions with the same m/z as the chosen fatty acids, no specific trend was observed on release of these ions. However upon spraying a mixture of ND, in which each of them were made with 1% of the fatty acid, a trend was observed for fatty acid release from ND with the greatest intensity for a fatty acid with a chain length of 22 carbons and the least for a fatty acid with 16 carbons. It is known that the longer the carbon chain of the fatty acid the more acidic it is in the gas phase[141]. However, the change in the acidity is not so great as to perturb the efficiency of the ionization. To validate the observed result two other ND types were made: One with incorporation of 1% of the four fatty acids and the other with incorporation of 1.5% of the four fatty acids. The results were consistent with the previous run. The longer carbon chain provides better interaction with

the DMPC carbon chain in ND and better incorporation of the fatty acid into ND. The results can be used for synthesis purposes where biologically important carbohydrates need a carbon chain in order to incorporate into the ND. In our case, we wanted to attach complex sugar molecules (From Dr. Bundle group, University of Alberta) to the fatty acid then incorporate them into ND. Unfortunately, due to the small amount of sugars received (owing to the complexity in the synthesis process) and low expected product yield from the reaction between the synthesized sugar and fatty acid, we changed the direction of the project. The current direction involves the incorporation of simpler carbohydrate sugars (From Dr. Lowary group, University of Alberta), into ND.

3.3 Surface Plasmon Resonance Measurement Using Nanodiscs

3.3.1 Introduction

Shiga toxin (Stx) is a protein toxin which contains a moiety that interacts with the cell surface. It is produced by *Shigella dysenteriae* and *Escherichia coli*, of which the strain O157: H7 has become known for its toxicity. This toxin causes gastrointestinal related diseases like diarrhea and hemolytic uremic syndrome and high mortality rate of most its recent outbreaks poses a serious threat to public health.

Fraser *et al.*[142] reported that binding of shiga toxin to Gb3 ganglioside on the cell membrane causes hemolytic uremic syndrome. Stx exists in two isoforms, Stx1 and Stx2. They have 56% homology[143]. Each Stx molecule is comprised of

six subunits in which five are labeled the B subunit and the other A. The B subunit of both Stx attaches to the Gb3 ganglioside[144]. Stx1 and 2 have highly similar structure but Stx2 is more toxic[145]. In my research, the B subunit of Stx1was used to investigate its interaction with Gb3-ND with SPR. Using ND as a native membrane model creates an opportunity to better investigate the interaction between the toxins and their receptor on cell surface that could clarify the difference between the toxicity of the two types of shiga toxin. To begin with, well known cholera toxin- GM1 interacting system was used. This test was performed by Borch *et al.* in 2008. Also in another experiment a well studied interacting partner was used as a model for ND using SPR, which is the P particle of norovirus and GM3 ganglioside. The P particle is the protruding domain found in the outmost surface of the viral capsid of norovirus which is believed to be essential to host interaction[146]. Recent report showed that the P particle interacts specifically with GM3 oligosaccharide but not with GD1b[147].

3.3.2 Experimental Sections

3.3.2.1 Materials

Cholera toxin B subunit (CTB) was purchased from Sigma-Aldrich (Oakville, Canada). Shiga Toxin B1 (StxB1) was a gift from Dr. Armstrong, University of Calgary. Stock solutions of StxB1 and CTB for SPR measurement was prepared by concentrating and dialyzing against 150 mM HEPES buffer (pH 7.4) using microconcentrators with a molecular weight cutoff of 10 kDa. 1,2-

dimyristoyl-*sn*-glycero-3-phosphocholine (DMPC) was purchased from Avanti Polar Lipids. Globotriaosylceramide (Gal(α1-4)Gal(β-4)Glc(β1)-ceramide, Gb3-Cer) was purchased from Abcam. CM5 and NTA sensor chips, Anti-His antibody Kit and Amine coupling Kit were provided from GE Healthcare Life Science. Other chemicals and detergents were purchased from Sigma Aldrich or Thermo Fisher Scientific Inc.

3.3.2.2 Sample Preparation

3.3.2.2.1 Nanodiscs Synthesis

ND with different percentages of GM1were prepared according to the protocol explained above. DMPC only ND was prepared for the reference cell. In addition, GD1b-ND and GM3-ND were prepared. Making of Gb3-ND was attempted as well. All NDs were buffer exchanged into HEPES buffer (10 mM HEPES, 150 mM NaCl and 3.33 mM EDTA).

3.3.2.2.2 Activating the Surface of NTA Sensor Chip for Capture of Ni^{2+} Ions

Nitrilotriacetic acid is covalently immobilized with carboxymethylated dextran on the NTA sensorchip. For chelating Ni ions by NTA, 0.5 mM $NiCl_2$ in HEPES buffer (pH 7.4) were injected over the sample and reference flow channels at 5 μg/min. This makes the sensor chip surface ready for capturing histidine- tagged proteins.

3.3.2.2.3 Immobilization of Anti-His Antibody on the Surface of CM5 Sensor Chip

The surface of CM5 sensor chip was modified by immobilization of Anti-his antibody through amine coupling according to the protocols provided by Biacore GE Healthcare. Briefly, the surface of the sensor chip activated through injection of 0.2 M (N-(3-dimethylaminopropyl)-N'-ethylcarbodiimide hydrochloride (EDC) solution and 0.05 M N-hydroxysuccinimide (NHS) solution. Then Anti-His antibody with concentration of 50 µg/mL was injected, followed by inactivation of the sensor chip surface by 1M ethanolamine hydrochloric acid solution (pH 8.5). HEPES buffer (pH 7.4) was used as running buffer (Figure 3.6).

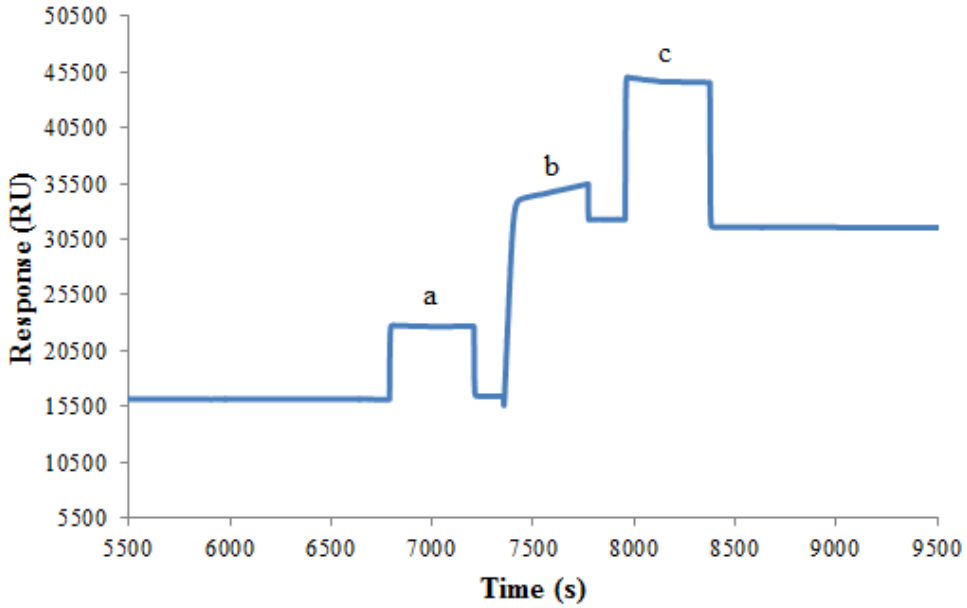

Figure 3.6 Sensorgram of immobilization of anti-his antibody on the surface of CM5 sensorchip a) Injection of EDC/NHS, b) Injection of anti-his antibody, c) Injection of ethanolamine hydrochloric acid.

Firstly, a NTA sensor chip was used as a test to examine its efficiency for capturing the his-tag attached to the MSP on the ND. This test was performed by Borch *et al.* in 2008. The well-known cholera toxin-GM1 interacting system was used. The sensor chip surface was activated by Ni^{2+} ions according to the abovementioned protocol. Then 2% GM1-ND (10 μg/mL) was injected over the sample flow channel at 5 μL/min. This was followed by injection of empty ND (10 μg/mL) at 5 μL/min on the two flow channels to block the direct capture of the analyte to the surface. Then cholera toxin (20 nM) was injected over both flow channels at 20 μL/min (Figure 3.7, 3.8). Regeneration buffer was 0.33 M EDTA, 10 mM HEPES and 150 mM NaCl (pH 8.2). The results show that even when the Ni^{2+} ions were blocked, cholera toxins were still able to attach to the reference cell albeit attachment was less than the sample cell. Also, it is important to note that there was ND release from the sensor chip due to its weak binding. The ND leakage happened at the end of ND injection. ND leakage and binding of CTB to the reference flow cell complicated data analysis. As such, for the experiments hereafter, CM5 sensor chip was used.

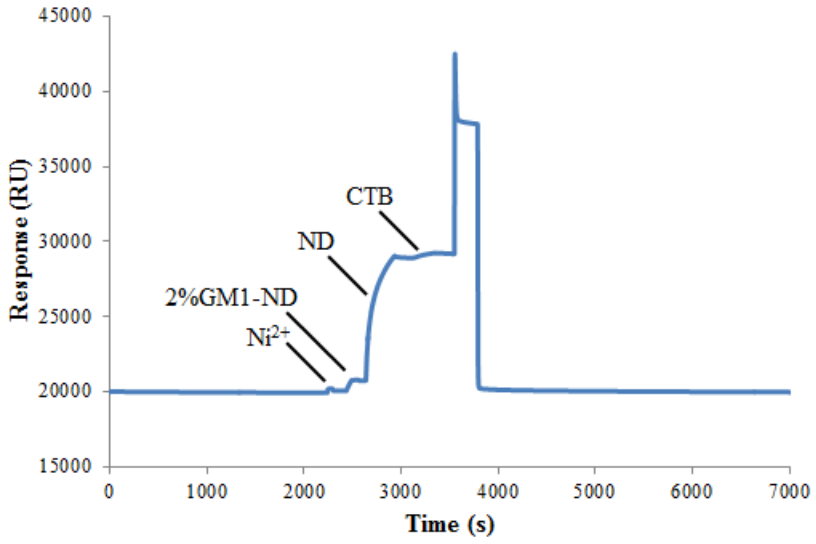

Figure 3.7 Binding of 20 nM CTB to 2% GM1-ND on NTA sensor chip.

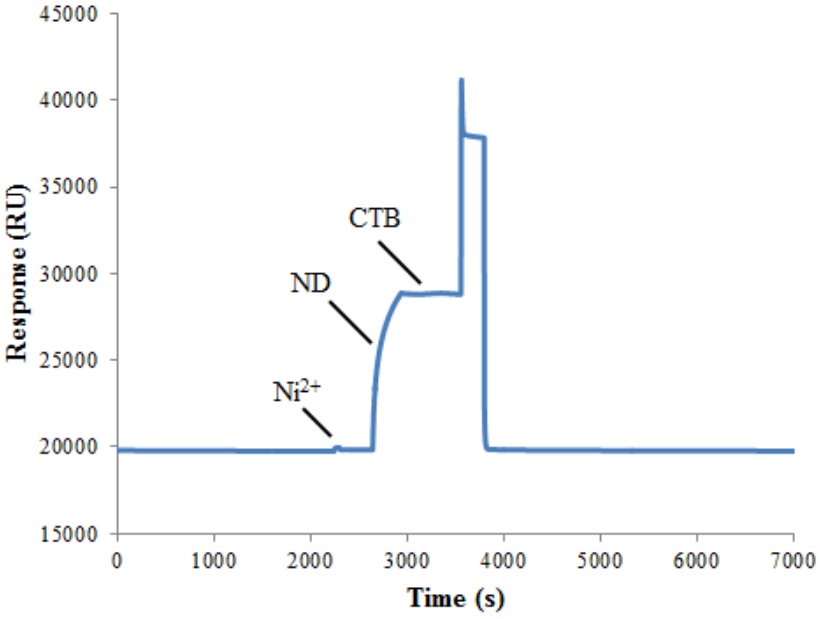

Figure 3.8 Binding of 20 nM CTB to reference flow cell containing empty NDs.

1% Gb3-ND was made according the abovementioned protocol. NDs made of DMPC only were used as the reference. Empty ND in 10 μg/mL was

injected in one flow cell and 1% Gb3-ND with 10 μg/mL was injected in another flow cell with a flow rate of 5 μL/min. The NDs was immobilized on the sensor chip surface through non covalent binding to the anti-his antibody. Running buffer was HEPES buffer (pH 7.4). StxB1 was buffer exchanged into the running buffer. Then the Stx (2 μM) was injected over the two flow channels at 20 μL/min. Finally, Glycine-HCl (pH 1.5) at flow rate of 30 μL/min was injected over the two flow channels to regenerate the surface of the sensor chip. No binding was detected by SPR, Figure 3.9; because of this we investigated whether Gb3 was correctly incorporated into ND. By using MS and tandem mass on the ND peak, no Gb3 was released from the ND (Figure 3.9). Due to inconclusive results with Stx B1 subunit and Gb3-ND interaction, we attempted another well studied interacting partner, which is P particle of norovirus and GM3 ganglioside, as model for ND using SPR.

5% GM3-ND and 5% GD1b-ND were made and incorporation of the gangliosides was confirmed by MS. The NDs were buffer exchanged into HEPES buffer. GD1b-ND was used as negative control. In one flow channel GD1b-ND (10 μg/mL) was injected with a flow rate of 5 μL/min and in another flow channel empty ND (10 μg/mL) was injected (5 μL/min). P particle (2 μM) was injected at 20 μL/min on both channels. As was expected, no binding was observed between GD1b-ND and P particle (Figure 3.11).

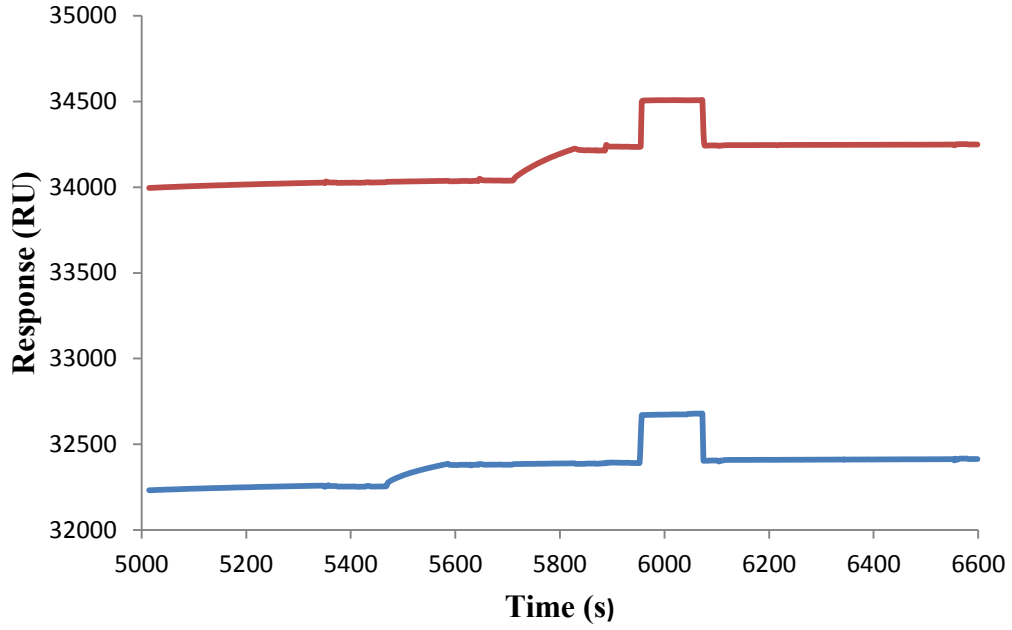

Figure 3.9 Sensorgram for immobilization of Gb3-ND (in red) and empty ND (in blue) on the surface of CM5 sensor chip. StxB1 was injected as analyte. No binding was detected.

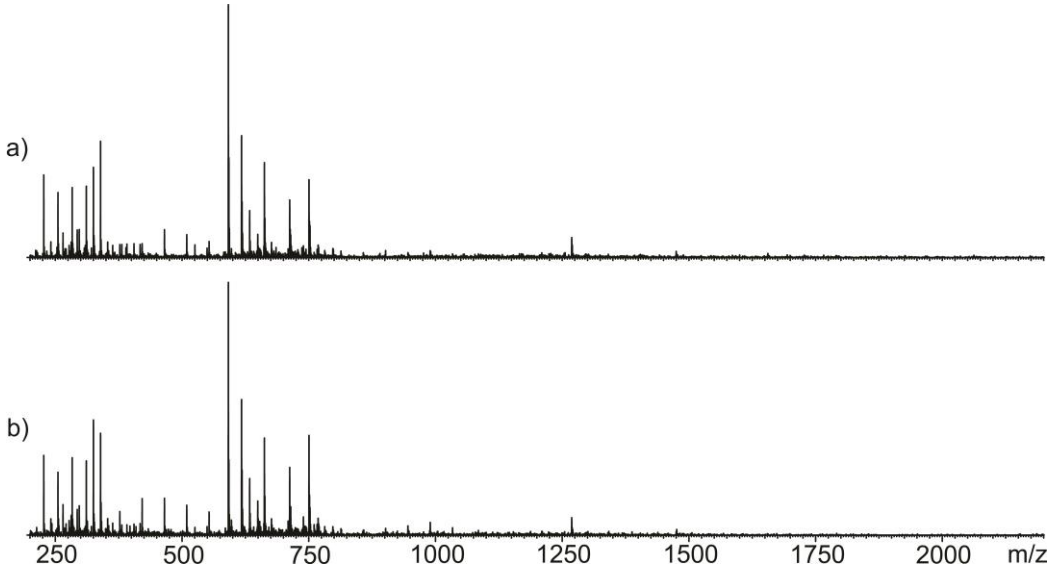

Figure 3.10 Tandem MS spectra acquired for 1% Gb3-ND at different m/z of: a) 10500 and b) 11500.

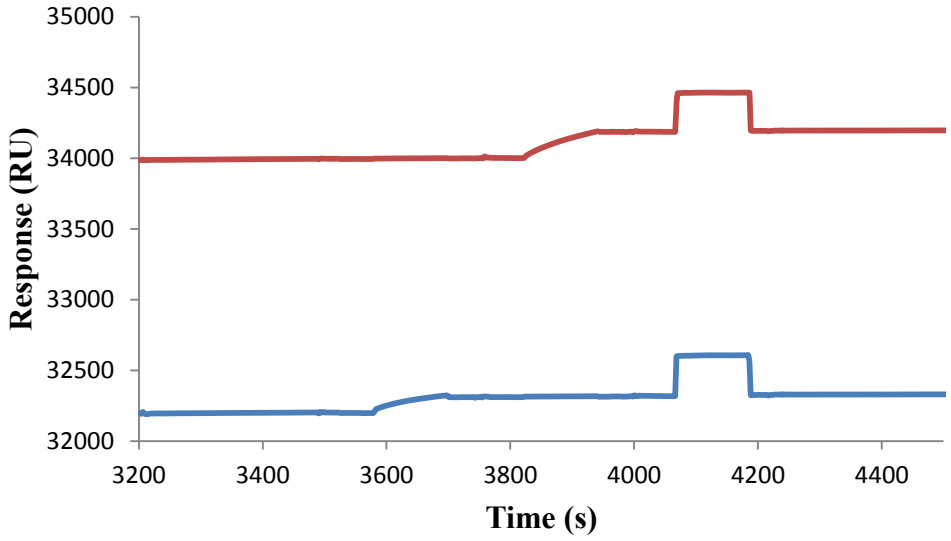

Figure 3.11 Sensorgram for immobilization of GD1b-ND (in red) and empty ND (in blue) on the surface of CM5 sensor chip. P particle (2 μM) was injected as analyte. No binding was detected as expected.

In another experiment GM3-ND was immobilized on the sensor chip surface and empty ND on the reference flow cell. This was performed following the protocol mentioned above. After injection of 2 μM P particle, no binding was observed (Figure 3.12). Running the experiment at an even higher concentration of P particle of 4 μM and more GM3 incorporated into ND (10% GM3-ND), did not indicate any binding between GM3-ND and P particle.

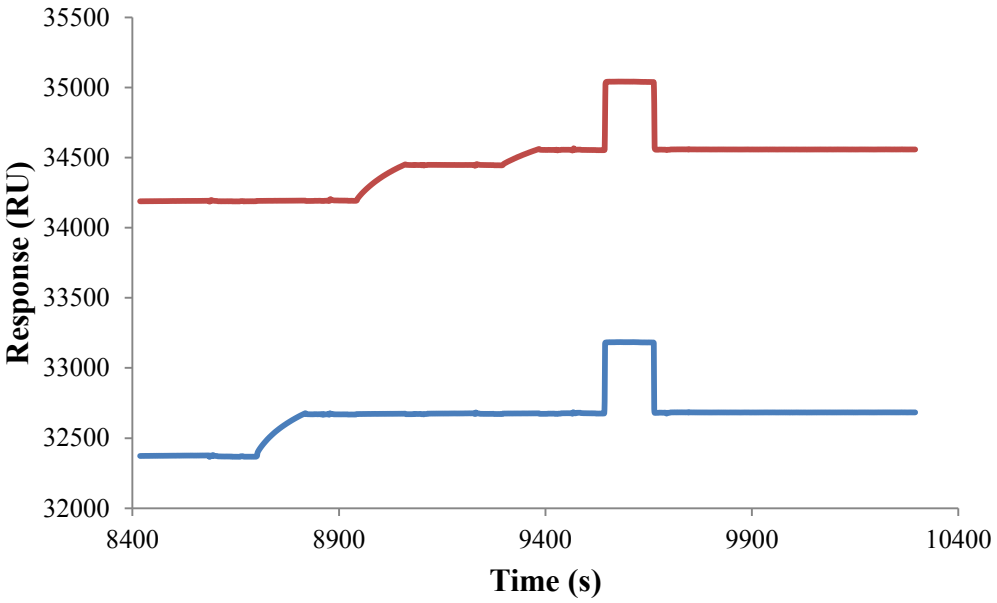

Figure 3.12 Sensorgram for immobilization of GM3-ND (in red) and empty ND (in blue) on the surface of CM5 sensor chip. P particle (2 μM) was injected as analyte. No binding was detected.

3.4 Conclusion

In the present work we tried to measure binding constant of different ganglioside with their cognate partner using ND technology with SPR spectroscopy. Using ND as a membrane model system opens up opportunities to observe binding interactions in near native conditions. Two different sensor chips were used. The NTA sensor chip immobilizes NDs through a capture method. Overall this kind of immobilization method suffers from leakages of the immobilized molecules from the sensor chip surface as was the case for the present work.

In another attempt, CM5 sensor chip was modified with anti-his antibody and the NDs were immobilized on the sensor chip surface through 6His-tag attached to the MSP. This method provided a very stable base line with no leakage of the NDs which was appropriate for kinetic measurements. Different NDs with different gangliosides were then used with the exception of Gb3-ND where Gb3 ganglioside was not successfully incorporated into ND. Although we were able to make the other NDs with their respective ganglioside, no binding between the GM3-ND and P particle was recorded despite their known interaction to each other[147]. Till now the only reported SPR binding data using ganglioside-ND system was from Borch et al in 2008 which the binding interaction was successfully reproduced in our lab (Appendix). The reason is probably because of the position of the binding site on the sugar attached to gangliosides. For GM3-ND and P particle tested here with SPR, GM3 binding site for P particle sugar moiety is sialic acid located near the phospholipid surface of ND which allows less accessibility to its proper receptor when ND immobilized on the sensor chip surface.

Even though no bindings were observed between the chosen ganglioside-ND systems and their cognate receptors for the SPR experiments, it opens up a new outlook for further analysis. It could be a good attempt to investigate the suppressing effect of ND system for those gangliosides with a binding site located near their ceramide part using SPR for known protein-ganglioside complexes. Incorporating gangliosides with a binding site at the top of the sugar into ND, like

the case for GM1 and CTB, can further clarify the effect of gangliosides' binding site position upon their successful interaction with their receptor using the ND system and SPR.

3.5 Literature cited

138. Bayburt, T. H.; Grinkova, Y. V.; Sligar, S. G., Self-assembly of discoidal phospholipid bilayer nanoparticles with membrane scaffold proteins. *Nano Letters* **2002,** *2* (8), 853-856.

139. Borch, J.; Roepstorff, P.; Møller-Jensen, J., Nanodisc-based co-immunoprecipitation for mass spectrometric identification of membrane-interacting proteins. *Molecular & Cellular Proteomics* **2011,** *10* (7), O110. 006775.

140. Zhang, Y.; Liu, L.; Daneshfar, R.; Kitova, E. N.; Li, C.; Jia, F.; Cairo, C. W.; Klassen, J. S., Protein–glycosphingolipid interactions revealed using catch-and-release mass spectrometry. *Analytical Chemistry* **2012,** *84* (18), 7618-7621.

141. Caldwell, G.; Renneboog, R.; Kebarle, P., Gas phase acidities of aliphatic carboxylic acids, based on measurements of proton transfer equilibria. *Canadian Journal of Chemistry* **1989,** *67* (4), 611-618.

142. Fraser, M. E.; Chernaia, M. M.; Kozlov, Y. V.; James, M. N., Crystal structure of the holotoxino from Shigella dysenteriae at 2.5 Å resolution. *Nature Structural & Molecular Biology* **1994,** *1* (1), 59-64.

143. Tesh, V.; O'brien, A., The pathogenic mechanisms of Shiga toxin and the Shiga-like toxins. *Molecular Microbiology* **1991,** *5* (8), 1817-1822.

144. Jackson, M. P.; Neill, R. J.; O'Brien, A. D.; Holmes, R. K.; Newland, J. W., Nucleotide sequence analysis and comparison of the structural genes

for Shiga-like toxin I and Shiga-like toxin II encoded by bacteriophages from Escherichia coli 933. *FEMS Microbiology Letters* **1987,** *44* (1), 109-114.

145. Milford, D.; Taylor, C.; Guttridge, B.; Hall, S.; Rowe, B.; Kleanthous, H., Haemolytic uraemic syndromes in the British Isles 1985-8: association with verocytotoxin producing Escherichia coli. Part 1: Clinical and epidemiological aspects. *Archives of Disease in Childhood* **1990,** *65* (7), 716-721.

146. Tan, M.; Fang, P.; Chachiyo, T.; Xia, M.; Huang, P.; Fang, Z.; Jiang, W.; Jiang, X., Noroviral P particle: structure, function and applications in virus–host interaction. *Virology* **2008,** *382* (1), 115-123.

147. Han, L.; Tan, M.; Kitova, E. N.; Xia, M.; Jiang, X.; Klassen, J. S., Gangliosides are Ligands for Human Noroviruses. *Journal of the American Chemical Society* **2014**.

Chapter 4

Conclusion and Future Work

In this work we extended the application of nanoESI-MS for quantifying the binding constant of an antibody and its cognate antigen. In addition, ND has been used as a native like membrane environment for solubilizing gangliosides and investigating their binding constants with their proper target proteins, using SPR spectroscopy. The effect of carbon chain length on effective incorporation of fatty acids into ND has also been investigated.

In chapter two, a new assay based on direct nanoESI-MS measurement was developed for an antibody with two binding sites to reveal specific interactions between antibodies and their specific antigens. This new MS quantification method allows direct calculation of the association constant for antibody-antigen interactions. This novel assay will surely be a complement to the current available methods for antibody-antigen interaction, identification and characterization. Studying antibody-antigen interactions with the new MS assay, we used antiGD2-mAb/GD2 sugar complex to quantify their interactions and the results were found to be consistent in both negative and positive ion modes and at different cone voltages. A clear application of this technique is for therapeutic mAb drug development.

In addition to quantitative measurement of the antibody-antigen reaction, qualitative examinations of cross-reactivity of different antibodies have been examined and the results showed that antibodies can have a wide range of cross-

reactivity. In order to further examine cross-reactivities, more mAb samples against a variety of target antigens need to be analyzed to obtain cross-reactivity profiling. As a new assay, it is recommended to further test the reliability and validity of the assay with more antibody-antigen systems with known binding data. Parameters such as pH, ionic strength and temperature, directly affect both antibody‘s stability, behavior and interaction towards their target antigen. Our newly developed strategy provides the opportunity to evaluate the influence of these conditions on binding interactions. This is of great importance in biological research for developing therapeutic mAbs for drug design.

In chapter three, we focused on the application of ND as a near native membrane model to solubilize and incorporate different fatty acids and gangliosides and use them in SPR and MS measurements. We examined fatty acids with different chain lengths to study their degree of incorporation into NDs by MS. The results are useful for synthesis purposes where carbohydrates with biological importance require a carbon chain for incorporation into NDs. We also tried to use ganglioside incorporated NDs and their target receptor to examine the kinetic interactions with SPR spectroscopy. Between NTA and CM5 sensor chips used in the experiments, CM5 showed better base line stability. With the exception of Gb3, the other gangliosides, GM1, GM3 and GD1b, were successfully incorporated into NDs.

In our attempt to measure binding constant using ND technology with SPR, the interaction between the P particle protein and GM3-ND was

investigated. It is known that the P particle protein has interaction with GM3 ganglioside but not GD1b[147]. As a negative control GD1b-ND immobilized on the sensor chip surface did not show interaction with the P particle. No binding was detected for the GM3-ND. Possible speculations may be due to the position of the binding sites on the sugar portion of the ganglioside. If the binding site of the ganglioside is near the ceramide chain, it may not be accessible to the target molecule when ganglioside incorporated into ND immobilizes on the sensor chip surface. Future work in this field may include the study of these suppressing effects of ganglioside incorporated ND to a known ganglioside protein interaction system to validate our observations. It is recommended to inverse the system by using ganglioside incorporated ND as the analyte and to have the target receptor immobilized on the sensor chip as ligand to compare the results with the previous system.

References

1. Norris, A. J.; Whitelegge, J. P.; Faull, K. F.; Toyokuni, T., Analysis of enzyme kinetics using electrospray ionization mass spectrometry and multiple reaction monitoring: Fucosyltransferase V. *Biochemistry* **2001,** *40* (13), 3774-3779.
2. Kapur, A.; Beck, J. L.; Sheil, M. M., Observation of daunomycin and nogalamycin complexes with duplex DNA using electrospray ionisation mass spectrometry. *Rapid Communications in mMass Spectrometry* **1999,** *13* (24), 2489-2497.
3. De Dominicis, E.; Commissati, I.; Suman, M., Targeted screening of pesticides, veterinary drugs and mycotoxins in bakery ingredients and food commodities by liquid chromatography-high-resolution single-stage Orbitrap mass spectrometry. *Journal of Mass Spectrometry* **2012,** *47* (9), 1232-1241.
4. Trauger, S. A.; Webb, W.; Siuzdak, G., Peptide and protein analysis with mass spectrometry. *Journal of Spectroscopy* **2002,** *16* (1), 15-28.
5. Hernández, F.; Portolés, T.; Pitarch, E.; López, F. J., Gas chromatography coupled to high-resolution time-of-flight mass spectrometry to analyze trace-level organic compounds in the environment, food safety and toxicology. *TrAC Trends in Analytical Chemistry* **2011,** *30* (2), 388-400.
6. Cubrilovic, D.; Biela, A.; Sielaff, F.; Steinmetzer, T.; Klebe, G.; Zenobi, R., Quantifying protein-ligand binding constants using electrospray

ionization mass spectrometry: a systematic binding affinity study of a series of hydrophobically modified trypsin inhibitors. *Journal of the American Society for Mass Spectrometry* **2012,** *23* (10), 1768-1777.

7. Xu, Y.; Falk, I. N.; Hallen, M. A.; Fitzgerald, M. C., Mass spectrometry- and lysine amidination-based protocol for thermodynamic analysis of protein folding and ligand binding interactions. *Analytical Chemistry* **2011,** *83* (9), 3555-3562.

8. Ohtsubo, K.; Marth, J. D., Glycosylation in cellular mechanisms of health and disease. *Cell* **2006,** *126* (5), 855-867.

9. Kakehi, K.; Oda, Y.; Kinoshita, M., Fluorescence polarization: analysis of carbohydrate–protein interaction. *Analytical Biochemistry* **2001,** *297* (2), 111-116.

10. Bundle, D. R.; Sigurskjold, B. W., Determination of accurate thermodynamics of binding by titration microcalorimetry. *Methods in Enzymology* **1994,** *247*, 288.

11. Smith, E. A.; Thomas, W. D.; Kiessling, L. L.; Corn, R. M., Surface plasmon resonance imaging studies of protein-carbohydrate interactions. *Journal of the American Chemical Society* **2003,** *125* (20), 6140-6148.

12. Chiodo, F.; Marradi, M.; Tefsen, B.; Snippe, H.; van Die, I.; Penadés, S., High sensitive detection of carbohydrate binding proteins in an ELISA-solid phase assay based on multivalent glyconanoparticles. *PLoS One* **2013,** *8* (8), e73027.

13. del Carmen Fernández-Alonso, M.; Díaz, D.; Berbis, M. Á.; Marcelo, F.; Cañada, J.; Jiménez-Barbero, J., Protein-carbohydrate interactions studied by NMR: from molecular recognition to drug design. *Current Protein & Peptide Science* **2012,** *13* (8), 816.

14. Wilcox, J. M.; Rempel, D. L.; Gross, M. L., Method of measuring oligonucleotide-metal affinities: Interactions of the thrombin binding aptamer with K+ and Sr2+. *Analytical Chemistry* **2008,** *80* (7), 2365-2371.

15. Oshannessy, D. J.; Brighamburke, M.; Soneson, K.; Hensley, P.; Brooks, I., Determination of rate and equilibrium binding constants for macromolecular interactions using surface plasmon resonance: use of nonlinear least squares analysis methods. *Analytical Biochemistry* **1993,** *212* (2), 457-468.

16. Jecklin, M. C.; Schauer, S.; Dumelin, C. E.; Zenobi, R., Label-free determination of protein–ligand binding constants using mass spectrometry and validation using surface plasmon resonance and isothermal titration calorimetry. *Journal of Molecular Recognition* **2009,** *22* (4), 319-329.

17. Larsen, K.; Thygesen, M. B.; Guillaumie, F.; Willats, W. G.; Jensen, K. J., Solid-phase chemical tools for glycobiology. *Carbohydrate Research* **2006,** *341* (10), 1209-1234.

18. Wishart, D., NMR spectroscopy and protein structure determination: applications to drug discovery and development. *Current Pharmaceutical Piotechnology* **2005,** *6* (2), 105-120.

19. Collie, J. N.; Patterson, H. S., On the Appearance of Helium and Neon in Vacuum Tubes. *Nature* **1913,** *90*, 699.

20. Fenn, J. B.; Mann, M.; Meng, C. K.; Wong, S. F.; Whitehouse, C. M., Electrospray ionization for mass spectrometry of large biomolecules. *Science* **1989,** *246* (4926), 64-71.

21. Kitova, E. N.; Kitov, P. I.; Bundle, D. R.; Klassen, J. S., The observation of multivalent complexes of Shiga-like toxin with globotriaoside and the determination of their stoichiometry by nanoelectrospray Fourier-transform ion cyclotron resonance mass spectrometry. *Glycobiology* **2001,** *11* (7), 605-611.

22. St. Hilaire, P. M.; Boyd, M. K.; Toone, E. J., Interaction of the Shiga-like toxin type 1 B-subunit with its carbohydrate receptor. *Biochemistry* **1994,** *33* (48), 14452-14463.

23. (a) Shoemaker, G. K.; Soya, N.; Palcic, M. M.; Klassen, J. S., Temperature-dependent cooperativity in donor–acceptor substrate binding to the human blood group glycosyltransferases. *Glycobiology* **2008,** *18* (8), 587-592; (b) ávan Dongen, W. D.; Albert, J., Binding of selected carbohydrates to apo-concanavalin A studied by electrospray ionization mass spectrometry. *Analyst* **2000,** *125* (4), 583-589.

24. Zeleny, J., The electrical discharge from liquid points, and a hydrostatic method of measuring the electric intensity at their surfaces. *Physical Review* **1914,** *3* (2), 69.

25. Kebarle, P.; Verkerk, U. H., Electrospray: from ions in solution to ions in the gas phase, what we know now. *Mass Spectrometry Reviews* **2009,** *28* (6), 898-917.

26. Cloupeau, M.; Prunet-Foch, B., Electrostatic spraying of liquids: main functioning modes. *Journal of Electrostatics* **1990,** *25* (2), 165-184.

27. Kebarle, P.; Tang, L., From ions in solution to ions in the gas phase-the mechanism of electrospray mass spectrometry. *Analytical Chemistry* **1993,** *65* (22), 972A-986A.

28. Wilm, M. S.; Mann, M., Electrospray and Taylor-Cone theory, Dole's beam of macromolecules at last? *International Journal of Mass Spectrometry and Ion Processes* **1994,** *136* (2), 167-180.

29. Dole, M.; Mack, L.; Hines, R.; Mobley, R.; Ferguson, L.; Alice, M. d., Molecular beams of macroions. *The Journal of Chemical Physics* **1968,** *49* (5), 2240-2249.

30. Banerjee, S.; Mazumdar, S., Electrospray ionization mass spectrometry: a technique to access the information beyond the molecular weight of the analyte. *International Journal of Analytical Chemistry* **2012,** *2012*.

31. Iribarne, J.; Thomson, B., On the evaporation of small ions from charged droplets. *The Journal of Chemical Physics* **1976,** *64* (6), 2287-2294.

32. Labowsky, M.; Fenn, J.; de la Mora, J. F., A continuum model for ion evaporation from a drop: effect of curvature and charge on ion solvation energy. *Analytica Chimica Acta* **2000,** *406* (1), 105-118.

33. Jecklin, M. C.; Touboul, D.; Bovet, C.; Wortmann, A.; Zenobi, R., Which electrospray-based ionization method best reflects protein-ligand interactions found in solution? A comparison of ESI, nanoESI, and ESSI for the determination of dissociation constants with mass spectrometry. *Journal of the American Society for Mass Spectrometry* **2008,** *19* (3), 332-343.

34. Pacholarz, K. J.; Garlish, R. A.; Taylor, R. J.; Barran, P. E., Mass spectrometry based tools to investigate protein–ligand interactions for drug discovery. *Chemical Society Reviews* **2012,** *41* (11), 4335-4355.

35. Joensson, H. N.; Samuels, M. L.; Brouzes, E. R.; Medkova, M.; Uhlén, M.; Link, D. R.; Andersson-Svahn, H., Detection and Analysis of Low-Abundance Cell-Surface Biomarkers Using Enzymatic Amplification in Microfluidic Droplets. *Angewandte Chemie International Edition* **2009,** *48* (14), 2518-2521.

36. Wilm, M.; Mann, M., Analytical properties of the nanoelectrospray ion source. *Analytical Chemistry* **1996,** *68* (1), 1-8.

37. Bahr, U.; Pfenninger, A.; Karas, M.; Stahl, B., High-sensitivity analysis of neutral underivatized oligosaccharides by nanoelectrospray mass spectrometry. *Analytical Chemistry* **1997,** *69* (22), 4530-4535.

38. Karas, M.; Bahr, U.; Dülcks, T., Nano-electrospray ionization mass spectrometry: addressing analytical problems beyond routine. *Fresenius' Journal of Analytical Chemistry* **2000,** *366* (6-7), 669-676.

39. Gobom, J.; Nordhoff, E.; Mirgorodskaya, E.; Ekman, R.; Roepstorff, P., Sample purification and preparation technique based on nano-scale reversed-phase columns for the sensitive analysis of complex peptide mixtures by matrix-assisted laser desorption/ionization mass spectrometry. *Journal of Mass Spectrometry* **1999,** *34* (2), 105-116.

40. Ho, C.; Lam, C.; Chan, M.; Cheung, R.; Law, L.; Lit, L.; Ng, K.; Suen, M.; Tai, H., Electrospray ionisation mass spectrometry: principles and clinical applications. *The Clinical Biochemist Reviews* **2003,** *24* (1), 3.

41. Watson, J. T.; Sparkman, O. D., *Introduction to mass spectrometry: instrumentation, applications, and strategies for data interpretation*. *John Wiley & Sons*: 2007.

42. Morris, M., Future paths of mass spectrometry in routine clinical chemistry. *Clinica Chimica Acta* **2010,** *411* (11), 905-906.

43. Mamyrin, B.; Shmikk, D., Linear mass reflectron. *Zh. Eksp. Teor. Fiz* **1979,** *76*, 1500-1505.

44. Clauser, K. R.; Baker, P.; Burlingame, A. L., Role of accurate mass measurement (±10 ppm) in protein identification strategies employing MS or MS/MS and database searching. *Analytical Chemistry* **1999,** *71* (14), 2871-2882.

45. Kitova, E. N.; El-Hawiet, A.; Schnier, P. D.; Klassen, J. S., Reliable determinations of protein–ligand interactions by direct ESI-MS measurements. Are we there yet? *Journal of the American Society for Mass Spectrometry* **2012,** *23* (3), 431-441.

46. Ganem, B.; Henion, J. D., Going gently into flight: analyzing noncovalent interactions by mass spectrometry. *Bioorganic & Medicinal Chemistry* **2003,** *11* (3), 311-314.

47. Kitova, E. N.; Kitov, P. I.; Paszkiewicz, E.; Kim, J.; Mulvey, G. L.; Armstrong, G. D.; Bundle, D. R.; Klassen, J. S., Affinities of Shiga toxins 1 and 2 for univalent and oligovalent Pk-trisaccharide analogs measured by electrospray ionization mass spectrometry. *Glycobiology* **2007,** *17* (10), 1127-1137.

48. Gross, J.; Xavier, A.; Gross, M. In *RNA Neomycin Complexes Analyzed by Electrospray and UV-MALDI-MS*, Papers, *49th ASMS Conference on Mass Spectrometry and Allied Topics*, 2001.

49. Gabelica, V.; Galic, N.; Rosu, F.; Houssier, C.; De Pauw, E., Influence of response factors on determining equilibrium association constants of non-covalent complexes by electrospray ionization mass spectrometry. *Journal of Mass Spectrometry* **2003,** *38* (5), 491-501.

50. Gabelica, V.; Rosu, F.; De Pauw, E., A simple method to determine electrospray response factors of noncovalent complexes. *Analytical Chemistry* **2009,** *81* (16), 6708-6715.

51. Sun, J.; Kitova, E. N.; Wang, W.; Klassen, J. S., Method for distinguishing specific from nonspecific protein-ligand complexes in nanoelectrospray ionization mass spectrometry. *Analytical Chemistry* **2006,** *78* (9), 3010-3018.

52. Deng, L.; Sun, N.; Kitova, E. N.; Klassen, J. S., Direct Quantification of Protein− Metal Ion Affinities by Electrospray Ionization Mass Spectrometry. *Analytical Chemistry* **2010,** *82* (6), 2170-2174.

53. Sun, J.; Kitova, E. N.; Klassen, J. S., Method for stabilizing protein-ligand complexes in nanoelectrospray ionization mass spectrometry. *Analytical Chemistry* **2007,** *79* (2), 416-425.

54. Taft, R. W.; Anvia, F.; Taagepera, M.; Catalan, J.; Elguero, J., Electrostatic proximity effects in the relative basicities and acidities of pyrazole, imidazole, pyridazine, and pyrimidine. *Journal of the American Chemical Society* **1986,** *108* (12), 3237-3239.

55. Bagal, D.; Kitova, E. N.; Liu, L.; El-Hawiet, A.; Schnier, P. D.; Klassen, J. S., Gas phase stabilization of noncovalent protein complexes formed by electrospray ionization. *Analytical Chemistry* **2009,** *81* (18), 7801-7806.

56. El-Hawiet, A.; Kitova, E. N.; Liu, L.; Klassen, J. S., Quantifying labile protein–ligand interactions using electrospray ionization mass spectrometry. *Journal of the American Society for Mass Spectrometry* **2010,** *21* (11), 1893-1899.

57. Wang, W.; Kitova, E. N.; Klassen, J. S., Influence of solution and gas phase processes on protein-carbohydrate binding affinities determined by nanoelectrospray Fourier transform ion cyclotron resonance mass spectrometry. *Analytical Chemistry* **2003,** *75* (19), 4945-4955.

58. Salamon, Z.; Macleod, H. A.; Tollin, G., Surface plasmon resonance spectroscopy as a tool for investigating the biochemical and biophysical

properties of membrane protein systems. II: Applications to biological systems. *Biochimica et Biophysica Acta (BBA)-Reviews on Biomembranes* **1997,** *1331* (2), 131-152.

59. Van Der Merwe, P. A., Surface plasmon resonance. *Oxford University Press*: New York, NY, USA: 2001; pp 137-170.

60. Patching, S. G., Surface plasmon resonance spectroscopy for characterisation of membrane protein–ligand interactions and its potential for drug discovery. *Biochimica et Biophysica Acta (BBA)-Biomembranes* **2014,** *1838* (1), 43-55.

61. Cooper, M. A.; Hansson, A.; Löfås, S.; Williams, D. H., A vesicle capture sensor chip for kinetic analysis of interactions with membrane-bound receptors. *Analytical Biochemistry* **2000,** *277* (2), 196-205.

62. Drescher, D. G.; Drescher, M. J.; Ramakrishnan, N. A., Surface plasmon resonance (SPR) analysis of binding interactions of proteins in inner-ear sensory epithelia. In *Auditory and Vestibular Research*, Springer: 2009; pp 323-343.

63. Andersson, K.; Areskoug, D.; Hardenborg, E., Exploring buffer space for molecular interactions. *Journal of Molecular Recognition* **1999,** *12* (5), 310-315.

64. Karlsson, R.; Fält, A., Experimental design for kinetic analysis of protein-protein interactions with surface plasmon resonance biosensors. *Journal of Immunological Methods* **1997,** *200* (1), 121-133.

65. Fahey, J. L., Antibodies and Immunoglobulins: II. Normal Development and Changes in Disease. *JAMA* **1965,** *194* (3), 255-258.

66. Harris, L. J.; Larson, S. B.; Hasel, K. W.; Day, J.; Greenwood, A.; McPherson, A., The three-dimensional structure of an intact monoclonal antibody for canine lymphoma. **1992**.

67. Carter, P. J., Potent antibody therapeutics by design. *Nature Reviews Immunology* **2006,** *6* (5), 343-357.

68. Zhang, Z.; Pan, H.; Chen, X., Mass spectrometry for structural characterization of therapeutic antibodies. *Mass spectrometry Reviews* **2009,** *28* (1), 147-176.

69. Schroeder Jr, H. W.; Cavacini, L., Structure and function of immunoglobulins. *Journal of Allergy and Clinical Immunology* **2010,** *125* (2), S41-S52.

70. Beck, A.; Wurch, T.; Bailly, C.; Corvaia, N., Strategies and challenges for the next generation of therapeutic antibodies. *Nature Reviews Immunology* **2010,** *10* (5), 345-352.

71. Thompson, N. J.; Rosati, S.; Rose, R. J.; Heck, A. J., The impact of mass spectrometry on the study of intact antibodies: from post-translational modifications to structural analysis. *Chemical Communications* **2013,** *49* (6), 538-548.

72. Beck, A.; Wagner-Rousset, E.; Bussat, M.-C.; Lokteff, M.; Klinguer-Hamour, C.; Haeuw, J.-F.; Goetsch, L.; Wurch, T.; Dorsselaer, A. V.; Corvaïa, N., Trends in glycosylation, glycoanalysis and glycoengineering

of therapeutic antibodies and Fc-fusion proteins. *Current Pharmaceutical Biotechnology* **2008,** *9* (6), 482-501.

73. Huang, L.; Biolsi, S.; Bales, K. R.; Kuchibhotla, U., Impact of variable domain glycosylation on antibody clearance: an LC/MS characterization. *Analytical Biochemistry* **2006,** *349* (2), 197-207.

74. Wormald, M. R.; Rudd, P. M.; Harvey, D. J.; Chang, S.-C.; Scragg, I. G.; Dwek, R. A., Variations in oligosaccharide-protein interactions in immunoglobulin G determine the site-specific glycosylation profiles and modulate the dynamic motion of the Fc oligosaccharides. *Biochemistry* **1997,** *36* (6), 1370-1380.

75. Oda, M.; Uchiyama, S.; Robinson, C. V.; Fukui, K.; Kobayashi, Y.; Azuma, T., Regional and segmental flexibility of antibodies in interaction with antigens of different size. *FEBS Journal* **2006,** *273* (7), 1476-1487.

76. Oda, M.; Uchiyama, S.; Noda, M.; Nishi, Y.; Koga, M.; Mayanagi, K.; Robinson, C. V.; Fukui, K.; Kobayashi, Y.; Morikawa, K., Effects of antibody affinity and antigen valence on molecular forms of immune complexes. *Molecular Immunology* **2009,** *47* (2), 357-364.

77. Harlow, E.; Lane, D., *Antibodies: a laboratory manual*. Cold Spring Harbor Laboratory Cold Spring Harbor, NY: 1988; Vol. 559.

78. Yokoyama, W. M.; Christensen, M.; Santos, G. D.; Miller, D.; Ho, J.; Wu, T.; Dziegelewski, M.; Neethling, F. A., Production of monoclonal antibodies. *Current Protocols in Immunology* **2006**, 2.5. 1-2.5. 29.

79. Lund, J.; Takahashi, N.; Pound, J. D.; Goodall, M.; Jefferis, R., Multiple interactions of IgG with its core oligosaccharide can modulate recognition by complement and human Fc gamma receptor I and influence the synthesis of its oligosaccharide chains. *The Journal of Immunology* **1996,** *157* (11), 4963-4969.

80. Dick, L. W.; Qiu, D.; Mahon, D.; Adamo, M.; Cheng, K. C., C-terminal lysine variants in fully human monoclonal antibodies: Investigation of test methods and possible causes. *Biotechnology and Bioengineering* **2008,** *100* (6), 1132-1143.

81. Dick, L. W.; Kim, C.; Qiu, D.; Cheng, K. C., Determination of the origin of the N-terminal pyro-glutamate variation in monoclonal antibodies using model peptides. *Biotechnology and Bioengineering* **2007,** *97* (3), 544-553.

82. Kaneko, Y.; Nimmerjahn, F.; Ravetch, J. V., Anti-inflammatory activity of immunoglobulin G resulting from Fc sialylation. *Science* **2006,** *313* (5787), 670-673.

83. Cui, W.; Rohrs, H. W.; Gross, M. L., Top-down mass spectrometry: recent developments, applications and perspectives. *Analyst* **2011,** *136* (19), 3854-3864.

84. Kaltashov, I. A.; Abzalimov, R. R., Do ionic charges in ESI MS provide useful information on macromolecular structure? *Journal of the American Society for Mass Spectrometry* **2008,** *19* (9), 1239-1246.

85. Zamani, L.; Lindholm, J.; Ilag, L. L.; Jacobsson, S. P., Discrimination among IgG1-κ monoclonal antibodies produced by two cell lines using

charge state distributions in nanoESI-TOF mass spectra. *Journal of the American Society for Mass Spectrometry* **2009,** *20* (6), 1030-1036.

86. Dillon, T. M.; Bondarenko, P. V.; Rehder, D. S.; Pipes, G. D.; Kleemann, G. R.; Ricci, M. S., Optimization of a reversed-phase high-performance liquid chromatography/mass spectrometry method for characterizing recombinant antibody heterogeneity and stability. *Journal of Chromatography A* **2006,** *1120* (1), 112-120.

87. Nallet, S.; Fornelli, L.; Schmitt, S.; Parra, J.; Baldi, L.; Tsybin, Y. O.; Wurm, F. M., Glycan variability on a recombinant IgG antibody transiently produced in HEK-293E cells. *New Biotechnology* **2012,** *29* (4), 471-476.

88. Remmele, R. L.; Callahan, W. J.; Krishnan, S.; Zhou, L.; Bondarenko, P. V.; Nichols, A. C.; Kleemann, G. R.; Pipes, G. D.; Park, S.; Fodor, S., Active dimer of Epratuzumab provides insight into the complex nature of an antibody aggregate. *Journal of Pharmaceutical Sciences* **2006,** *95* (1), 126-145.

89. Johnson, K. A.; Paisley-Flango, K.; Tangarone, B. S.; Porter, T. J.; Rouse, J. C., Cation exchange–HPLC and mass spectrometry reveal C-terminal amidation of an IgG1 heavy chain. *Analytical Biochemistry* **2007,** *360* (1), 75-83.

90. Kükrer, B.; Filipe, V.; van Duijn, E.; Kasper, P. T.; Vreeken, R. J.; Heck, A. J.; Jiskoot, W., Mass spectrometric analysis of intact human

monoclonal antibody aggregates fractionated by size-exclusion chromatography. *Pharmaceutical Research* **2010,** *27* (10), 2197-2204.

91. Atmanene, C. agner-Rousset, E. Malissard, M. Chol, B. Robert, A. Corva a, N. Dorsselaer, A. . Beck, A. Sanglier-Cianf rani, S.-. Extending mass spectrometry contribution to therapeutic monoclonal antibody lead optimization: characterization of immune complexes using noncovalent ESI-MS. *Analytical Chemistry* **2009,** *81* (15), 6364-6373.

92. Kaltashov, I. A.; Bobst, C. E.; Abzalimov, R. R.; Wang, G.; Baykal, B.; Wang, S., Advances and challenges in analytical characterization of biotechnology products: mass spectrometry-based approaches to study properties and behavior of protein therapeutics. *Biotechnology Advances* **2012,** *30* (1), 210-222.

93. Chelius, D.; Xiao, G.; Nichols, A. C.; Vizel, A.; He, B.; Dillon, T. M.; Rehder, D. S.; Pipes, G. D.; Kraft, E.; Oroska, A., Automated tryptic digestion procedure for HPLC/MS/MS peptide mapping of immunoglobulin gamma antibodies in pharmaceutics. *Journal of Pharmaceutical and Biomedical Analysis* **2008,** *47* (2), 285-294.

94. Fornelli, L.; Damoc, E.; Thomas, P. M.; Kelleher, N. L.; Aizikov, K.; Denisov, E.; Makarov, A.; Tsybin, Y. O., Analysis of intact monoclonal antibody IgG1 by electron transfer dissociation Orbitrap FTMS. *Molecular & Cellular Proteomics* **2012,** *11* (12), 1758-1767.

95. Houde, D.; Arndt, J.; Domeier, W.; Berkowitz, S.; Engen, J. R., Characterization of IgG1 conformation and conformational dynamics by

hydrogen/deuterium exchange mass spectrometry. *Analytical Chemistry* **2009,** *81* (7), 2644-2651.

96. Manikwar, P.; Majumdar, R.; Hickey, J. M.; Thakkar, S. V.; Samra, H. S.; Sathish, H. A.; Bishop, S. M.; Middaugh, C. R.; Weis, D. D.; Volkin, D. B., Correlating excipient effects on conformational and storage stability of an IgG1 monoclonal antibody with local dynamics as measured by hydrogen/deuterium-exchange mass spectrometry. *Journal of Pharmaceutical Sciences* **2013,** *102* (7), 2136-2151.

97. Nath, A.; Atkins, W. M.; Sligar, S. G., Applications of phospholipid bilayer nanodiscs in the study of membranes and membrane proteins. *Biochemistry* **2007,** *46* (8), 2059-2069.

98. Numata, M.; Grinkova, Y. V.; Mitchell, J. R.; Chu, H. W.; Sligar, S. G.; Voelker, D. R., Nanodiscs as a therapeutic delivery agent: inhibition of respiratory syncytial virus infection in the lung. *International Journal of Nanomedicine* **2013,** *8*, 1417.

99. Denisov, I.; Grinkova, Y.; Lazarides, A.; Sligar, S., Directed self-assembly of monodisperse phospholipid bilayer Nanodiscs with controlled size. *Journal of the American Chemical Society* **2004,** *126* (11), 3477-3487.

100. Civjan, N. R.; Bayburt, T. H.; Schuler, M. A.; Sligar, S. G., Direct solubilization of heterologously expressed membrane proteins by incorporation into nanoscale lipid bilayers. *Biotechniques* **2003,** *35* (3), 556-563.

101. Bayburt, T. H.; Sligar, S. G., Self-assembly of single integral membrane proteins into soluble nanoscale phospholipid bilayers. *Protein Science* **2003,** *12* (11), 2476-2481.

102. Boldog, T.; Grimme, S.; Li, M.; Sligar, S. G.; Hazelbauer, G. L., Nanodiscs separate chemoreceptor oligomeric states and reveal their signaling properties. *Proceedings of the National Academy of Sciences* **2006,** *103* (31), 11509-11514.

103. Nath, A.; Grinkova, Y. V.; Sligar, S. G.; Atkins, W. M., Ligand Binding to Cytochrome P450 3A4 in Phospholipid Bilayer Nanodiscs THE EFFECT OF MODEL MEMBRANES. *Journal of Biological Chemistry* **2007,** *282* (39), 28309-28320.

104. Alami, M.; Dalal, K.; Lelj-Garolla, B.; Sligar, S. G.; Duong, F., Nanodiscs unravel the interaction between the SecYEG channel and its cytosolic partner SecA. *The EMBO Journal* **2007,** *26* (8), 1995-2004.

105. Bayburt, T. H.; Leitz, A. J.; Xie, G.; Oprian, D. D.; Sligar, S. G., Transducin activation by nanoscale lipid bilayers containing one and two rhodopsins. *Journal of Biological Chemistry* **2007,** *282* (20), 14875-14881.

106. Schuler, M. A.; Denisov, I. G.; Sligar, S. G., Nanodiscs as a new tool to examine lipid–protein interactions. In *Lipid-Protein Interactions*, Springer: 2013; pp 415-433.

107. Öjemyr, L. N.; von Ballmoos, C.; Gennis, R. B.; Sligar, S. G.; Brzezinski, P., Reconstitution of respiratory oxidases in membrane nanodiscs for

investigation of proton-coupled electron transfer. *FEBS Letters* **2012,** *586* (5), 640-645.

108. Borch, J.; Torta, F.; Sligar, S. G.; Roepstorff, P., Nanodiscs for immobilization of lipid bilayers and membrane receptors: kinetic analysis of cholera toxin binding to a glycolipid receptor. *Analytical Chemistry* **2008,** *80* (16), 6245-6252.

109. Mould, D. R.; Sweeney, K. R., The pharmacokinetics and pharmacodynamics of monoclonal antibodies-mechanistic modeling applied to drug development. *Current Opinion in Drug Discovery and Development* **2007,** *10* (1), 84.

110. Nimmo, I.; Atkins, G. L.; Strange, R. C.; Percy-Robb, I. W., An evaluation of ways of using equilibrium dialysis to quantify the binding of ligand to macromolecule. *Biochem. J* **1977,** *165*, 107-110.

111. Bee, C.; Abdiche, Y. N.; Pons, J.; Rajpal, A., Determining the Binding Affinity of Therapeutic Monoclonal Antibodies towards Their Native Unpurified Antigens in Human Serum. *PLoS One* **2013,** *8* (11), e80501.

112. Stoop, M. P.; Dekker, L. J.; Titulaer, M. K.; Burgers, P. C.; Sillevis Smitt, P. A.; Luider, T. M.; Hintzen, R. Q., Multiple sclerosis-related proteins identified in cerebrospinal fluid by advanced mass spectrometry. *Proteomics* **2008,** *8* (8), 1576-1585.

113. Thamilarasan, M.; Hecker, M.; Goertsches, R. H.; Paap, B. K.; Schröder, I.; Koczan, D.; Thiesen, H.-J.; Zettl, U. K., Glatiramer acetate treatment

effects on gene expression in monocytes of multiple sclerosis patients. *Journal of Neuroinflammation* **2013,** *10* (1), 126.

114. Rolak, L. A.; Fleming, J. O., The differential diagnosis of multiple sclerosis. *The Neurologist* **2007,** *13* (2), 57-72.

115. Fuhr, P.; Borggrefe-Chappuis, A.; Schindler, C.; Kappos, L., Visual and motor evoked potentials in the course of multiple sclerosis. *Brain* **2001,** *124* (11), 2162-2168.

116. Seehusen, D. A.; Reeves, M. M.; Fomin, D. A., Cerebrospinal fluid analysis. *American Family Physician* **2003,** *68* (6), 1103-1108.

117. de Graaf, M. T.; de Jongste, A. H.; Kraan, J.; Boonstra, J. G.; Smitt, P. A.; Gratama, J. W., Flow cytometric characterization of cerebrospinal fluid cells. *Cytometry Part B: Clinical Cytometry* **2011,** *80* (5), 271-281.

118. Noga, M. J.; Dane, A.; Shi, S.; Attali, A.; van Aken, H.; Suidgeest, E.; Tuinstra, T.; Muilwijk, B.; Coulier, L.; Luider, T., Metabolomics of cerebrospinal fluid reveals changes in the central nervous system metabolism in a rat model of multiple sclerosis. *Metabolomics* **2012,** *8* (2), 253-263.

119. Jia, Y.; Wu, T.; Jelinek, C. A.; Bielekova, B.; Chang, L.; Newsome, S.; Gnanapavan, S.; Giovannoni, G.; Chen, D.; Calabresi, P. A., Development of protein biomarkers in cerebrospinal fluid for secondary progressive multiple sclerosis using selected reaction monitoring mass spectrometry (SRM-MS). *Clin Proteomics* **2012,** *9* (9).

120. Kanda, T.; Iwasaki, T.; Yamawaki, M.; Tai, T.; Mizusawa, H., Anti-GM1 antibody facilitates leakage in an in vitro blood–nerve barrier model. *Neurology* **2000,** *55* (4), 585-587.

121. Vyshkina, T.; Kalman, B., Autoantibodies and neurodegeneration in multiple sclerosis. *Laboratory Investigation* **2008,** *88* (8), 796-807.

122. Krebs, J. F.; Siuzdak, G.; Dyson, H. J.; Stewart, J. D.; Benkovic, S. J., Detection of a catalytic antibody species acylated at the active site by electrospray mass spectrometry. *Biochemistry* **1995,** *34* (3), 720-723.

123. Bennett, K. L.; Smith, S. V.; Lambrecht, R. M.; Truscott, R. J.; Sheil, M. M., Rapid characterization of chemically-modified proteins by electrospray mass spectrometry. *Bioconjugate Chemistry* **1996,** *7* (1), 16-22.

124. Siuzdak, G.; Krebs, J. F.; Benkovic, S. J.; Dyson, H. J., Binding of hapten to a single-chain catalytic antibody demonstrated by electrospray mass spectrometry. *Journal of the American Chemical Society* **1994,** *116* (17), 7937-7938.

125. Uetrecht, C.; Heck, A. J., Modern biomolecular mass spectrometry and its role in studying virus structure, dynamics, and assembly. *Angewandte Chemie International Edition* **2011,** *50* (36), 8248-8262.

126. Rostom, A. A.; Robinson, C. V., Detection of the intact GroEL chaperonin assembly by mass spectrometry. *Journal of the American Chemical Society* **1999,** *121* (19), 4718-4719.

127. Tito, M. A.; Miller, J.; Walker, N.; Griffin, K. F.; Williamson, E. D.; Despeyroux-Hill, D.; Titball, R. W.; Robinson, C. V., Probing molecular interactions in intact antibody: antigen complexes, an electrospray time-of-flight mass spectrometry approach. *Biophysical Journal* **2001,** *81* (6), 3503-3509.

128. Rosati, S.; Yang, Y.; Barendregt, A.; Heck, A. J., Detailed mass analysis of structural heterogeneity in monoclonal antibodies using native mass spectrometry. *Nature Protocols* **2014,** *9* (4), 967-976.

129. Rose, R. J.; Labrijn, A. F.; van den Bremer, E. T.; Loverix, S.; Lasters, I.; van Berkel, P. H.; van de Winkel, J. G.; Schuurman, J.; Parren, P. W.; Heck, A. J., Quantitative analysis of the interaction strength and dynamics of human IgG4 half molecules by native mass spectrometry. *Structure* **2011,** *19* (9), 1274-1282.

130. Thompson, N. J.; Rosati, S.; Heck, A. J., Performing native mass spectrometry analysis on therapeutic antibodies. *Methods* **2014,** *65* (1), 11-17.

131. Houde, D.; Peng, Y.; Berkowitz, S. A.; Engen, J. R., Post-translational modifications differentially affect IgG1 conformation and receptor binding. *Molecular & Cellular Proteomics* **2010,** *9* (8), 1716-1728.

132. Collin, M.; Olsén, A., EndoS, a novel secreted protein from Streptococcus pyogenes with endoglycosidase activity on human IgG. *The EMBO Journal* **2001,** *20* (12), 3046-3055.

133. Kitova, E. N.; Bundle, D. R.; Klassen, J. S., Thermal dissociation of protein-oligosaccharide complexes in the gas phase: Mapping the intrinsic intermolecular interactions. *Journal of the American Chemical Society* **2002,** *124* (20), 5902-5913.

134. Kaur, D.; Lowary, T. L.; Vissa, V. D.; Crick, D. C.; Brennan, P. J., Characterization of the epitope of anti-lipoarabinomannan antibodies as the terminal hexaarabinofuranosyl motif of mycobacterial arabinans. *Microbiology* **2002,** *148* (10), 3049-3057.

135. Sarkar, S.; Tang, X. L.; Das, D.; Spencer, J. S.; Lowary, T. L.; Suresh, M. R., A bispecific antibody based assay shows potential for detecting tuberculosis in resource constrained laboratory settings. *PLoS One* **2012,** *7* (2), e32340.

136. Klinman, D.; Banks, S.; Hartman, A.; Steinberg, A., Natural murine autoantibodies and conventional antibodies exhibit similar degrees of antigenic cross-reactivity. *Journal of Clinical Investigation* **1988,** *82* (2), 652.

137. James, L. C.; Tawfik, D. S., The specificity of cross-reactivity: promiscuous antibody binding involves specific hydrogen bonds rather than nonspecific hydrophobic stickiness. *Protein Science* **2003,** *12* (10), 2183-2193.

138. Bayburt, T. H.; Grinkova, Y. V.; Sligar, S. G., Self-assembly of discoidal phospholipid bilayer nanoparticles with membrane scaffold proteins. *Nano Letters* **2002,** *2* (8), 853-856.

139. Borch, J.; Roepstorff, P.; Møller-Jensen, J., Nanodisc-based co-immunoprecipitation for mass spectrometric identification of membrane-interacting proteins. *Molecular & Cellular Proteomics* **2011,** *10* (7), O110. 006775.

140. Zhang, Y.; Liu, L.; Daneshfar, R.; Kitova, E. N.; Li, C.; Jia, F.; Cairo, C. W.; Klassen, J. S., Protein–glycosphingolipid interactions revealed using catch-and-release mass spectrometry. *Analytical Chemistry* **2012,** *84* (18), 7618-7621.

141. Caldwell, G.; Renneboog, R.; Kebarle, P., Gas phase acidities of aliphatic carboxylic acids, based on measurements of proton transfer equilibria. *Canadian Journal of Chemistry* **1989,** *67* (4), 611-618.

142. Fraser, M. E.; Chernaia, M. M.; Kozlov, Y. V.; James, M. N., Crystal structure of the holotoxino from Shigella dysenteriae at 2.5 Å resolution. *Nature Structural & Molecular Biology* **1994,** *1* (1), 59-64.

143. Tesh, V.; O'brien, A., The pathogenic mechanisms of Shiga toxin and the Shiga-like toxins. *Molecular Microbiology* **1991,** *5* (8), 1817-1822.

144. Jackson, M. P.; Neill, R. J.; O'Brien, A. D.; Holmes, R. K.; Newland, J. W., Nucleotide sequence analysis and comparison of the structural genes for Shiga-like toxin I and Shiga-like toxin II encoded by bacteriophages

from Escherichia coli 933. *FEMS Microbiology Letters* **1987,** *44* (1), 109-114.

145. Milford, D.; Taylor, C.; Guttridge, B.; Hall, S.; Rowe, B.; Kleanthous, H., Haemolytic uraemic syndromes in the British Isles 1985-8: association with verocytotoxin producing Escherichia coli. Part 1: Clinical and epidemiological aspects. *Archives of Disease in Childhood* **1990,** *65* (7), 716-721.

146. Tan, M.; Fang, P.; Chachiyo, T.; Xia, M.; Huang, P.; Fang, Z.; Jiang, W.; Jiang, X., Noroviral P particle: structure, function and applications in virus–host interaction. *Virology* **2008,** *382* (1), 115-123.

147. Han, L.; Tan, M.; Kitova, E. N.; Xia, M.; Jiang, X.; Klassen, J. S., Gangliosides are Ligands for Human Noroviruses. *Journal of the American Chemical Society* **2014**.

Appendix

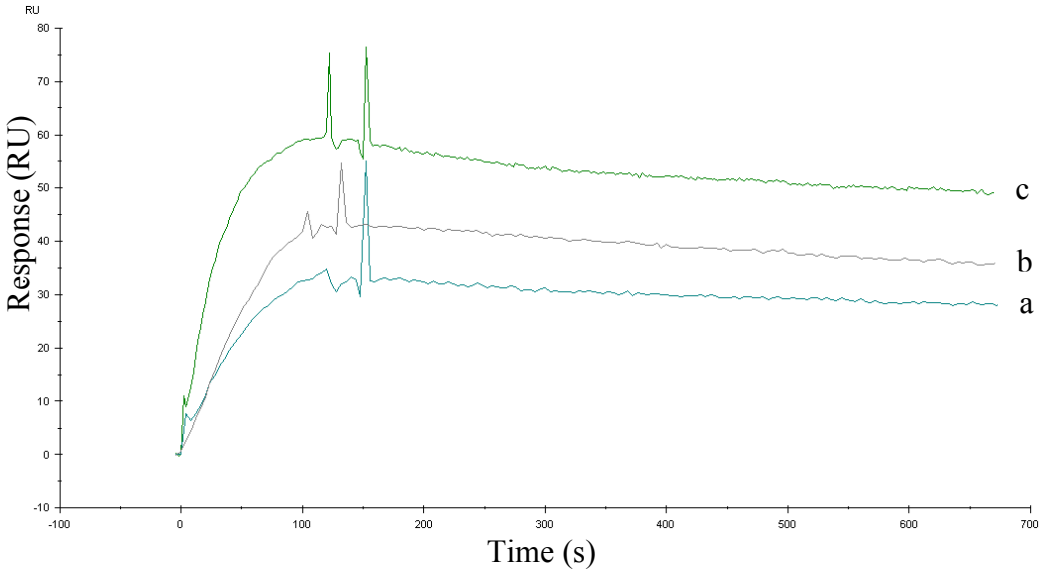

Figure A: Sensorgram for binding of a) 1.5, b) 4.5 and c) 13.5 nM CTB to 1%GM1-ND immobilized on the surface of CM5 sensor chip.